Universitat de Girona

CHARACTERIZATION OF CYTOTOXIC RIBONUCLEASES: FROM THE INTERNALIZATION PATHWAY TO THE IMPORTANCE OF DIMERIC STRUCTURES

Montserrat RODRÍGUEZ MAYNOU

ISBN: 978-84-690-4263-2
Dipòsit legal: GI-256-2007

UNIVERSTITAT DE GIRONA

DEPARTAMENT DE BIOLOGIA
LABORATORI D'ENGINYERIA DE PROTEÏNES
ÀREA DE BIOQUÍMICA I BIOLOGIA MOLECULAR

Tesi Doctoral

Characterization of cytotoxic ribonucleases: from the internalization pathway to the importance of dimeric structures

Montserrat Rodríguez Maynou

2006

UNIVERSTITAT DE GIRONA

DEPARTAMENT DE BIOLOGIA
LABORATORI D'ENGINYERIA DE PROTEÏNES
ÀREA DE BIOQUÍMICA I BIOLOGIA MOLECULAR

Characterization of cytotoxic ribonucleases: from the internalization pathway to the importance of dimeric structures

Memòria presentada per adquirir el grau de
Doctor per la Universitat de Girona, per

Montserrat Rodríguez Maynou

Vist-i-plau
La Directora de Tesi

Dra. Maria Vilanova i Brugués
Catedràtica
de Bioquímica i Biologia Molecular

Vist-i-plau
El Director de Tesi

Dr. Antoni Benito i Mundet
Professor Titular
de Bioquímica i Biologia Molecular

Girona, Octubre de 2006

A l’Antonio i en Pau

AGRAÏMENTS

Són molts els noms que em venen al cap que han fet possible que aquesta tesi arribés a enquadernar-se, però sobretot que m'han fet gaudir del dia a dia durant la realització d'aquest treball. Tot i que no veig possible expressar el meu agraïment en unes poques frases, voldria almenys intentar-ho. Gràcies, sincerament:

A la Dra. Maria Vilanova i al Dr. Antoni Benito per l'orientació, direcció i correcció d'aquesta tesi, la confiança dipositada en mi i en especial per les enriquidores converses, per explicar resultats de difícil interpretació, per animar-me a continuar en els moments difícils i per mostrar-me la seva part humana.

El Ministerio de Ciencia y Tecnología per la concessió d'una beca predoctoral de *Formació de Personal Investigador* i a la Universitat Autònoma de Barcelona per la concessió d'una *Beca de Formació i Suport a la Recerca*. Així mateix vull agrair al Ministerio de Educación y Ciencia i a la Generalitat de Catalunya, els quals han finançat, a través dels ajuts BMC2000-01380CO2-02, BMC2003-08485-CO2-02 i SGR00-00064 respectivament, el projecte en què s'emmarca aquesta tesi.

Al Dr. Marc Ribó d'una forma especial pels seus consells necessaris per a avançar dia a dia en els moments difícils.

Als companys del "LAB 107": la Teresa, en Pep, en Gerard, en Pere i la Jess, amb qui he compartit moltes hores de laboratori amb moments de riure, tristesa, alegria, desesperació, ironia, ajudes...A més, a mesura que escric aquestes paraules em venen al cap una gran quantitat de moments que no podré oblidar mai.

Als companys del Departament de Biologia pels moments distesos de xerrades al passadís, a l'hora de dinar o a la màquina de cafè.

Al Dr. Bruno Beaumelle per donar-me la oportunitat d'iniciar-me en l'experimentació dels cultius cel·lulars i permetre'm realitzar una part de la tesi al seu laboratori de Montpellier. Vull agrair en especial tot l'ajut i col·laboració que vaig rebre durant la meva estada per part de tots els components del grup: Juliette, Fabianne, Jocelyn i l'Anne.

A la Dra. M.Victòria Nogués per donar-me la oportunitat de realitzar l'estudi cinètic en el seu laboratori de la Universitat Autònoma de Barcelona. No voldria oblidar-me de l'incondicional ajut en aquesta estada de tots els membres d'aquest grup, la Susana, en Zoran, l'Elisabet, en Marc i en especial en Mohamed per estar sempre disponible en les incomptables ocasions en què he necessitat el seu ajut ni que fos a hores intempestives.

A l’Ester, el César, l’Alicia, el Llucià, la Lourdes i en Josep que encara que no han entès massa a què em dedico m’han soportat moltes crisis. La Odette i la Mònica que tot i no poder-nos veure el dia a dia sempre sabem que són un puntal on ens podem recolzar. La Lucia, una madrilenya especial, que em va fer “Viure i Riure” a Montpellier.

A en Jordi i l’Eva que en moments d’estrés han hagut d’aguantar-me a mi, l’ordinador i els meus nervis d’última hora.

Finalment i el més important..., un càlid petó per el Pare, la Mare, i L’Antonio per donar-me suport incondicional al llarg d’aquest camí i mostrar haver cregut en mi fins i tot quan jo no hi creia.

Un petó a tots i moltes gràcies.

Índex

ÍNDEX ABREVIATURES

ε	Coeficient d'extinció molar
λ	Longitud d'ona
A	Adenina
Å	Amstrong
AAP	Aminopeptidasa d'*Aeromonas proteolytica*
Abs, A	Absorbància
AG	Aparell de Golgi
Ang	Angiogenina
Amp, Ap	Ampicil·lina
ATP	Adenosina-5'-trifosfat
B	Subseti per a la fixació de bases
BSA	Albúmina de serum boví
BS-RNasa	Ribonucleasa bovina seminal
C	Citidina
cCMP, C>p	Citidina 2',3'-fosfat cíclic
CCV	Vesícules recobertes de clatrina
C-terminal	Carboxi-terminal
Da, KDa	Dalton, quiloDalton
DMEM	*Dulbecco's eagle modified medium*
DMSO	Dimetilsulfòxid
DNA	Àcid desoxiribonuclèic
dNTP	Desoxiribonucleòtid-5' trifosfat
DO	Densitat òptica
DTT	1,4-ditio-DL-treitol
E. coli	*Escherichia coli*
ECP	Proteïna catiònica d'eosinòfil
ECV/MVB	*Endosomal carrier vesicle // multivesicular body*
EDN	Neurotoxina derivada d'eosinòfil
EDTA	Àcid etilendiamina-tetraacètic
EE	Endosomes primaris
EGF	Factor de creixement epidèrmic
EGFR	Receptor de l'EGF
ER	Reticle endoplasmàtic
FCS	Sèrum fetal boví
G	Guanina
Gnd-HCl	Clorur de guanidini
GSH	Glutatió reduït
GSSG	Glutatió oxidat
HPLC	Cromatografia Líquida d'Alta Resolució
HP-RNasa	Ribonucleasa pancreàtica humana
IC_{50}	Concentració de proteïna que inhibeix el 50% la síntesi proteica cel·lular
IPTG	Isopropil-β-D-tiogalactopiranòsid
k_{cat}	Constant catalítica
K_m	Constant de Michaelis Menten
LacZ	Gen de la β-galactosidasa
L-Arg	L-Arginina
LB	Medi Luria-Bertani
LBPA	Àcid lisobifosfatídic
LE	Endosomes secundaris
LYS	Lisosomes
Mes	Àcid 2(N-morfolino)etanosulfònic
M6PR	Receptor de la manosa-6-fosfat
NLS	Senyal de importació nuclear
N-terminal	Amino-terminal
ONC	Onconasa
P	Subseti per a la fixació de fosfats
PAGE	Electroforesi en gel de poliacrilamida
PBS	Tampó fosfat salí
PCR	Reacció en cadena de la polimerasa
PDB	Banc de dades de proteïnes
Poli(A)	Àcid poliadenílic
Poli(C)	Àcid policitidílic
Poli(U)	Àcid poliuridílic
Pyr	Àcid piroglutámic
R	Subseti per a la fixació de riboses
RE	Endosomes de reciclatge
RI	Inhibidor proteic de ribonucleases
pRI	Inhibidor d'origen humà
RNA	Àcid ribonucleic
mRNA	RNA missatger
rRNA	RNA ribosòmic
tRNA	RNA de transferència
RNasa	Ribonucelasa
RNasa A	Ribonucleasa de pàncrees boví
SDS	Dodecil sulfat sòdic
ssDNA	DNA de cadena senzilla
T	Timina
$T_{1/2}$	Temperatura en la qual el 50% de la proteïna està desnaturalitzada
TAE	Tamó amortidor Tris/Acètic/EDTA
TCA	Àcid tricloroacètic
Temed	N,N,N',N'-tetrametiletilendiamina
Tf	Transferrina
TrR	Receptor de la transferrina
TFA	Àcid trifluoroacètic
TGN	Xarxa trans de l'AG
Tris	Tris-hidroximetil-aminometà
TRITC	Isotiocianat tetrametil rodamina
UV	Ultraviolat
$V_{màx}$	Velocitat màxima

RESUM

En aquesta tesi s'ha caracteritzat la ruta d'internalització de l'onconasa, una ribonucleasa que és citotòxica per a cèl·lules tumorals i que es troba en fase III d'assajos clínics per al tractament del mesotelioma maligne. Aquest fet ha portat a què l'onconasa sigui considerada una proteïna model entre les RNases citotòxiques. Els resultats d'aquest treball indiquen que l'onconasa entra a les cèl·lules per la via dependent de clatrina i del complex AP-2 i que seguidament es dirigeix al compartiment dels endosomes de reciclatge a l'igual que la transferrina. Així mateix els resultats demostren que aquesta és la ruta a través de la qual aquesta proteïna exerceix la seva citotoxicitat. L'increment de la concentració d'onconasa en aquests endosomes, resultat de l'expressió transitòria de la toxina tetànica en aquestes cèl·lules, té com a resultat un increment de la mort cel·lular, indicant que els endosomes de reciclatge són el compartiment a través del qual l'onconasa pot translocar al citosol. Aquesta destinació intracel·lular sembla ser específica per a l'onconasa, a diferència d'altres RNases, que segueixen la ruta de degradació lisosomal. En aquest treball, també es mostra que la neutralització del pH endosomal incrementa notablement la toxicitat de l'onconasa, probablement degut a què facilita la seva translocació al citosol.

Per altra banda, en treballs previs del grup de recerca s'havia descrit que la variant de la HP-RNasa anomenada PE5 malgrat no escapar l'acció de l'RI presentava activitat citotòxica i era transportada activament al nucli cel·lular *in vitro*. L'import nuclear de proteïnes té lloc a través de seqüències específiques que les permeten unir-se a certs receptors anomenats importines, els quals les transporten a través dels complexes de porus nuclears. Aquestes seqüències s'anomenen senyals de localització nuclear (NLS) i les més caracteritzades són les corresponents a NLSs monopartits i bipartits. Els resultats d'aquest treball de tesi demostren que PE5 interacciona amb la importina α mitjançant diferents residus bàsics entre els quals hi ha la Lys1 i els triplets d'Arg 31-33 i 89-91. Tot i que aquests residus es troben allunyats en la seqüència, es troben propers en l'estructura tridimensional d'aquesta proteïna i la seva disposició topològica té una gran similitud amb un NLS bipartit clàssic.

Una altra estratègia utilitzada per a l'obtenció de variants RNases citotòxiques és la seva oligomerització, procés que es dóna de forma natural en la BS-RNasa i està descrit com a responsable de la citotoxicitat d'aquesta ribonucleasa. En el nostre grup de recerca s'havia obtingut l'estructura cristal·logràfica d'una variant dimèrica de l'HP-RNasa, anomenada PM8, que constituïa un dímer per intercanvi de dominis N-terminal, tot i que en solució aquosa predominava la forma monomèrica. En aquesta tesi s'han buscat les condicions en les quals s'afavoreix la formació d'estructura dimèrica en solució. S'ha provat que a 29ºC i en un tampó que conté 20% d'etanol una fracció important de la proteïna apareix en forma dimèrica sense la

presència d'altres oligòmers de mida superior. L'estructura dimèrica, també s'ha estabilitzat a partir d'una variant de PM8 anomenada PM8E103C, per la introducció d'un enllaç disulfur entre les dues subunitats. Aquests dímers es s'han aïllat mitjançant cromatografia d'exclusió molecular i estudiat per una banda la seva activitat citotòxica i per l'altra el procés de dimerització. Pel que fa a l'activitat citotòxica, la variant dimèrica PM8E103C no presenta una activitat citotòxica significativa. Aquests resultats poden ser deguts a què l'entorn citosòlic, on les RNases exerceixen la seva acció citotòxica, presenta un caràcter reductor que podria induir la dissociació del dímer i per tant el monòmer generat podria ser capturat per l'RI. Per altra banda, en l'estudi del procés de dimerització, s'ha determinat la constant de dissociació del dímer de PM8 (5 mM a 29ºC) que és dos ordres de magnitud inferior a l'estimada per a la HP-RNasa nativa. L'anàlisi de la dependència del procés de dimerització respecte a la temperatura mostra que, al contrari del que succeeix amb la seva homòloga bovina, en disminuir la temperatura, l'equilibri monòmer-dimer es desplaça cap a la forma dimèrica. Així mateix, els resultats obtinguts indiquen que primer té lloc el procés de dimerització i seguidament la separació del domini intercanviable respecte del domini principal. S'ha caracteritzat el procés d'intercanvi de dominis a partir de la variant PM8E103C i s'ha comprovat que el domini intercanviable es troba majoritàriament disposat sobre l'altra subunitat del dímer. Aquests resultats suggereixen un model per a la dimerització de PM8 diferent del postulat per la RNasa A. En aquest model, primer es forma la interfície secundària i després s'estableixen interaccions entre residus de les dues subunitats que estabilitzen el pèptid xarnera en una conformació que afavoreix l'intercanvi de dominis.

A més, en aquesta tesi, s'ha analitzat el patró de trencament de poli(C) i d'un tetranucleòtid per la HP-RNasa. Els resultats indiquen que l'enzim no actua de forma aleatòria sinó que prefereix el trencament de substrats llargs i que segueix un patró més endonucleolític que la RNasa A. L'enzim trenca especialment enllaços fosfodiéster que estan situats com a mínim entre 9-11 residus comptats a partir d'un extrem de la molècula de substrat. Amb l'eliminiació de dues càrregues positives a l'extrem N-terminal (R4 i K6) es modifica el patró de trencament del tetranucleòtid generant una proteïna molt més exonucleolítica. Per contra, l'addició de càrregues positives a la supefície de la proteïna, en la cara on es troba situat el centre actiu (R89 i R90) sembla crear un nou lloc d'ancoratge de l'enzim per a substrats llargs. Finalment, també s'ha caracterizat cinèticament una variant dimèrica de l'HP-RNasa (PM8E103C).

SUMMARY

In this thesis the internalization pathway of onconase has been characterized. Onconase is a ribonuclease with antitumor activity at the present is in Phase III of clinical trials for the treatment of malignan mesothelioma. It is considered a model protein among cytotoxic RNases. Here, we show that onconase enters cells using AP-2/ clathrin mediated endocytosis and it is then routed, together with transferrin, to the receptor recycling compartment. In addition, the results show that this is the route used by onconase to perform its cytotoxic activity. Increasing onconase concentration in the recycling endosomes using tetanus toxin light chain expression enhanced onconase toxicity, indicating that this compartment is a key cellular structure for onconase cytosolic delivery. This intracellular destination is specific to onconase since other RNases follow the default pathway to late endosomes/lysosomes. Neutralization of endosomal pH strongly enhances onconase toxicity, probably by facilitating its access to the cytosol.

On the other hand, our group has previously described an HP-RNase variant, named PE5, which shows cytotoxic activity although it is sensible to RI. It is actively transported to the nucleus *in vitro*. Nuclear import of proteins is determined by specific sequences that allow them to bind to receptors, namely importins, which transport the proteins through the nuclear pore complex. These sequences are termed nuclear localization signals (NLS) and the most characterized ones correspond to monopartite and bipartite NLSs. The present results show that PE5 interacts with importin α through different basic residues including Lys1 and the arginine clusters 31-33 and 89-91. Although these residues are scattered along the sequence, they are close in the three-dimensional structure of the protein and their topological disposition strongly resembles that of a classical bipartite nuclear localization signal.

Another strategy to obtain cytotoxic variants consists in its oligomerization, a natural process that takes place in BS-RNase, which is responsible of its cytotoxicity. We have previously described the structure of an HP-RNase variant, namely PM8, which constitutes a dimer by the exchange of an amino terminal domain, although in an aqueous solution it is found mainly as a monomer. In this thesis, the solution conditions that favour the dimerization of this variant have been investigated. It has been found that at 29ºC in a 20% ethanol buffer a significant fraction of the protein is found in dimeric form without the appearance of higher oligomers. A new variant of PM8, called PM8E103C, has been created in which the dimeric structure is stabilized by a disulfide bond between the two subunits. Both dimers were isolated by size exclusion chromatography and their cytotoxic activity and the dimerization process were investigated. PM8E103 was not cytotoxic likely because the cytosol, where RNases exert their cytotoxic activity, is a reductive environment that can induce the dissociation of the dimer. Thus generated monomer can be inhibited by RI. On the other hand, the dissociation constant of the

dimeric form of PM8 has been measured (5 mM at 29ºC) being this value two orders of magnitude lower than the one estimated for native HP-RNase. Analysis of the dependence of the dimerization process on temperature shows that unlike RNase A, a decrease in the temperature shifts the monomer-dimer equilibrium to the latter form. Also, it is shown that a previous dissociation of the exchangeable domain from the main protein body does not take place before the dimerization process. The domain swapping process has been characterized using the variant PM8E103C. In this variant the exchangeable domain is completely located on the other subunit. Our results suggest a model for the dimerization of PM8 that is different to that postulated for the dimerization of the homologous bovine pancreatic ribonuclease. In our model, first an open interface is formed and then intersubunit interactions stabilize the hinge loop in a conformation that completely displaces the equilibrium between non-swapped and swapped dimers to the latter ones.

In addition, in this thesis, the pattern of oligonucleotide formation by HP-RNase has been analysed using poly(C) and tetranucleotide as substrates. The results show that the enzyme does not act randomly and follows a more endonucleolytic pattern when compared with RNase A. The enzyme prefers the binding and cleavage of longer substrate molecules especially when the phosphodiester bond cleaved is between 9 and 11 nucleotides apart from at least one end of the substrate molecule. Deletion of two positive charges on the N-terminus (Arg4 and Lys6) modifies this pattern of external/internal phosphodiester bond cleavage preference leading to a more exonucleolytic enzyme. Addition of positives charges on the surface of the active site face (Arg89 and Arg90) seems to generate a new binding site for large substrates. Finally, a dimeric variant of HP-RNase (PM8E103C) has been kinetically characterized.

Introducció

1. CARACTERÍSTIQUES GENERALS DE LES RIBONUCLEASES

1.1. Definició

Les ribonucleases (RNases) són enzims que catalitzen el trencament dels enllaços fosfodièster dels àcid ribonucleics, tant en la degradació no específica de l'RNA com en nombroses formes de processament específiques dels diferents tipus de RNA (Mishra, 1995). D'aquí, es pot intuir que són un grup d'enzims extremadament heterogeni, tant pel que fa a la seva estructura com per la funció biològica que realitzen, i que es troben presents en tots els éssers vius. Tot i que el terme ribonucleasa s'utilitza generalment per a designar proteïnes amb activitat ribonucleolítica, existeixen àcids nuclèics que presenten funcions similars, com és el cas dels ribozims i de les ribonucleoproteïnes, com l'RNasa P (Deutscher, 1998; Deutscher, 1993).

1.2. Classificació

L'establiment d'un sistema de classificació adequat per a aquest grup tant ampli de molècules no és una tasca senzilla. A fi d'organitzar agrupacions més o menys homogènies es poden utilitzar criteris bioquímics, funcionals o evolutius. La dificultat en l'establiment d'una classificació general rau en el fet que una mateixa ribonucleasa pot acomplir més d'un dels criteris a utilitzar per a l'establiment de les diverses agrupacions. Així doncs, les ribonucleases es poden classificar:

- Segons l'actuació de l'enzim sobre el seu substrat. Es poden diferenciar en exoribonucleases, quan catalitzen la formació de mononucleòtids a partir d'un extrem 5' o 3' lliure de la cadena d'RNA o en endoribonucleases, si catalitzen l'escissió d'enllaços fosfodièster de l'interior d'una cadena de RNA, produint oligonucleòtids.
- Segons la seva especificitat per substrat. Per una banda distingim les ribonucleases inespecífiques, que catalitzen la degradació de tot tipus de molècules d'RNA, com és el cas de la nucleasa de *Serratia* i la nucleasa estafilocòccica. Per l'altra, les que presenten especificitat de base, com l'RNasa A, que hidrolitza les cadenes d'RNA a l'extrem 3' de residus de pirimidina. Per últim, les ribonucleases específiques, que reconeixen característiques concretes (de seqüència o d'estructura) en el seu substrat, i que estan implicades normalment en processos de maduració de l'RNA, com ara l'RNasa III.
- En funció del lloc on els enzims duen a terme la seva acció. Les ribonucleases es poden classificar com a extracel·lulars si actuen fora de la cèl·lula que l'ha sintetitzat, o com a intracel·lulars si actuen en el seu interior i estan implicades en el metabolisme de l'RNA. Les ribonucleases extracel·lulars solen ser inespecífiques i de massa molecular

molt baixa; al contrari que les intracel·lulars, que estan implicades en el metabolisme de l'RNA cel·lular, tenen una elevada especificitat per substrat i són estructuralment complexes.

Tradicionalment, les ribonuleases de mamífer i d'altres vertebrats s'han classificat en dos grans grups (Sierakowska i Shugar, 1977), les ribonucleases de *tipus secretori* i les de *tipus no secretori*. La nomenclatura no fa referència a la capacitat d'aquests enzims a ser o no secretats, sinó que té relació amb els òrgans a partir de les quals es van caracteritzar i purificar les primeres ribonucleases. Com a tipus secretori es van definir les que eren similars a la ribonucleasa produïda pel pàncrees, i com a tipus no secretori les que eren semblants a la purificada a partir del fetge o la melsa. Degut a la confusió que generava l'ordenació precedent, Sorrentino i Libonati (1997) van proposar utilitzar el terme *tipus pancreàtic* en comptes de *secretor* per classificar classificar les ribonucleases per identitat de seqüència, d'estructura i de propietats catalítiques amb les de l'RNasa A, malgrat que es trobin en teixits i fluids diferents als pancreàtics. La designació de *tipus no pancreàtic* enlloc de *no secretor* fa referència a ribonucleases que es troben en diversos fluids i en teixits diferents al pàncrees, caracteritzades per presentar identitat de seqüència i propietats catalítiques similars a les de l'RNasa K2 de ronyó boví o a les de l'EDN humana.

Per últim, en funció del nivell de conservació de seqüència i estructura, sobretot en els residus que intervenen en el procés de catàlisi, s'ha establert una sistemàtica de les ribonuclesases que engloba grups evolutius relacionats. En base a aquesta darrera classificació, els enzims dels quals es parla en aquest treball formen part de l'anomenada *superfamília de l'RNasa A* (Beintema *et al.*, 1988), categoria que comprèn endoribonucleases pirimidina específiques, tant de tipus pancreàtic com no pancreàtic, amb ponts difulfur en la seva estructura, la tríada catalítica His-Lys-His (veure apartat 1.4.), i una distribució filogenètica restringida als vertebrats (Beintema i Kleineidam, 1998).

En els vertebreats, els enzims pertanyents a la superfamíla de la RNasa A es troben àmpliament distribuïts en diversos òrgans i fluids. Els seus membres presenten diferents patrons d'expressió i mostren activitats catalítiques diverses enfront de substrats de RNA específics. A part de la funció digestiva, dels membres del tipus pancreàtic (RNasa 1), es desconeixen encara moltes de les seves funcions fisiològiques (veure apartat 1.3.). Fins al moment, s'han caracteritzat 8 famílies diferents pertanyents a aquesta superfamília en humans. La nomenclatura proposada inicialment (Zhou i Strydom, 1993) es basa en l'estructura primària de les proteïnes i va incloure inicialment cinc famílies. Posteriorment l'agrupació es va ampliar per l'addició de la família RNasa 6 (o RNasa K6) (Rosenberg i Dyer, 1996) i, més recentment, per les famílies RNasa 7 i 8 (Harder i Schroder, 2002; Zhang *et al.*, 2002). A la taula 1.1 es presenten les 8 famílies conegudes fins al moment.

Taula 1.1. Classificació de la superfamília de ribonucleases en humans

Família	Descripció	Tipus
RNasa 1	Ribonucleasa pancreàtica (HP-RNasa)	Pancreàtic
RNasa 2	Neurotoxina derivada d'eosinòfil (EDN)	No pancreàtic
RNasa 3	Proteïna catiònica d'eosinòfil (ECP)	No pancreàtic
RNasa 4	Ribonucleasa aïllada de plasma humà	Mixt
RNasa 5	Angiogenina (Ang)	No pancreàtic
RNasa 6	Ribonucleasa K6	No pancreàtic
RNasa 7	Ribonucleasa antimicrobial aïllada de teixit epitelial	No pancreàtic
RNasa 8	Ribonucleasa aïllada de placenta	No pancreàtic

1.3. Funcions de les RNases

Tal i com ja s'ha comentat, les ribonucleases tenen un paper central en el metabolisme de l'RNA i es troben en tots els organismes exercint funcions diverses i sovint vitals (Deutscher, 1993). Molts organismes secreten ribonucleases per tal de digerir l'RNA de l'entorn cel·lular en productes que puguin ser absorbits per les cèl·lules. Per a molts microorganismes i plantes aquesta funció és essencial, perquè la disponibilitat de fosfat inorgànic representa el factor més limitant pel seu creixement. En altres casos, les ribonucleases poden estar involucrades en processos de replicació i transcripció, ser responsables de transformacions postranscripcionals de l'RNA, prevenir l'autopol·linització en plantes o participar en mecanismes de resposta cel·lular a virus o microorganismes (Schein, 1997). A la taula 1.2 es presenta un llista de les diferents funcions conegudes de les ribonucleases, així com exemples representatius dins de cada grup.

El contingut de ribonucleases en una cèl·lula depèn de la seva síntesi endògena i de la internalització dels enzims presents en el medi extracel·lular, secretats pel pàncrees o per altres glàndules (Bartholeyns *et al.*, 1975, Reddi, 1975). Una mateixa cèl·lula pot arribar a contenir fins a 20 tipus de ribonucleases diferents alhora i amb especificitats superposades, provinents tant del seu medi extern com intern. Alguns d'aquests enzims poden ser components de complexes supramoleculars, funcionant de manera coordinada amb altres enzims (Deutscher i Li, 2001).

Les ribonucleases intracel·lulars són les que participen en la maduració, processament i recanvi dels diversos tipus d'RNA cel·lular, amb una elevada especificitat de substrat, tant en procariotes com en eucariotes. L'estricta regulació d'aquestes ribonucleases és essencial, donat que el metabolisme de l'RNA és essencial per a l'expressió gènica (Deutscher, 1988).

Pel que fa a les ribonucleases extracel·lulars, la funció fisiològica es desconeix encara en la majoria dels casos. Pel que fa a l'RNasa 1, s'accepta que intervé activament en processos

digestius, sobretot en herbívors remugants, com a conseqüència de la gran quantitat d'RNA d'origen microbià que s'ha de degradar en l'intestí d'aquests organismes (Barnard, 1969).

Taula 1.2. Principals funcions de les ribonucelases: selecció d'exemples representatius

Funció	Ribonucleasa	Organisme
Digestió RNA extracel·lular	RNasa A	*Bos taurus*
	RNasa T1	*Aspergillus oryzae*
	Nucleasa de *Serratia*	*Serratia marcescens*
	Nucleasa estafilococal	*Staphylococcus aureus*
	Nucleasa P1	*Penicillum citrinum*
Maduració RNA	RNasa III	*Escherichia coli*
	'Complexe de trencament' per al processament en l'extrem 3' de pre-mRNAs eucariotes	*Bos taurus*
Degradació RNA intracel·lular	RNasa E	*Escherichia coli*
	RNasa HI	*Escherichia coli*
	Exoribonucleasa específica poli(A)	*Homo sapiens*
Apoptosi	Nucleasa anticodó	*Escherichia col*
	RNasa L	*Homo sapiens*
Defensa	α-sarcina	*Aspergillus giganteus*
	ECP i EDN	*Homo sapienss*
	RNasa 7	*Homo sapiens*
Aspermatogència i immunotòxica	BS-RNasa	*Bos taurus*
	RNasa 4	*Homo sapiens*
Control de creixement	Angiogenina	*Homo sapiens*
	S-RNases	*Nicotiana alata*

Tanmateix s'ha comprovat que diversos membres de la superfamília de la RNasa A presenten accions biològiques especials, a banda del simple paper degradatiu que clàssicament s'ha establert per aquests enzims. Aquestes ribonucleases s'agrupen sota el terme 'RISBASES' (*Ribonucleases endowed with special bioactions*) (D'Alessio, 1997; Irie, 1997). Aquestes proteïnes es caracteritzen per ser en la majoria dels casos proteïnes bàsiques, tenir un pèptid senyal i ponts disulfur a la seva estructura. Aquest grup inclou, entre d'altres, les ribonucleases que presenten propietats citotòxiques (veure apartat 3).

1.4. Mecanisme de catàlisi

El mecanisme de catàlisi s'ha estudiat sobretot per la RNasa A, però malgrat això, totes les RNases pancreàtiques ja que presenten un pH d'activitat òptim al voltant de 8 per a la degradació de RNA, prefereixen com a substrat poly(C) en relació al poli(U) i són capaces d'hidrolitzar nucleotids 2',3'-fosfat cíclic. La RNasa A catalitza el trencament dels enllaços 3'-5'-fosfodièster de les cadenes senzilles d'RNA mitjançant una reacció en dues etapes (Figura 1.1a). La primera etapa és una reacció de tranfosforilació des de la posició 5' d'un nucleòtid a la posició 2' del nucleòtid adjacent, generant-se un extrem 2',3'-fosfat cíclic i un extrem 5'-OH

lliure. Durant la segona etapa es produeix la hidròlisi del grup fosfodièster cíclic, generant-se un grup 3'-fosfat terminal. La base en la posició 3' de l'enllaç que s'escindeix ha de ser una pirimidina (citidina o uracil) mentre que la base en la posició 5' pot ser tant una pirimidina com una purina tot i que l'enzim mostra una certa preferència per purines. La reacció de transfosforilació es produeix a una velocitat molt superior a la de hidròlisi i presenta una naturalesa reversible.

En el mecanisme de catàlisi de les RNases (Figura 1.1b) intervenen principalment els dos anells imidazol dels dos residus histidina del centre actiu (His 12, His 119). En la reacció de transfosforilació, la His-12 actua de base, desprotonant l'oxigen-2' de la molècula de substrat facilitant l'atac sobre l'àtom de fòsfor (Findlay *et al.*, 1961; Usher *et al.*, 1970a; Usher *et al.*, 1970b). El grup imidazol de la histidina 119 actua com a àcid protonant l'oxigen-5' facilitant el seu desplaçament i debilitant l'enllaç P-O5'. En la reacció d'hidròlisi, la His-119 capta un protó d'una molècula d'aigua i facilita la hidròlisi de l'enllaç 2',3'-fosfat cíclic, mentre la His-12 protona el grup O2'. Durant el procés es forma un complex intermediari de fosfat pentavalent que està estabilitzat principalment per la Lys-41 (Borkakoti, 1983; Wlodawer i Sjolin, 1983).

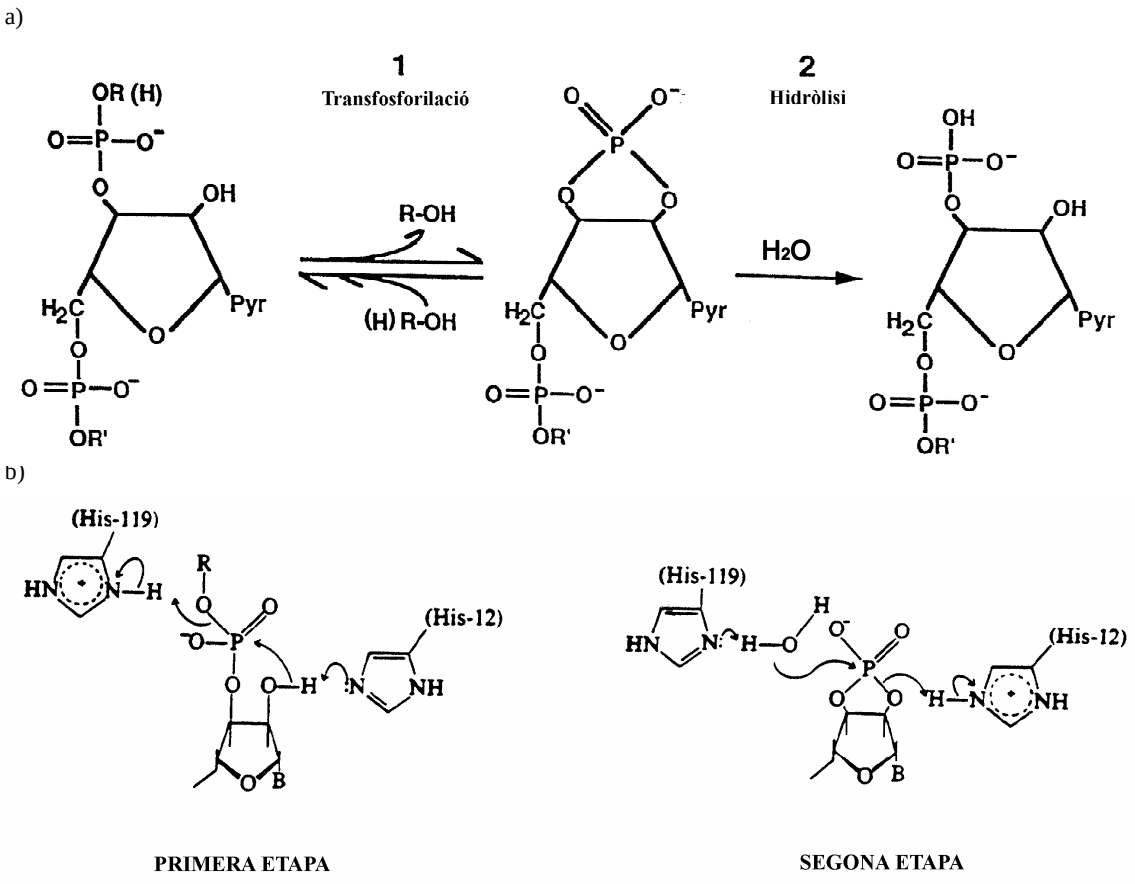

Figura 1.1. Mecanisme de catàlisi de les RNases.

a) Esquema de les dues etapes de trencament de l'RNA (reproduït de Cuchillo *et al.*, 1993). b) Esquema dels desplaçaments electrònics originats durant la catàlisi àcid-base segons el mecanisme catalític acceptat actualment (reproduït de Cuchillo *et al.*, 1997).

Estudis sobre el mecanisme de catàlisi de l'RNasa A (Cuchillo *et al.*, 1993; Thompson *et al.*, 1994) indiquen que no és correcte considerar la reacció com un procés seqüencial, amb la formació d'un intermediari associat a l'enzim, sinó que més aviat s'hauria de parlar de processos catalítics separats, fins al punt que la reacció de hidròlisis pràcticament no es produeix fins que no finalitza el trencament de tots els enllaços 3',5'-fosfodièster que l'enzim té disponibles. Per aquesta raó, els autors suggereixen que seria més acurat catalogar l'enzim de transferasa i no de hidrolasa (Cuchillo *et al.*, 1993).

L'enzim pot associar-se tant a desoxiribonucleòtids com a ribonucleòtids, però només pot hidrolitzar els darrers, ja que el grup 2'-OH de la ribosa és necessari pel mecanisme catalític.

1.4.1. Interacció RNasa-RNA

L'RNasa A exhibeix una clara preferència per a pirimidines en la posició 3' en relació a l'enllaç fosfodièster a escindir, hidrolitzant el substrat poli(C) aproximadament 20 vegades més ràpid que el poli(U). Tanmateix, l'especificitat de la reacció de transfosforilació no és absoluta, ja que l'enzim també es capaç de catalitzar la degradació de poli(A), per bé que amb una eficiència 10^3-10^4 vegades inferior a la que degrada poli(U) (delCardayré i Raines, 1994; Sorrentino i Libonati, 1994). Paral·lelament a aquesta especificitat primària, s'ha observat que la composició dels nucleòtids adjacents té una gran influència en l'eficiència catalítica (k_{cat}/K_m) d'aquest enzim. S'ha descrit una especificitat secundària per la base del nucleòtid en posició 5' en relació a l'enllaç que s'escindeix, seguint l'ordre A>G>C>U (Follmann *et al.*, 1967; Rushizky *et al.*, 1961; Witzel i Barnard, 1962 a i b). La segona etapa de la reacció és molt més específica i només s'hidrolitzen els èsters fosfat cíclic que tenen una pirimidina com a base nitrogenada (Cuchillo *et al.*, 1993; Nogués *et al.*, 1995).

Estudis estructurals, cinètics i de modificació química han proposat i demostrat l'existència de diferents subsetis en el centre actiu de l'enzim que uneixen per diversos punts d'interacció els fosfats (p_0...p_n), les bases (B_0...B_n) i les riboses (R_0...R_n) del substrat polimèric contribuint a la seva correcta disposició (Richards i Wyckoff, 1971) (Figura 1.2). p_1 és el centre catalític que interacciona amb el grup fosfat de l'enllaç fosfodièster que s'escindeix, B_1, és el seti principal específic per pirimidines i B_2 és el subseti d'interacció amb la base que ocupa la posició 5' de l'enllaç que s'escindeix. Els treballs on s'ha estudiat la participació dels diferents subsetis de l'RNasa A han estat revisats per Cuchillo *et al.* (1997), Gilliland (1997) i Nogués *et al.* (1998).

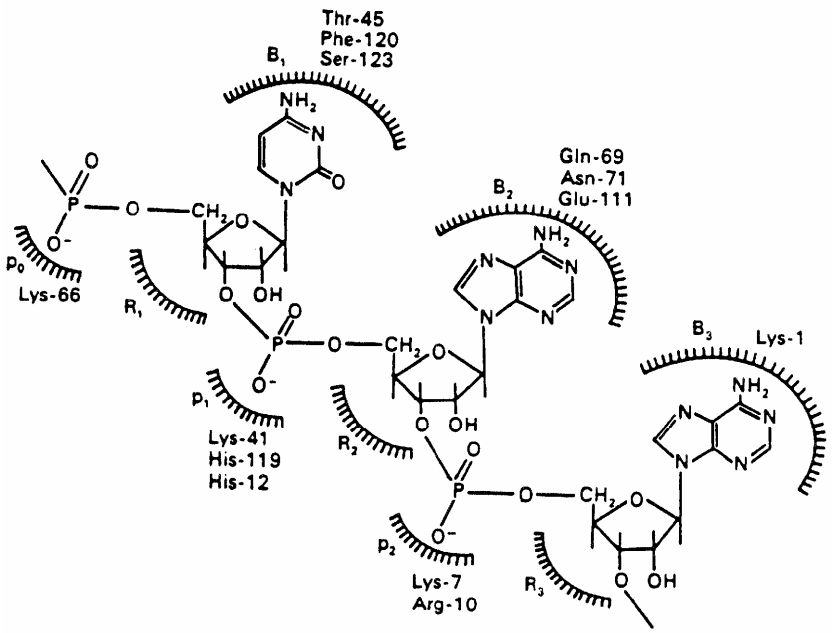

Figura 1.2. Representació esquemàtica de la interacció d'un fragment d'RNA amb l'RNasa A. B, R i p fan referència als subsetis de fixació de les bases, riboses i fosfats respectivament. Els mononucleòtids 3'-pirimidines interaccionen a $B_1R_1p_1$ i els 3'-AMP a $B_2R_2p_2$. S'indiquen els residus que podrien participar en cada subseti. Reproduït de Parés *et al.*, (1991).

L'eficiència catalítica de l'RNAsa A s'incrementa amb la longitud de la cadena de l'oligonucleòtid (Irie *et al.*, 1984a; Irie *et al.*, 1984b). El coneixement que es té de l'estructura i localització dels subsetis d'unió a fosfats, així com de les propietats cinètiques de l'enzim, demostren que la millor eficiència catalítica observada pels substrats d'elevat pes molecular s'origina per la unió múltiple i cooperativa del substrat amb l'enzim (Cuchillo *et al.*, 1997; Moussaoui *et al.*, 1996).

1.4.2. Accions sobre RNA de doble cadena i DNA-RNA

La RNasa A és pràcticament inactiva en RNA de doble cadena (Barnard, 1969) en les condicions fisiològiques que estabilitzen l'estructura secundària dels àcids nucleics. Sota aquestes condicions però, la ribonucelasa bovina seminal, proteïna homodimèrica que pertany a la superfamília de la RNasa A, (BS-RNasa, Matousek *et al.*, 1973) presenta activitat enfront RNA de doble cadena i enfront a complexes poli(A)-poli(U) (Libonati i Floridi, 1969) i cadenes híbrides de DNA-RNA (Taniguchi i Libonati, 1974). Cal destacar que dímers de la RNasa A obtinguts per liofilització (Libonati, 1969) són capaços de degradar RNA de doble cadena i híbrids de DNA-RNA (Libonati 1975a). Malgrat tot, la capacitat de degradar RNA de doble cadena no depèn necessàriament de l'existència d'una estructura dimèrica ja que la ribonucleasa pancreàtica humana (HP-RNasa) que presenta estructura monomèrica té la capacitat de degradar

tant RNA de cadena senzilla com doble cadena en condicions fisiològiques (Sorrentino i Libonati, 1997; Libonati i Sorrentino, 2001; Sorrentino *et al.*, 2003). Els determinants estructurals d'aquesta activitat peculiar s'han atribuït a la desestabilització local de l'estructura secundària dels àcids nucleics induïda per l'enzim. Aquest efecte s'ha relacionat amb el nombre i disposició de càrregues positives dins de l'HP-RNasa i la seva interacció amb el substrat polianiònic de doble hèlix (Sorrentino *et al.*, 2003).

1.4.3. Propietats alostèriques

Tot i que la BS-RNasa és capaç de trencar enllaços de dinucleòtids com a substrats de la primera reacció, on s'obté una cinètica tipus Michaelià (Piccoli *et al.*, 1982), en la hidròlisis de 2',3'-fosfats cíclics (productes de la primera reacció i substrats de la segona) s'obté una corba cinètica d'aspecte diferent. A baixes concentracions, el substrat indueix cooperativitat negativa, mentre que a elevades concentracions aquest mateix substrat genera cooperativitat positiva. Aquest enzim presenta cooperativitat mixta, amb un pronunciat esglaó en la corba de saturació de substrat, localitzat en el rang de concentracions entre la cooperativitat positiva i negativa. Aquestes propietats alostèriques només s'observen en la forma que presenta intercanvi de dominis de la BS-RNasa (veure apartat 2.1. de la introducció) i això s'ha relacionat amb la possible existència d'un centre alostèric localitzat en la zona del pèptid xarnera (D'Alessio *et al.*, 1997).

Mitjançant estudis d'interacció enzim-substrat (Donadio *et al.*, 1986), s'ha proposat el següent model del mecanisme alostèric de la BS-RNasa (Piccoli *et al.*, 1988):

a) A baixes concentracions de substrat, l'ocupació d'un dels dos possibles centres actius fa que aquest prengui una conformació de transició que inactiva l'altra centre. Aquesta cooperativitat negativa fa que s'observi la meitat de la reactivitat enzimàtica, malgrat que els subsetis no catalítics romanen actius.

b) A elevades concentracions de substrat, es produeix un segon canvi conformacional que fa possible que el segon centre catalític s'activi, generant-se així la cooperativitat positiva.

2 . RIBONUCLEASES DIMÈRIQUES

2.1. Dimerització per intercanvi de dominis

Moltes proteïnes han evolucionat de la forma monomèrica cap a la forma oligomèrica. Els determinants estructurals que provoquen l'estat oligomèric són molts cops difícils d'identificar ja que solen ser la suma de molts canvis petits i sobtats. Malgrat tot, l'anàlisi estructural d'aquests oligòmers, pot ajudar a comprendre quins són aquests determinants i per tant servir de base pel disseny de noves estructures oligomèriques.

L'intercanvi de dominis (Bennett *et al.*, 1995; Heringa i Taylor 1997) és un mecanisme pel qual dues o més molècules formen un dímer o oligòmer intercanviant un domini sencer i idèntic entre les subunitats que el constitueixen. Aquest tipus d'associació té un interès especial ja que es genera tant en mecanismes d'oligomerització reversible com en oligomeritzacions patològiques irreversibles com són la formació de fibres amiloides. Per fer més entenedora la descripció resulta útil dividir la molècula monomèrica de RNasa en tres regions; un domini intercanviat, un pèptid xarnera, i un domini principal. La Figura 1.3. presenta una descripció més gràfica d'aquesta simplificació estructural. El domini intercanviat es plega sobre el domini principal de la subunitat veïna de la mateixa manera com ho faria en el monòmer original i pot correspondre tant a un domini globular com a un o varis elements d'estructura. El pèptid xarnera és un segment de cadena polipeptídica que uneix el domini intercanviat amb el domini principal. Aquest pèptid adopta diferents conformacions segons es trobi en el monòmer o en el dímer que presenta intercanvi de dominis. La interacció entre els dos dominis es dóna a través de dues interfícies: una interfície primària o tancada definida com aquelles interaccions entre dominis que també es produeixen a la forma monomèrica i una interfície secundària o oberta que correspondria a aquelles noves interaccions que s'estableixen únicament en la forma oligomèrica (Figura 1.3. A i B).

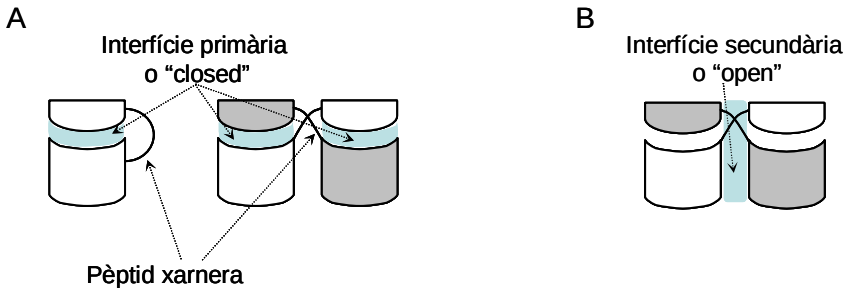

Figura 1.3.: Representació esquemàtica dels principals termes que defineixen l'intercanvi de dominis. A. En l'intercanvi de dominis, el domini intercanviat adopta la mateixa conformació que en el monòmer original però no així el pèptid xarnera. La interfície primària és el conjunt d'interaccions que es produeixen entre el domini intercanviat i el domini principal que existeixen tant en la forma oligomèrica com en el monòmer. **B.** La interfície secundària correspon al conjunt d'interaccions que existeixen només en el dímer que presenta intercanvi de dominis i que no estan presents en el monòmer.

Apart de la BS-RNasa i la RNasa A, fins al moment, s'han descrit més de 40 estructures proteiques que presenten intercanvi de dominis. Aquesta disposició es dóna en proteïnes tan diverses com l'α-espectrina (Yan *et al.*, 1993) (proteïna del citoesquelet), la CksMs2 (Parge *et al.*, 1993) (proteïna reguladora del cicle cel·lular), la nucleasa estafilococal (Green *et al.*, 1995), la proteïna de prió humana (Knaus *et al.*, 2001) o la cistatina C humana (Janowski *et al.*, 2001); aquestes dues últimes relacionades amb la formació de fibres i malalties amiloides.

L'anàlisi de les estructures que presenten intercanvi de dominis caracteritzades fins al moment revela que la majoria d'intercanvis s'observen en els extrems N- i C-terminals**,** tot i que no sempre és així, i que presenten diversitat tant en la seva estructura primària com en la secundària. La diversitat de longitud i de seqüència dels dominis intercanviats indiquen que les interfícies primàries de les proteïnes que presenten intercanvi de dominis són diferents entre elles. A més a més**,** les interaccions que es formen en les interfícies primàries poden ser de diferents tipus des d'interaccions hidrofòbiques a electroestàtiques o fins i tot ponts disulfur (Diederichs *et al.*, 1991; Milburn *et al.*, 1993; Knaus *et al.*, 2001).

2.2. Descripció de les RNases dimèriques

La primera RNasa que es va descriure que podia presentar-se en forma de dímer fou la RNasa A la qual forma estructures dimèriques durant la seva liofilització en presència d'àcid acètic (Crestfield *et al.*, 1962). Estudis posteriors han mostrat l'existència de dos tipus de dímers d'aquesta proteïna, un d'ells més abundant que l'altre (Libonati *et al.*, 1996; Gotte *et al.* 1999). La resolució de les dues estructures dimèriques va revelar que en el dímer minoritari s'intercanvia un domini N-terminal (Liu *et al.*, 1998), mentre que en l'altre tipus de dímer s'intercanvia l'extrem C-terminal de la cadena polipeptídica (Liu *et al.*, 2001). La RNasa A també forma estructures oligomèriques superiors (Gotte *et al.*, 1999a; Gotte *et al.*, 1999b) basades en l'intercanvi simultani de dominis N- i C-terminals: s'ha observat un trímer lineal format per intercanvis N- i C-terminals (Liu *et al.*, 2001) , i un trímer minoritari format per l'intercanvi d'extrems C-terminals que s'ha pogut cristal·litzar (anomenat també trímer cíclic; Liu *et al.*, 2002), també tetràmers (Gotte and Libonati, 2004), pentàmers i hexàmers (Gotte *et al.*, 2005).

L'únic membre de la superfamília de les ribonucleases pancreàtiques que dimeritza de forma natural és la BS-RNasa. Aquesta estructura està estabilitzada covalentment mitjançant dos ponts disulfur. L'estructura tridimensional de la forma dimèrica de la BS-RNasa mostra que cada centre actiu està format per aminoàcids que pertanyen a les dues cadenes polipeptídiques (forma MxM) a través de l'intercanvi de dominis dels seus extrems N-terminals (Mazzarella *et al.*, 1993), tot i que també s'ha caracteritzat una segona forma dimèrica en equilibri amb la forma MxM en la qual els centres actius no estan formats per aminoàcids que pertanyen a les dues subunitats ja que no es produeix intercanvi dels dominis N-terminals (forma M=M) (Piccoli *et al.*, 1992; Kim i Raines, 1993).

Recentment s'ha descrit una variant de l'HP-RNasa anomenada PM8 que incorpora els 20 primers residus de la BS-RNasa a més de la substitució de la Pro101 per una Gln (Canals *et al.*, 1999) l'estructura cristal·logràfica de la qual (Canals *et al.*, 2001) és un dimer basat en l'intercanvi de dominis N-terminals.

Tal i com s'ha comentat abans, el pèptid xarnera presenta una flexibilitat intrínseca que li permet d'adoptar diferents conformacions en el monòmer i en els oligòmers amb intercanvi de dominis. Aquesta flexibilitat es fa evident en la RNasa A, BS-RNasa i PM8. La RNasa A i la BS-RNasa mostren un 80% d'identitat de seqüència i la BS-RNasa i PM8 comparteixen el mateix pèptid xarnera. Totes elles intercanvien el domini N-terminal, però malgrat tot, les orientacions relatives de les seves subunitats en els seus dímers són diferents, generant diferents conformacions pels tres pèptids xarnera (Mazzarella *et al.*, 1993; Liu *et al.*, 1998; Canals *et al.*, 2001). Aquesta flexibilitat també s'observa en el pèptid xarnera C-terminal de la RNasa A ja que la mateixa estructura secundària adopta diferents conformacions en el monòmer, el dimer C-terminal i en el trimer C-terminal d'aquesta proteïna.

2.3. Mecanisme d'intercanvi de dominis

Malgrat que el mecanisme pel qual s'estableix l'intercanvi de dominis roman encara desconegut, si que s'han establert alguns principis per tal que es produeixi aquest intercanvi: a) aquest tipus d'intercanvi és independent de l'estructura primària i secundària de la proteïna; b) el pèptid xarnera i les regions d'interacció són zones molt flexibles tot i que provenen de diferents seqüències i estructures secundàries.

Tampoc és clar si existeix un mecanisme general d'intercanvi de dominis tot i que s'ha plantejat (Bennet *et al.*, 1995) que les proteïnes que dimeritzen per intercanvi de dominis durant el seu procés de plegament, com per exemple l'espectrina, seguirien un camí diferent d'aquelles en les que l'intercanvi es forma a partir d'un monòmer estable per a formar un dímer metaestable, com és el cas de la RNasa A. Per a aquestes, s'ha plantejat que el monòmer estable es sotmetria temporalment a condicions que afavorissin la dissociació del domini a intercanviar, p.e. la liofilització en presència d'àcid acètic. Quan es restablissin les condicions d'estabilització del monòmer es produiria l'intercanvi de dominis, especialment a elevades concentracions de proteïna (Bennet *et al.*, 1995). El cas de la BS-RNasa és especial ja que, tot i que de manera natural és un dímer, s'ha observat que l'intercanvi de dominis es produeix en condicions fisiològiques a partir de monòmers estables però amb la prèvia formació del dímer a partir de l'establiment de dos enllaços disulfur ubicats en la interfície oberta.

S'han comparat les estructures en solució de la RNasa A i la estructura monomèrica de la BS-RNasa ja que poden ajudar a revelar els detalls estructurals que indueixen l'intercanvi d'extrems N-terminals en la BS-RNasa. L'estructura en solució de la forma monomèrica de la BS-RNasa, obtinguda per RMN 3D heteronuclear, mostra una elevada similitud amb la RNasa A en totes les regions caracteritzades per elements regulars de l'estructura secundària. Malgrat tot, s'han observat grans diferències en la flexibilitat del pèptid en el segment 16-22 de les dues proteïnes; postulant-se que aquestes diferències en l'estructura terciària podrien ser les bases moleculars per explicar l'habilitat de la BS-RNasa per intercanviar els seus dominis N-terminals

(Avitabile *et al.*, 2003). Per tal d'identificar els determinants molecular que promouen l'intercanvi de dominis en la BS-RNasa s'ha analitzat l'efecte produït per la substitució de la Pro19, situada en el pèptid xarnera, i la Leu28, localitzada a la interfície secundària, pels corresponents aminoàcids en aquestes posicions presents en la RNasa. S'han comparat les propietats estructurals de la forma monomèrica de les dues variants respecte a la proteïna salvatge, i per altra banda, els canvis cinètics que es produeixen en formar-se els seus corresponents dímers. S'ha observat que la mutació P19A incrementa de forma notable l'estabilitat tèrmica de la proteïna monomèrica, però que no modifica la tendència a l'intercanvi de dominis en el dímer. Per contra, la variant L28Q presenta canvis significatius tant en la dimerització com en l'intercanvi de dominis però no en l'estabilitat tèrmica del monòmer (Ercole *et al.*, 2003). També s'ha observat (Picone *et al.*, 2005) que variants de la BS-RNasa en les que s'ha substituït la Pro19 o la totalitat de la seqüència del pèptid xarnera pels residus corresponents de la RNasa A, presenten una constant d'associació i uns paràmetres cinètics d'intercanvi de dominis similars als obtinguts per la proteïna salvatge. Aquests conjunt de resultats indiquen que el pèptid xarnera no és el responsable de modular l'equilibri en l'intercanvi de dominis i que residus localitzats en el pèptid xarnera (Pro19) i en la interfície secundària (Leu28) semblen actuar de forma cooperativa per tal de potenciar la formació de l'estructura quaternària per intercanvi de dominis (Sica *et al.*, 2004).

2.4. Propietats biològiques dels dímers

Algunes RNases han estat considerades clàssicament com a models per a l'estudi de diferents problemes biològics. L'interès en el seu estudi va renéixer a principis dels anys 90 arran del descobriment que algunes ribonucleases presentaven funcions biològiques especials (RISBASES) (veure apartat 1.3.). Les ribonucleases presenten un ampli rang d'accions biològiques, a més del simple paper digestiu i de la seva participació en el manteniment del contingut cel·lular d'RNA. Per aquesta raó, aquests enzims presenten un important potencial com a agents terapèutics per a determinats desordres humans, incloent el càncer i la SIDA. Per altra banda també tenen la possibilitat de servir com a marcadors moleculars de determinades disfuncions biològiques. Les dues RNases dimèriques que es coneixen: la BS-RNasa i els oligòmers de la RNasa A presenten un ampli ventall de funcions especials que es detallen a continuació.

2.4.1. Propietats biològiques de la BS-RNasa

El paper fisiològic de la BS-RNasa sembla estar relacionat amb un efecte immunosupressor, que protegeix les cèl·lules espermàtiques del fluid seminal del sistema immunitari de l'organisme femella. Amb tot, la BS-RNasa presenta un ampli ventall d'activitats biològiques com són l'aspermatogènesi (Hlinak *et al.*, 1981), l'activitat antitumoral (Matousek i

Grozdanovic, 1973; Vescia *et al.*, 1980), embriotòxica (Matousek i Grozdanovic, 1973), immunosupressiva (Tamburrini *et al.*1990) i antiviral (Youle *et al.*, 1994). S'ha comprovat també que la BS-RNasa exerceix una potent acció citotòxica contra cèl·lules tumorals, tant en experiments *in vitro* com *in vivo*. Les bases d'aquesta activitat citotòxica però, es desconeixen tot i que s'ha demostrat que les activitats són estrictament dependents de l'activitat ribonucleolítica de la proteïna (D'Alessio, 1997) i estan associades només a la forma dimèrica que presenta intercanvi de dominis (Soucek *et al.*, 1996).

2.4.2. Propietats biològiques dels oligòmers de la RNasa A

La RNasa A nativa, monomèrica, no presenta cap activitat biològica, tot i que fa uns 50 anys, Ledoux va comunicar que aquest enzim (administrat a elevades concentracions) presentava activitat citotòxica pels carcinomes de Ehrlich i Krebs en ratolins i Walker en rates (Ledoux, L., 1955 a i b). Però en canvi, els oligomers de la RNasa A adquireixen una remarcable activitat antitumoral i aspermatogènica. (Matousek *et al.*, 2003). Aquest fet, avui per avui, no sorprèn si es té en compte que dimers estabilitzats covalentment (Bartholeyns i Baudhuin, 1976; Tarnowski et al 1976) i trímers (Gotte *et al.*, 1997) de RNasa A, igualment que la RNasa A monomèrica conjugada amb polietilenglicol (Matousek *et al.*, 2002), presenten activitat citotòxica enfront diferents tipus de cèl·lules tumorals. A més a més, els dímers i oligòmers superiors de la RNasa A poden tenir la mateixa activitat antitumoral i aspermatogènica que la BS-RNasa, amb qui comparteix en un 80% d'homologia de seqüència (D'Alessio *et al.*, 1997; Youle *et al.*, 1997).

3. RIBONUCLEASES AMB PROPIETATS ANTITUMORALS

D'entre les funcions biològiques especials que presenten algunes ribonucleases de la família de la RNasa A, ja s'ha destacat la seva activitat antitumoral. Es coneixen quatre RNases que tenen activitat citotòxica específica per a cèl·lules tumorals. Aquestes són l'onconasa, la BS-RNasa, i les lectines de *Rana Catesbeiana* i *Rana japonica*. L'estudi d'aquestes RNases ha permès el desenvolupament de noves RNases dissenyades per a tenir una acció citotòxica amb interès clínic com a substitut o complement dels agent quimioterapèutics d'ús estàndard.

3.1. Bases moleculars del mecanisme de citotoxicitat

Tot i que molts aspectes de les bases moleculars de la citotoxicitat de les RNases romanen encara desconeguts en un grau important, els estudis realitzats tant amb RNases citotòxiques, com l'onconasa (Darzynkiewicz *et al.*, 1988) o la BS-RNasa (Matousek *et al.*, 1973), o no

citotòxiques, com ara la RNasa A, a més de variants citotòxiques d'aquestes, han permès l'establiment d'un model d'acció que és generalment acceptat. Aquest model postula que, per tal d'exercir la citotoxicitat, cal la interacció de la RNasa amb la membrana cel·lular i la seva internalització per endocitosi, amb una posterior translocació al citotsol, on la degradació del RNA cel·lular induiria la mort cel·lular per apoptosi. L'eficiència amb la qual una RNasa pot superar cada una d'aquestes etapes es pot correlacionar amb la seva potència com a agent citotòxic.

A continuació es descriu el que es coneix sobre cadascuna de les etapes que proposa aquest model.

3.1.1. Unió a la superfície cel·lular i endocitosi

Com a pas previ a la internalització, la RNasa interacciona amb la membrana cel·lular de la cèl·lula diana. El mecanisme d'interacció no ha estat encara del tot dilucidat, i per moltes RNases és encara desconegut. En alguns casos hi ha indicis de què es produeix de manera específica, mitjançant receptors de membrana, o bé mitjançant interaccions electrostàtiques amb components de la bicapa.

En el cas de la BS-RNasa, s'ha descrit l'existència d'un receptor específic a la matriu extracel·lular dels fibroblasts de ratolí Balb/C3T3 la unió al qual és necessària per a la citotoxicitat de l'enzim (Mastronicola *et al.*, 1995). No s'ha pogut demostrar la presència d'un receptor específic a la membrana cel·lular, i algunes dades suggereixen que la interacció amb la membrana es podria produir per un mecanisme d'adsorció, enlloc de mediada per receptor (Kim *et al.*, 1995). S'ha proposat també un mecanisme alternatiu, segons el qual la BS-RNasa interacciona amb la membrana plasmàtica a través dels grups sulfidril de la superfície cel·lular (Bracale *et al.*, 2003).

En el cas de la onconasa, l'existència d'un receptor específic és controvertida, i probablement depèn de la línia cel·lular assajada. Per una banda, s'ha descrit l'existència d'un receptor de membrana específic en cèl·lules de glioma 9L (Wu *et al.*, 1993). Tot i que no s'ha pogut encara determinar la seva naturalesa, el fet que la competència amb àcid siàlic o altres sucres simples, així com el tractament amb neuramidasa, no comprometin la citotoxicitat de l'onconasa apunten a un receptor diferent del caracteritzat per les lectines aïllades de *Rana catesbeiana* i *Rana japonica* (jSBL, cSBL; Nitta *et al.*, 1987; Sakakibara *et al.*, 1979). Per altra banda, el fet que la internalització de l'onconasa no sigui saturable en cèl·lules HeLa (Haigis i Raines, 2003) ni es vegi afectada per tractaments amb proteases posa en qüestió l'existència d'un receptor proteic, almenys en aquesta línia cel·lular.

Hi ha indicis que apunten que la interacció amb la membrana pot ser de tipus electrostàtic. Les RNases citotòxiques comparteixen un caràcter bàsic, i s'ha descrit que la cationització incrementa l'eficiència d'internalització de cSBL (Iwama *et al.*, 2001; Ogawas *et al.*, 2002).

Aquest augment en l'eficiència d'internalització ha estat interpretada com que aquestes RNases estableixen interaccions electrostàtiques amb la superfície cel·lular, carregada negativament. A més, estudis d'internalització en les línies cel·lulars A431 i K562 de variants citotòxiques de l'RNasa A i l'HP-RNasa (Haigis i Raines, 2003; Bosch *et al.*, 2004), apunten a què aquestes s'internalitzen per endocitosi en fase fluida.

La fusió de RNases citotòxiques a lligands de membrana com la transferrina, factors de creixement o anticossos potencien la seva internalització cel·lular, cosa que es tradueix en l'adquisició de propietats citotòxiques (Rybak i Newton, 1999). En conjunt, es pot afirmar que una diferència important entre les RNases citotòxiques i les no citotòxiques és l'habilitat de les primeres per interaccionar de manera específica amb les cèl·lules.

Després de la unió a la superfície cel·lular, és necessària la internalització, la qual es produeix per un mecanisme que resta encara per identificar. Aquesta necessitat ve il·lustrada pel fet que, quan la interacció d'una RNasa amb la membrana cel·lular no ve seguida de la seva internalització, l'enzim no provoca la mort cel·lular. De fet, s'ha observat el desenvolupament, en cèl·lules de leucèmia P388, d'una resistència a l'exposició continuada a cSBL, aparentment deguda a un mecanisme defectiu d'internalització (Nitta *et al.*, 1994b). La BS-RNasa (Bracale *et al.*, 2002), l'onconasa (Haigis i Raines, 2003) i una variant citotòxica de l'HP-RNasa (Bosch *et al.*, 2004) s'han localitzat en endosomes, i en varis d'aquests casos s'ha demostrat que la seva citotoxicitat es veu compromesa amb la inhibició del procés d'endocitosi depenent d'energia (Haigis *et al.*, 2002, Bracale *et al.*, 2002; Wu *et al.*, 1995). En el cas de l'onconasa i variants citotòxiques de l'RNasa A s'ha descrit que l'endocitosi segueix una ruta independent de clatrina i dinamina (Haigis i Raines, 2003).

3.1.2. Trànsit intracel·lular

Tot i que comparativament no s'han observat diferències en el grau d'internalització de la BS-RNasa en diferents línies cel·lulars, la seva citotoxicitat és més important sobre línies cel·lulars tumorals (Mastronicola *et al.*, 1995; Vescia *et al.*, 1980, Youle i D'Alessio, 1997). Aquest fet planteja la possibilitat que una RNasa pugui seguir diferents rutes intracel·lulars, d'entre les quals només algunes permetrien el trànsit fins al citosol. Per tal de dilucidar el camí seguit per diferents RNases citotòxiques entre els endosomes i el citosol s'han realitzat dues aproximacions diferents.

En primer lloc, s'ha comparat la citotoxicitat d'aquestes RNases en presència de diferents drogues que actuen desorganitzant el transport intracel·lular. Els resultats obtinguts amb l'onconasa suggereixen que el camí seguit exclou el reticle endoplasmàtic i l'aparell de Golgi (Haigis i Raines, 2003; Wu *et al.*, 1995; Newton *et al.*, 1998) i la seva internalització a diferència d'altres drogues citotòxiques, com ara la toxina colèrica, és aparentment independent d'un pH àcid en les vesícules que transporten l'enzim (Haigis i Raines, 2003).

Un segon enfoc es basa en la colocalització, amb marcadors específics per orgànuls cel·lulars, de RNases marcades fluorescentment. Amb aquesta metodologia s'ha demostrat que la internalització de l'onconasa es realitza a través d'endosomes acídics (Haigis i Raines, 2003), mentre que la BS-RNasa s'ha localitzat a la xarxa trans-Golgi de cèl·lules malignes tractades, cosa que suggereix que aquest orgànul podria actuar com a lloc efectiu de la translocació de la BS-RNasa (Bracale *et al.*, 2002). Mitjançant aquesta segona aproximació ha estat possible determinar la localització d'una variant citotòxica d'HP-RNasa en endosomes acídics/lisosomes però no s'ha localitzat ni en el reticle endoplasmàtic ni a l'aparell de Golgi de cèl·lules A431 (Bosch *et al.*, 2004).

3.1.3. Translocació a través de la membrana lipídica

La RNasa A té activitat citotòxica només en el cas de ser microinjectada directament al citoplasma, tal com s'ha determinat amb oòcits de granota (Saxena *et al.*, 1991; Rybak *et al.*, 1991), cosa que indica la necessitat d'un mecanisme de translocació de la RNasa cap al citoplasma des d'un determinat compartiment subcel·lular.

En el cas de la BS-RNasa s'ha observat com la forma dimèrica, que a diferència de la monomèrica és citotòxica, presenta la capacitat d'alterar i penetrar membranes artificials amb fosfolípids carregats negativament (Mancheño *et al.*, 1994). Tot i això, no s'ha determinat encara la manera com les RNases citotòxiques, altament estables i hidrofíliques, aconsegueixen arribar al citosol des de l'orgànul a través del qual penetren a la cèl·lula. Altres toxines, com ara la ricina, l'exotoxina A de *Pseudomonas* o la toxina de la diftèria, presenten dos dominis diferenciats, un amb activitat catalítica i un altre amb la capacitat de travessar determinades membranes biològiques. Diferents fets indiquen que aquestes toxines penetren al citoplasma a través dels complexes de translocació proteica. Per una banda s'ha comprovat que interaccionen amb Sec61, una proteïna que constitueix part del complex responsable de la translocació de proteïnes a través de la membrana del reticle endoplasmàtic (Schmitz *et al.*, 2000). A més a més s'ha descrit que aquestes toxines pateixen un procés de desplegament per tal d'arribar al citosol (Argent *et al.*, 1994). Diversos factors indiquen que les RNases citotòxiques utilitzen un mecanisme diferent per travessar la bicapa lipídica. Per una banda, les rutes intracel·lulars que s'han determinat per a diverses RNases citotòxiques, en cap cas comprenen un trànsit pel reticle endoplasmàtic. De fet, quan s'ha buscat direccionar la BS-RNasa cap a aquest compartiment mitjançant l'addició, al seu extrem C-terminal, de la seqüència consens de direccionalització a reticle endoplamàtic, KDEL, aquesta variant perd bona part de la seva citotoxicitat (Bracale *et al.*, 2002). En segon lloc, el fet que s'hagi observat una correlació entre l'estabilitat conformacional (i per tant la resistència al desplegament) i la citotoxicitat observada per diferents variants de la RNasa A (Klink i Raines, 2000; Leland *et al.*, 2001) indica que les RNases no són transferides al citoplasma de forma desplegada. Aquesta correlació es deu

probablement a una major resistència d'aquestes a les proteases intracel·lulars i extracel·lulars deguda a la major resistència al desplegament.

3.1.4. Acció al citosol

Un cop en el citosol, les RNases actuen sobre el RNA de la cèl·lula, degradant-lo. S'ha observat que RNases citotòxiques perden aquesta capacitat en ser privades de la seva activitat RNasa, bé sigui mitjançant modificacions químiques (Wu *et al.*, 1995; Vescia *et al.*, 1980), o bé sigui per mutagènesi dirigida sobre els residus implicats en el procés de catàlisi (Kim *et al.*, 1995).

Les cèl·lules de vertebrat posseeixen un inhibidor proteic de RNases, el RI (Wu *et al.*,1993; Lee i Valle, 1993), que és capaç d'actuar sobre un ventall ampli de membres de la superfamília de les RNases pancreàtiques. Aquest presenta una estructura formada per 15 repeticions de motius β-α riques en leucina, disposades en forma de ferradura (Kobe i Deisenhofer, 1993). Té la capacitat d'unir-se específicament a l'HP-RNasa (Boix *et al.*, 1996), RNasa A i angiogenina (Lee *et al.*, 1989) amb una relació estequiomètrica 1:1, i presentant constants de dissociació de l'ordre de fM (Lee *et al.*, 1989; Vicentini *et al.*, 1990). L'elevada inhibició de l'activitat RNasa és deguda a què alguns dels residus importants en la unió entre el RI i la RNasa estan implicats en l'activitat catalítica de l'enzim (Kobe i Deisenhofer, 1996). Es postula que el RI serviria com a mecanisme per evitar que les RNases extracel·lulars puguin penetrar accidentalment al citosol i realitzar-hi la seva acció degradadora.

El fet que les lectines d'amfibi, l'onconasa i la BS-RNasa no resultin inhibides pel RI ha portat a suggerir que l'evasió al RI és un requisit necessari per tal que una RNasa sigui citotòxica, però aquesta hipòtesi és controvertida.

L'estudi de RNases amb citotoxicitat natural, així com variants citotòxiques obtingudes a partir de RNases no citotòxiques, ha permès establir tres estratègies per a l'evasió al RI.

a) Disminució de l'afinitat per l'RI. Una baixa afinitat entre la RNasa i el RI es tradueix en una baixa inhibició. L'onconasa presenta una constant de dissociació del complex que forma amb l'inhibidor unes 10^7 vegades superior que el valor trobat per la RNasa A (Boix *et al.*, 1996), cosa que li permet evadir l'acció del RI *in vitro*. El fet que un increment dels nivells citoplasmàtics de RI (Iwama *et al.*, 2001) no tingui cap tipus d'efecte en el grau de citotoxicitat de l'onconasa apunta a què aquesta evasió també es dóna *in vivo*, cosa que permetria la degradació del RNA cel·lular.

En el cas de la BS-RNasa, la interacció entre la forma dimèrica citotòxica i el RI no es pot establir a causa dels impediments estèrics derivats de la dimerització. Aquesta estructura dimèrica es manté durant la internalització de la BS-RNasa (Bracale *et al.*, 2003), i també sembla ser important en el trànsit a través de la bicapa lipídica (Mancheño *et al.*, 1994), però el manteniment del caràcter dimèric de la BS-RNasa al citosol no és clar. De fet, en cèl·lules amb

el RI silenciat s'observa una major sensibilitat a la BS-RNasa (Monti i D'alessio, 2004), cosa que indica que el RI actua en certa mesura inhibint la seva acció. Les condicions reductives del citosol podrien derivar en una dissociació de la forma dimèrica citotòxica, generant-se així monòmers lliures que serien inhibits. Els monòmers estables de BS-RNasa, obtinguts mitjançant la reducció selectiva dels ponts disulfur que uneixen les dues subunitats i la posterior alquilació dels sulfidrils lliures, són sensibles al RI i no resulten citotòxics (Kim *et al.*, 1995; Murthy *et al.*, 1996).

Mitjançant mutagènesi dirigida per oligonucleòtid s'han obtingut variants de la RNasa A i HP-RNasa en les quals s'han modificat residus implicats en la unió al RI (Leland *et al.*, 2001; Leland *et al.*, 1998), i alternativament s'han generat formes dimèriques d'aquestes RNases (Di Donato *et al.*, 1994; Di Gaetano *et al.*, 2001; Piccoli *et al.*, 1999) que no poden unir-se al RI per impediments estèrics. Mitjançant les dues estratègies s'han obtingut variants que són capaces d'evadir el RI i que són citotòxiques. L'afebliment posterior de la unió amb l'inhibidor introduint noves mutacions s'ha traduït en un augment de la citotoxicitat d'aquestes noves variants (Haigis *et al.*, 2002).

b) Saturació del RI. El RI citoplasmàtic representa entre el 0.01 i el 0.1% del contingut proteic total de la cèl·lula (Lee i Valle, 1993). En el cas que una quantitat suficient de RNasa penetri al citoplasma, es pot produir la saturació de la totalitat del RI, de manera que les noves RNases que penetressin a la cèl·lula podrien lliurement exercir la seva acció degradadora sobre el RNA cel·lular. D'aquesta manera es podria explicar la citotoxicitat d'algunes variants de RNasa que es troben unides, bé sigui químicament, bé per enginyeria genètica, a lligands específics de receptors de cèl·lules tumorals i que són inhibides *in vitro* en presència de RI. En aquestes, la presència d'aquests lligands assegura que en ser aplicades sobre cèl·lules tumorals es produeixi una internalització suficientment eficient per saturar l'inhibidor intracel·lular. Relacionat amb això, s'ha observat en cèl·lules de glioma 9L pretractades amb àcid retinoic que l'aplicació de l'HP-RNasa o l'angiogenina, les quals no són habitualment citotoxiques, provoca la mort d'aquestes cèl·lules (Wu *et al.*, 1995). L'aplicació d'àcid retinoic provoca la desorganització de l'aparell de Golgi, cosa que pot facilitar l'arribada d'aquestes proteïnes al citosol a través d'aquest orgànul.

c) *Unió a altres molècules que obstaculitzen la captura de la RNasa per part del RI.* El citoplasma és un ambient altament concentrat en diferents tipus de biomolècules, en el qual la interacció entre RNases i RI observada *in vitro* no necessàriament s'ha de donar amb la mateixa eficiència. La unió de RNases a d'altres molècules ha permès, en dos casos evitar la seva captura per part del RI.

S'ha observat que en el cas de la BS-RNasa, la seva unió al RNA pot ajudar en l'evasió al RI. De fet, existeixen dues formes dimèriques de la BS-RNasa, que són interconvertibles. Una d'elles es troba estabilitzada per dos enllaços disulfur entre les dues subunitats (forma M=M), mentre que l'altra presenta, a més a més, l'intercanvi del domini N-terminal (forma MxM). En l'ambient reductor del citoplasma, la forma M=M monomeritza i pot ser inhibida pel RI, mentre que la forma MxM es pot mantenir per les interaccions no covalents dels dominis intercanviats. De totes maneres, com que les formes M=M i MxM es troben en equilibri, i l'ambient reductor assegura la desaparició de la forma M=M, per la llei d'acció de masses també s'hauria de produir una progressiva desaparició de la forma dimèrica MxM. De totes maneres, la unió de la forma MxM al RNA l'estabilitza, impedint la seva conversió en la forma M=M (Murthy *et al.*, 1996; Murthy i Sirdeshmukh, 1992).

En el grup de recerca en el qual s'ha portat a terme aquesta tesi, s'ha obtingut una variant citotòxica de HP-RNasa sensible a l'RI, anomenada PE5 (Bosch *et al.*, 2004), la qual presenta un grau de citotoxicitat equivalent a la d'altres variants no inhibides pel RI (Leland *et al.*, 2001). Aquesta variant incorpora els canvis G89R i S90R, els quals la doten d'una senyal de localització nuclear (NLS) que la dirigeix al nucli, on no s'ha detectat la presència de RI (Roth i Juster, 1972), de manera que pot desenvolupar la seva activitat RNasa. La zona d'interacció entre PE5 i la importina, membre de la maquinària de transport nuclear, comprèn residus implicats en la unió al RI, de manera que en el citosol s'estableix una competència entre la importina i el RI per unir-se a PE5. El fet que aquesta variant presenti un lleuger escapament al inhibidor permet que petites quantitats d'aquesta RNasa restin capturables per la importina; la qual, per altra banda es troba molt més concentrada. La translocació de la RNasa al nucli produeix una disminució de la forma lliure disponible, cosa que afavoreix la dissociació del complex amb el RI i una acumulació progressiva al nucli, principalment al nucleol (Bosch *et al.*, 2004).

3.1.5. Mecanisme de mort cel·lular.

Tot i que el substrat comú a les RNases citotòxiques sigui el RNA intracel·lular i que *in vitro* aquestes degradin amb la mateixa intensitat rRNA i tRNA, s'han observat preferències en la naturalesa del RNA degradat *in vivo*. Així, mentre que la BS-RNasa i la cSBL actuen preferentment sobre rRNA (Mastronicola *et al.*, 1995; Liao *et al.*, 1996), l'onconasa degrada tRNA sense afectar el rRNA ni el mRNA (Lin *et al.*, 1994; Saxena *et al.*, 1996; Saxena *et al.*, 2002; Iordanov *et al.*, 2000a). Les diferents especificitats es poden deure a la localització subcel·lular de les diferents RNases i RNA, a l'acció protectora de les diferents proteïnes que podem trobar unides al RNA o a possibles modificacions de les RNases en el citosol. En tot cas, la degradació del RNA cel·lular té com a conseqüència l'aturada de la síntesi proteica i la inducció de l'apoptosi en les cèl·lules afectades. La via a través de la qual s'indueix l'apoptosi

roman encara per dilucidar, però presenta també certes diferències segons quina sigui la RNasa citotòxica inductora del procés, i fins i tot, en el cas de l'onconasa, la inhibició de la síntesi proteica sembla no ser l'únic desencadenant d'aquest procés. En aquest cas s'ha suggerit que l'onconasa podria actuar sobre RNA no codificant, com ara els siRNA o els microRNA, els quals funcionen com a reguladors de l'expressió gènica (Ardelt *et al.*, 2003).

3.2.Especificitat antitumoral

No es coneix la causa per la qual aquestes RNases presenten especificitat vers les cèl·lules tumorals. Per una banda, s'ha plantejat la possibilitat que interaccionin preferentment amb la membrana de les cèl·lules tumorals ja que s'ha descrit que aquestes presenten a la superfície de la membrana una major densitat de càrregues negatives (Kojima, 1993). El caràcter més aniònic de la membrana cel·lular potenciaria l'adsorció de les RNases citotòxiques, que tenen un marcat caràcter bàsic. Tot i això, en el cas de la BS-RNasa no s'observen diferències en el grau d'unió a la membrana entre cèl·lules normals i cèl·lules tumorals (Mastronicola *et al.*, 1995; Vescia *et al.*, 1980). Per altra banda, la selectivitat es pot explicar en base a diferències en la ruta intracel·lular seguida durant la internalització, que en el cas de cèl·lules tumorals facilitaria la translocació al citosol. També en el cas de la BS-RNasa, s'ha observat com aquesta apareix en les cisternes trans-Golgi de cèl·lules tumorals, mentre que aquesta localització no es dóna en cèl·lules normals (Bracale *et al.*, 2002). Finalment, aquesta especificitat es podria explicar per l'existència de diferències en la sensibilitat de les cèl·lules tumorals a la degradació del RNA respecte de les cèl·lules normals.

Tot i la toxicitat renal que genera (Vasandani *et al.*, 1996; Vasandani *et al.*, 1999), l'onconasa es troba en fase III d'assajos clínics per al tractament de mesotelioma maligne. Actualment, les RNases, especialment la RNasa A i la HP-RNasa, es troben en la base del desenvolupament de nous fàrmacs antitumorals. El coneixement del mecanisme d'acció de les RNases citotòxiques, així com de les característiques implicades en aquesta activitat, ha de repercutir en el desenvolupament de noves drogues que ajudin a combatre el desenvolupament de processos cancerígens minimitzant els efectes secundaris.

4. OBJECTIUS

L'estudi dels membres de la superfamília de les ribonucleases de tipus pancreàtic ha permès descobrir que alguns d'aquests presenten activitats biològiques especials, en aparença allunyades de la seva funció biològica principal relacionada amb la degradació del RNA, bé sigui com a part del processament i renovació del RNA cel·lular, bé sigui amb funcions digestives. Aquestes funcions atípiques inclouen les activitats antimicrobiana, antivírica, antihelmíntica, angiogènica, aspermatogènica, embriotòxica i immunosupressora. A més d'aquestes, destaca pel seu interès l'activitat antitumoral, que ha obert el camí a la possibilitat d'utilitzar les ribonucleases com a agents terapèutics en la lluita contra el càncer.

Molts dels factors moleculars que determinen la capacitat tòxica de les ribonucleases romanen encara desconeguts. S'accepta que el procés s'inicia amb la unió de l'enzim a la superfície cel·lular, seguit de la seva endocitosi i la seva translocació al citoplasma. Un cop en el citosol, l'enzim haurà de superar l'activitat inhibidora del inhibidor citoplàsmatic de ribonucleases (RI) per tal de dur a terme la degredació de l'RNA, induint així la mort cel·lular.

Els objectius generals del grup de recerca d'Enginyeria de Proteïnes, on s'ha dut a terme aquest treball, són per una banda aprofundir en les bases moleculars de la toxicitat d'aquestes ribonucleases i per l'altra el disseny de noves variants de la HP-RNasa amb activitat antitumoral. La generació de variants de HP-RNasa amb propietats similars a les descrites per a altres ribonucleases d'origen no humà (com l'onconasa i la BS-RNasa) ofereix la possibilitat de desenvolupar nous agents quimioterapèutics que, en humans probablement mostrarien una millor tolerància immunològica.

En els darrers anys, diferents grups han construït mitjançant enginyeria de proteïnes, variants de la RNasa A o de la HP-RNasa que han estat dissenyades per tal que aquests enzims adquireixin propietats citotòxiques. Aquestes modificacions confereixen a la molècula o bé una major capacitat d'internalització (Rybak i Newton, 1999) o bé la capacitat d'escapar al RI (Leland et al., 1998; Leland et al., 2001; Piccoli et al., 1999). L'obtenció, per part del nostre grup, d'una variant de la HP-RNasa, anomenada PE5, que no evadeix l'RI tot i ser citotòxica, pot haver obert el camí a una nova estratègia de construcció de RNases antitumorals. La seqüència de PE5 conté una senyal de localització nuclears (NLS) atípica, la qual li permet transitar fins al nucli cel·lular mitjançant la unió a unes proteïnes específiques de transport nuclear anomenades importines. Es postula que la base molecular del comportament citotòxic de PE5 radica en què les importines competeixen amb l'RI per unir-se a PE5. Així, part de la fracció de molècules de PE5 que assolirien el citoplasma serien transportades al nucli, on no hi ha RI, sense estar complexades amb aquest. Com a conseqüència de la desaparició de molècules del citoplasma, l'equilibri entre la HP-RNasa lliure i la HP-RNasa complexada amb el RI es desplaçaria cap a la

primera forma. Un cop al nucli, la degradació del RNA nuclear induiria la mort cel·lular.
Una altra estratègia d'obtenció de ribonucleases que presenten activitat citotòxica consisteix en dotar a aquestes proteïnes d'estructura quaternària com és el cas de la BS-RNasa (D'Alessio et al., 1997) o dímers artificials de la HP-RNasa o de la RNasa A (Catanzano et al., 1997; Piccoli et al., 1999). L'obtenció en el grup de la variant de la HP-RNasa denominada PM8 (Canals et al., 2001) que presenta una estructura cristal·logràfica dimèrica amb intercanvi de dominis N-terminals va fer pensar en la possibilitat de què aquesta nova variant pogués ésser utilitzada com a proteïna citotòxica.

En base als antecedents esmentats, els objectius d'aquest treball foren:

1. Estudi de la ruta endocítica de l'onconasa, una ribonucleasa d'origen amfibi que, per la seva elevada citotoxicitat i gràcies a l'elevada selectivitat enfront de cèl·lules tumorals es troba actualment en fase III d'assajos clínics per al tractament de determinats tipus de neoplàsies. Aquesta ribonucleasa ha esdevingut un model en els estudis de la citotoxicitat de les RNases.

2. Identificació dels residus importants per la seqüència de localització nuclear present en PE5.

3. Obtenció d'una variant dimèrica estable de PM8 per tal de poder avaluar el seu potencial com a proteïna citotòxica.

4. Caracterització del procés de dimerització per intercanvi de dominis N-terminals de la variant humana, PM8.

5. Caracterització cinètica de la HP-RNasa i d'una variant dimèrica utilitzant diferents substrats per a l'estudi del seu patró de trencament.

Resultats i Discussió

Capítol I:

FROM COATED PITS TO THE RECYCLING COMPARTMENT: THE INTERNALIZATION PATHWAY OF ONCONASE

FROM COATED PITS TO THE RECYCLING COMPARTMENT: THE INTERNALIZATION PATHWAY OF ONCONASE

Montserrat Rodríguez, Gerard Torrent, Fabienne Rayne*, Jean-François Dubremetz*, Marc Ribó, Antoni Benito, Maria Vilanova and Bruno Beaumelle*

Laboratori d'Enginyeria de Proteïnes, Departament de Biologia, Facultat de Ciències, Universitat de Girona, Campus de Montilivi s/n E-17071 Girona, Spain
*UMR 5539 CNRS, Département Biologie-Santé, Université Montpellier II, 34095 MONTPELLIER Cedex 05, France.

Total number of words ~ 5800.

Short title: Onconase internalization pathway

Key words: Onconase, RNase, coated pits, recycling endosomes, endocytosis, translocation.

Corresponding author:

Bruno Beaumelle
UMR 5539 CNRS
Case 107
Université Montpellier II
34095 MONTPELLIER Cedex 05
France

Tel + 33.467.14.33.98 Fax +33.467.14.42.86

Email: beaumel@univ-montp2.fr

Summary

Onconase® is an RNase with a very specific property since it is selectively toxic to transformed cells. Onconase is thought to recognize cell surface receptors. Moreover, the protection confered by metabolic poisons against Onconase toxicity indicated that this RNase relies on endocytic uptake to kill cells. Nevertheless, the Onconase internalization pathway has yet to be unraveled. We show here that Onconase enters cells using AP-2/ clathrin mediated endocytosis. It is then routed, together with transferrin, to the receptor recycling compartment. Increasing the Onconase concentration in this structure using tetanus toxin light chain expression enhanced Onconase toxicity, indicating that recycling endosomes are a key compartment for Onconase cytosolic delivery. This intracellular destination is specific to Onconase since other (and much less toxic) RNases follow the default pathway to late endosomes/lysosomes. Neutralization of endosomal pH strongly enhances Onconase toxicity (up to 100-fold), probably by facilitating its access to the cytosol.

Introduction

Onconase® (Onco) is an interesting member of the RNase superfamily since it is an anticancer molecule. Indeed, this amphibian RNase was shown to be cytotoxic to transformed cells (Darzynkiewicz et al., 1988) and to possess potent in vivo antitumour activity (Mikulski et al., 1990). Onco can be used in synergy with standard chemotherapeutic agents (Rybak and Newton, 1999) and is currently undergoing phase III clinical trials for the treatment of malignant pleural mesothelioma (Favaretto, 2005). One of the most most relevant features of Onco is that it provides a non-mutagenic alternative to the conventional DNA-damaging cancer therapy (Costanzi et al., 2005; Favaretto, 2005).

Onco toxicity is thought to result from its ability to degrade tRNAs (Saxena et al., 2002), although alternative substrate candidates have been proposed (Ardelt et al., 2003). This multi-targeted effect of Onco might explain its synergistic interactions with other chemotherapeutic agents (Rybak and Newton, 1999). Earlier steps of the Onco intoxication procedure, i.e. intracellular routing which enables its delivery to the cytosol, remains elusive. Pioneer studies showed that Onco binding to cells was saturable and likely involved membrane receptors. Metabolic poisons were found to protect cells against Onco toxicity, indicating that this toxin does not access the cytosol by direct transport across the plasma membrane, and that endocytosis is required for cytotoxicity (Wu et al., 1993).

Several receptors enter cells using clathrin-mediated endocytosis (CME). These receptors interact with adaptors that also bind to clathrin, enabling receptor sequestration within coated pits (Conner and Schmid, 2003). Quantitatively, adaptor protein complex-2 (AP-2) is the major adaptor involved in CME (Traub, 2003). Several proteins are required for this process. For instance, Eps15, which is constitutively associated with AP-2, is needed for endocytosis of the transferrin (Tf) receptor, which is the paradigm for receptors entering cells by AP-2 mediated CME (Benmerah et al., 1999). Some CME effectors are also involved in other endocytosis pathways, such as caveolae-mediated uptake. This is the case for intersectin (Predescu et al., 2003) and dynamin II (Henley et al., 1998). The latter protein is a GTPase that enables fission of endocytic buds from the plasma membrane to generate a free vesicle (Conner and Schmid, 2003). GTP hydrolysis by dynamin is required for vesicle scission and the involvement of dynamin in internalization processes is usually studied using the dynamin-K44A

mutant that has a weak affinity for GTP and acts in a dominant negative manner (Damke et al., 1994). Most ligand uptake pathways studied so far, with the exception of GPI-anchored protein internalization, were found to be dynamin-dependent (Parton and Richards, 2003). Regarding Onco, toxicity was found to be slightly enhanced upon dynamin-K44A expression by stably transfected and inducible HeLa cells, indicating that Onco internalization is dynamin independent (Haigis and Raines, 2003).

Following initial uptake, endocytosed tracers are delivered to sorting endosomes. From there they can be directed to the endosome recycling compartment located in the pericentriolar region of the cell. This is the case for recycling ligands such as Tf. Alternatively, endocytosed proteins can be transported to late endosomes/lysosomes (Gruenberg and Maxfield, 1995). Most RNases seem to follow this degradation pathway, since neither RNase A (Haigis and Raines, 2003) nor a human pancreatic RNase A variant colocalized with Tf upon uptake. The latter mutant was very slowly endocytosed by A431 cells (over a 24 h period) and accumulated within late endosomes/lysosomes (Bosch et al., 2004). Onco intracellular routing is usually evaluated using drugs such as those able to increase acidic endosomal pH, which is in the pH 5.5–6.5 range (Gruenberg and Maxfield, 1995). Among these molecules, ammonium chloride did not show any effect, while monensin enhanced Onco toxicity by 10-fold. The fungal metabolite brefeldin A that prevents retrograde transport to the ER either had no effect (Wu et al., 1993) or potentiated Onco toxicity by 10-fold (Haigis and Raines, 2003). Both studies concluded that Onco likely gains access to the cytosol from endosomes and not from the Golgi or the ER (Haigis and Raines, 2003; Wu et al., 1993). Accordingly, Onco could be visualized within unidentified intracellular vesicles (Haigis and Raines, 2003). The role of endosome acidification in Onco toxicity has yet to be precised.

In this work, we assessed the Onco uptake pathway using several CME molecular effectors. Routing within the endocytic network was then examined using morphological examination as well as transport interference by expression of rab5-or rab7-dominant negative mutants. Our results show that Onco is taken up by AP-2/CME before routing to pericentriolar recycling endosomes, just like Tf. This recycling compartment is a key location for Onco access to the cytosol. This translocation step seems to be facilitated by endosome neutralization.

MATERIALS AND METHODS

Protein expression, purification and labeling

Recombinant Onco (rOnco) was produced from E. coli BL21 (DE3) cells (Novagen) transformed with the pOnc plasmid (Leland et al., 1998). The pOncS72C plasmid was created from pET11d-(Met-1)-Onco(M23L) (Boix et al., 1996) using the QuikChange site-directed mutagenesis kit (Stratagene), according to the manufacturer's instructions. This new plasmid directs the expression of (Met-1)-Onco with mutations at positions 1, 23 and 72 substituted by Gln, Leu and Cys, respectively (OncoS72C).

Mutant and wild-type Onco were expressed in BL21(DE3) cells using the T7 expression system and the recombinant proteins were purified and activated by generating an N-terminal pyroglutamic acid, essentially as described in (Ribo et al., 2001; Ribo et al., 2004).

Tf was labeled with Cy5 according to the recommendations of the labeling-kit manufacturer (Amersham Biosciences). Alexa Fluor 594 C5 maleimide (Molecular Probes) was conjugated to OncoS72C as described earlier (Bosch et al., 2004) to obtain Onco-Red. For pH measurement, Tf was simultaneously labeled with fluorescein and rhodamine succinimidyl esters (Molecular Probes) to obtain Fl-Tf-Rh as described (Presley et al., 1997). All labeling was followed by extensive dialysis against PBS at 4°C.

Cell culture and transfections

HeLa (cervix carcinoma), A431 (epidermoid carcinoma) and Jurkat (T lymphocytes) human cell lines were from the American Type Culture Collection. They were grown in DMEM or RPMI 1640 media (Invitrogen) containing 10% (v/v) heat-inactivated FCS (Invitrogen), 2 mM L-glutamine, 100 units/ml penicillin, and 100 μg/ml streptomycin. pCi vector was from Promega. Plasmids pEGFP (Clontech) containing Eps15 DIIIΔ2, Eps15Δ95/295 (Benmerah et al., 1999), intersectin SH3 domain (Simpson et al., 1999), as well as pCMV5-Dynamin II (WT or K44A (Lamaze et al., 2001)) and vectors coding for tetanus toxin light chain (TeNT LC, WT or the E234Q inactive mutant (Proux-Gillardeaux et al., 2005)), Rab5a (WT, Q79L or S34N (Mukhopadhyay et al., 1997)) or Rab7 (WT, Q67L, N125I (Vitelli et al., 1997)) have been described. Rab4-GFP and Rab5-GFP expression plasmids were provided by Anne Blangy (CRBM, Montpellier, France) and Rab11-GFP by Jean Salamero (Institut Curie, Paris, France).

HeLa cells were transfected using Superfect (Qiagen). Jurkat cells (9×10^6 cells) were electroporated with 20 μg of effector plasmid (Vendeville et al., 2004). Jurkat transfection efficiencies were determined using pEGFP and fluorescence-activated cell sorting (FACS) analysis. They ranged from 40 to 60%. Cells were used 24 h after transfection.

Immunofluorescence

HeLa cells were seeded onto 12 mm diameter coverslips in 24-well plates (8×10^4 cells/well) the day before the experiment. They were labeled for 45 min with 250 nM Onco-Red and 100 nM Tf-Cy5 in DMEM containing 2% FCS and, when indicated, 1 mg/ml of 66 kDa fluorescein-labeled dextran (Sigma). Cells were then fixed using 3.7% paraformaldehyde and permeabilized with saponin as described (Bosch et al., 2004). Anti-lamp (lysosomal-associated membrane protein) -1, -2 and -3 mAbs were supplied by the Iowa Developmental Studies Hybridoma Bank, anti-calnexin was from BD Biosciences and anti-lysobisphosphatidic acid (LBPA) was provided by Jean Gruenberg (Geneva, Switzerland). These antibodies were revealed using fluorescein-conjugated goat anti-mouse antibodies (Sigma). Sheep antibodies against human TGN46 (a marker for the trans-Golgi network) (Serotec) were detected using fluorescein-labeled donkey anti-sheep antibodies (Nordic). Finally, cells were mounted and examined under a Leica confocal microscope using a 63 x lens. To prevent passage of AlexaFluor 594 fluorescence into the blue (Cy5) channel, Onco-red fluorescence was imaged after acquiring the green (FITC or GFP) and blue (Cy5) images, which were collected simultaneously. Median optical sections were recorded. Colocalisation quantitations were performed using Metamorph software (Molecular Devices).

Transfected Jurkat cells were labeled with 250 nM Onco-Red and 100 nM Tf-Cy5 for 45 min at 37 ºC. Cells (1.5×10^6) in PBS were allowed to adhere for 3 min onto 18 mm poly-L-Lysine-coated coverslips in a 12-well plate. They were then fixed and mounted as described above for HeLa cells.

Quantitative fluorescence microscopy

The procedure for endosome-pH measurements has been described in detail (Dunn et al., 1994; Presley et al., 1997). Cells were first labeled for 40 min with Fl-Tf-Rh in DMEM supplemented with 1 mg/ml BSA. To prepare a calibration curve, cells were then washed with PBS and fixed before equilibration for 15 min in buffers containing 10 µM nigericin, within the pH 5-7.5 range. Fluorescence images from > 40 cells were obtained for both channels simultaneously using band-pass filters and taking care to avoid detector saturation. After quantitation of the signal from internalized Fl-Tf-Rh using ImageQuant (Amersham Biosciences), the Fl/Rh image ratio was plotted against the pH. The Fl/ Rh ratio increased 2.5-fold between pH 5 and pH 7 (data not shown), as documented earlier (Dunn et al., 1994). This calibration curve was then used for endosomal pH measurements in live cells (n>50).

Electron microscopy

Onco was conjugated to 10 nm diameter colloidal gold at pH 9.0 as described (Beaumelle and Hopkins, 1989). Jurkat cells in RPMI supplemented with 2% FCS were labeled with Onco-gold for 10 min at 37°C before chilling on ice, washes and fixation in Karnovsky fluid. Pellets were then processed for conventional electron microscopy.

Cytotoxicity assays on transfected cells

A FACS-based procedure was used to monitor Onco-induced apoptosis of transfected Jurkat cells. One day after transfection with pEGFP and the indicated effector (Eps15, dynamin, intersectin, rab5 rab7 or TeNT-LC), cells were treated with 6 μM rOnco for 24 h. They were then labeled with Annexin V-Cy5 as recommended by the manufacturer (BD Biosciences) and analyzed by FACS, gating on transfected cells using EGFP fluorescence. Apoptosis was monitored using annexin-Cy5 binding to these cells. Around 20% of the cells became Annexin-V positive upon Onco treatment (see Results). 10000 events were collected for each assay, which was performed in duplicate using a four-color FACScalibur analysis cytometer. Results are the mean ± S.E of three separate experiments.

Cytotoxicity assays with lysosomotropic agents

HeLa or A431 cells were preincubated with 0.1 μM bafilomycin A1 (Baf) (Sigma), 0.5 μM monensin (Sigma) or 20 mM NH_4Cl (Merck) before adding Onco. Cytotoxicity was assayed after 24 h. For HeLa cells, we used an assay monitoring the reduction of MTT (Sigma) to formazan. To this end, the medium was removed and replaced with 100 μl of fresh medium with 10 μl of MTT. After 3 h, the medium was replaced with 100 μl of DMSO and the absorption was read at 570 nm. We assessed the viability of A431 cells by monitoring ^{35}S-methionine incorporation into proteins (Bosch et al., 2004).

RESULTS

Design of an Onco variant suitable for fluorescent labeling

To visualize the internalization of Onco by human cells, we introduced a Cys residue into Onco so that it could be available for labeling. We selected position 72 because this residue is located in a solvent-exposed surface loop remote from the active site (Fig. 1). We prepared OncoS72C and checked that, after fluorescent labeling, this mutant was as toxic as Onco (i.e. IC_{50} of 1 μM for A431 cells) and therefore biologically active. We then examined Onco intracellular routing using the fluorescently-labeled variant.

Onco is endocytosed via an AP-2/ clathrin-dependent pathway

We used well-established CME inhibitors to assess the Onco initial uptake pathway. Overexpression of a dominant-negative mutant of Eps15 selectively inhibits clathrin/AP-2-dependent endocytosis (Benmerah et al., 1999), without affecting internalization mediated by lipid rafts (Lamaze et al., 2001). Overexpression of the intersectin SH3 domain also impairs clathrin-dependent uptake (Simpson et al., 1999). In most cases, the K44A mutation within the dynamin GTPase site blocks ligand internalization (Lamaze et al., 2001; Parton and Richards, 2003).

We individually and transiently overexpressed these constructs in Jurkat cells and monitored the capacity of transfected cells, identified by the EGFP tag of the construct (or by cotransfection with EGFP in the case of dynamin), to internalize fluorescent Onco. Cells transfected with the control version of Eps15 (Eps15D3Δ2) or dynamin (WT) internalized both Onco and the early endosome marker Tf (Fig. 2). As detailed below, endocytosed Onco co-localized with Tf. Dominant-negative constructions impairing coated vesicle formation (i.e. Eps15Δ95/295, the intersectin SH3A domain and dynamin K44A) prevented, with approximately the same efficiency, Tf and Onco uptake. Taken together these results indicated that Jurkat cells endocytosed Onco through an Eps15-, intersectin- and dynamin-dependent route, most presumably the well-characterized clathrin/AP-2-mediated endocytic pathway.

Onco is concentrated within coated pits at the plasma membrane

We then examined Onco localisation at the plasma membrane by EM. Since RNases are conserved proteins it is difficult to raise good antibodies against them (Beintema and Kleineidam, 1998). We therefore directly labeled Onco with gold and incubated Jurkat cells at 37°C with this conjugate. Onco-gold was found within coated pits (Fig.3). A morphometric analysis showed that more than 20% of plasma membrane associated Onco localized within these structures. Since coated pits occupy ~2% of the cell surface in T-cells (Foti et al., 1997), we concluded that Onco is specifically concentrated within coated pits at the plasma membrane.

Inhibition of clathrin mediated endocytosis decreases Onco toxicity

Morphological evidence that the bulk of Onco entered cells via a clathrin-dependent pathway did not necessarily mean that this was the pathway responsible for toxicity. It was indeed possible that a small amount of Onco, below the microscope detection thresholds, was internalized through an alternative pathway and that this small fraction only was responsible for cytotoxicity. To examine this possibility, we used the CME effectors described above to assess whether they would protect cells against Onco toxicity. This type of experiment requires specific monitoring of Onco toxicity to transfected cells. Since Onco is known to kill cells by

inducing apoptosis (Grabarek et al., 2002; Iordanov et al., 2000), we set up a FACS assay to quantify Onco toxicity to transfected cells using fluorescent annexin-V binding to GFP-cotransfected cells (see Materials and Methods for details).

While Onco-induced apoptosis was not significantly affected by overexpression of the control construction EGFP, Eps15-D3Δ2 and dynamin WT (Fig.4), all the dominant-negative constructs inhibited Onco toxicity with an efficiency ranging from 32% (Dynamin-K44A) to 54% (Eps15 Δ95/295). Hence, Onco enters cells using clathrin-mediated uptake and this enables its subsequent delivery to the cytosol.

Onco is routed to the receptor recycling compartment

We then examined Onco routing along the endocytic network. This study was performed on HeLa cells that enable easier visualization and compartment discrimination than lymphocytes, which are small cells with a large nucleus. It was shown earlier, using K562 erythroleukemic cells, that Onco internalization proceeded rapidly and that maximum cell labelling was achieved after 45 min of uptake only (Bosch et al., 2004). We obtained similar data on HeLa cells (data not shown). These observations are consistent with the finding that Onco uses coated pits to enter cells since the clathrin pathway usually enables efficient ligand entry within this time scale (Conner and Schmid, 2003). Onco-Red was internalized in the same endosomal structures as Tf-Cy5 (Figs 2, 5A). Contrary to other RNases that enter cells slowly and are directed to the degradative pathway (Bosch et al., 2004; Haigis and Raines, 2003), endocytosed Onco-Red did not significantly colocalize with established late endosome/lysosome markers such as lysosomal membrane proteins (Lamp-1, Lamp-2, Lamp-3), internalized dextran, LBPA (Fig.5A) or the mannose 6-phosphate receptor (data not shown). Onco-containing structures were negative for calnexin or TGN46, indicating that this protein is not transported to the endoplasmic reticulum or the trans-Golgi network (Fig.5A). Onco intracellular routing was actually restrained to Tf-positive structures, and the efficiency of Onco colocalization with Tf (75-80%, Fig.5B) was the same as that observed when using two Tf bearing different fluorophores (Sabharanjak et al., 2002). Hence, Onco remains within early endosomes after uptake. More specifically, Onco seemed to concentrate within a compartment at the center of the cell where fluorescent Tf is known to accumulate upon labeling, i.e. the recycling compartment (Mallard et al., 1998).

Recycling endosomes are the sole structure in the endocytic pathway where the small GTPase Rab11 is present. Hence, the recycling compartment can be efficiently labeled using Rab11-GFP and, to a lesser extent, with Rab4- or Rab5-GFP (Sonnichsen et al., 2000). When HeLa cells were transfected with Rab4-, Rab5- or Rab11-GFP, internalized Onco colocalized very efficiently with Rab11-GFP and Tf in the pericentriolar recycling compartment at the

center of the cell (Fig.6). Altogether these data indicated that Onco follows Tf internalisation, from coated pits to the recycling compartment.

Onco uptake depends on Rab5 but not on Rab7

Rab5 and Rab7 small GTPases control traffic along the endocytic pathway (Gruenberg and Maxfield, 1995). To further confirm that Onco endocytosis followed a similar pathway as Tf internalization and that Onco was not, as other RNases, targeted to lysosomes (Bosch et al., 2004), we monitored the effects of overexpressing Rab5 or Rab7 mutants on Onco endocytosis. A dominant negative mutant of Rab5 (Rab5S34N, defective in GDP-binding) is known to slow down endocytosis of ligands, whether they are destined to the recycling compartment, such as Tf (Stenmark et al., 1994) or to degradation within late endosomes/lysosomes, such as low-density lipoproteins (Vitelli et al., 1997). A dominant negative version of Rab7 (Rab7N125I) prevents tracer delivery to late endosomes, but does not significantly inhibit Tf uptake (Bucci et al., 2000; Vitelli et al., 1997) . Neither the activated version of Rab5 (Ceresa et al., 2001) nor of Rab7 (Bucci et al., 2000; Vitelli et al., 1997) were found to influence uptake of Tf or lysosome-targeted molecules. Accordingly, we observed that the WT or the activated version of Rab5 and Rab7 did not significantly affect Onco or Tf internalization (Fig.7). Regarding dominant-negative mutants, Onco and Tf uptake was strongly inhibited in cells overexpressing Rab5S34N, but was not affected by Rab7N125I (Fig.7). Hence, Onco endocytosis is regulated by Rab5 but not by Rab7.

Onco toxicity is regulated by Rab5 but not Rab7

It was possible that, although Onco was not efficiently transported to late endosomes/lysosomes, it nevertheless required such routing to access the cytosol. In such a case, dominant-negative Rab7 expression should protect cells against Onco cytotoxicity. To examine this possibility, we transfected Jurkat cells with Rab5 or Rab7 mutants and monitored Onco toxicity to transfected cells by FACS. None of the Rab7 effectors (WT, dominant negative or activated version) significantly affected Onco toxicity. Cells overexpressing WT Rab5 were as sensitive to Onco as control cells. Not surprisingly, cells transfected by the dominant negative version of Rab5 (Rab5S34N) were partially resistant to Onco (-25% toxicity, Fig.8). The activated version of Rab5 (Rab5Q79L) weakly but significantly protected cells against Onco (-10%). This effect could be explained by the ability of this construct to produce enlarged sorting endosomes (Ceresa et al., 2001; Vendeville et al., 2004), thereby interfering not with bulk Tf recycling (Ceresa et al., 2001) but with transport to the recycling compartment. Indeed, Rab5Q79L is already known to inhibit tracer delivery to late endosomes, indicating that this

activated version of Rab5 interferes with the sorting process taking place at the sorting endosome level (Rosenfeld et al., 2001).

Altogether with morphological examination, the Rab5 data showed that Onco internalization is regulated by this small GTPase. The result that dominant negative Rab7 affects neither Onco intracellular routing nor its toxicity confirmed that the Onco intracellular pathway is restricted to early endosomes, and that Onco does not need delivery to late endosomes/lysosomes to reach the cytosol and kill cells.

The recycling compartment is a key intermediate for Onco toxicity

To examine whether recycling endosomes were implicated in Onco toxicity we transfected cells with TeNT-LC, a highly specific protease that cleaves and inactivates cellubrevin, a SNARE protein present on different types of vesicles but colocalizing with Tf at the recycling endosome level only (Wilcke et al., 2000). Cellubrevin is required for efficient Tf recycling, although 70% of Tf recycling is cellubrevin independent (Galli et al., 1994). In close agreement with these findings, TeNT-LC expression enhanced Onco toxicity by 32% whereas the proteolytically inactive E234Q mutant had no significant effect (Fig.8). This result is consistent with the view that the recycling compartment enables Onco translocation to the cytosol and that a higher Onco concentration at this level favors toxicity.

Onco toxicity is enhanced upon endosome neutralization

Studies on the role of endosomal low pH in Onco toxicity used 20-30 mM ammonium chloride to neutralize endosomes and failed to reveal any effect of this treatment on Onco toxicity. The less specific drug monensin that also affects Golgi structure nevertheless enhanced toxicity by 10-fold on 9L and K562 cells. It was concluded that Onco toxicity was insensitive to endosome neutralization (Haigis and Raines, 2003; Wu et al., 1993). We reexamined these findings by additionally using bafilomycin A1 (Baf), which is a specific inhibitor of the vacuolar ATPase responsible for endosome acidification (Crider et al., 1994). For these experiments, we used both HeLa and A431 cells, and monitored the endosomal pH using double-labeled fluorescent Tf for the latter cell line.

In agreement with previous findings (Haigis and Raines, 2003; Wu et al., 1993), we observed that ammonium chloride either did not affect (HeLa) or moderately sensitized (5-fold for A431) cells to Onco (Fig.9A). Nevertheless, this molecule alone (20 mM) only increased endosomal pH by 0.4 pH units (from pH 5.2 to pH 5.6, Fig.9B) and only when mixed with methylamine (20 mM) was it able to almost neutralize endosomes (20 mM methylamine + 20 mM NH_4Cl raised endosomal pH to 6.5). Monensin (0.25 µM) enhanced Onco toxicity by 5-80 fold while efficiently increasing the endosomal pH to pH 6.5. Baf enhanced Onco toxicity by 20-100 fold and completely neutralized the endosomal pH. We concluded that (i) neutralization

of low endosomal pH enhances Onco toxicity by more than one log and (ii) this sensitization effect cannot be obtained using NH_4Cl alone that weakly increases the endosomal pH. How can endosome neutralization enhance Onco toxicity? Endosome neutralizing drugs do not affect the routing of ligands that are addressed to the recycling compartment, such as Tf (Presley et al., 1997), Pseudomonas exotoxin (PE) (Alami et al., 1998) or shiga toxin (Mallard et al., 1998). Consistent with these findings, we found that Baf did not modify the efficiency of Onco colocalisation with established markers of the endocytic pathway (Fig.5B), indicating that endosome neutralisation did not affect Onco intracellular routing. When Jurkat cells were labeled with ^{125}I-Onco before purification of endosomes to test Onco translocation in a cell-free assay (Alami et al., 1998; Vendeville et al., 2004), ^{125}I-Onco efficiently translocated in the presence of Baf (data not shown). Collectively, our results show that Onco likely escapes to the cytosol from recycling endosomes and that this process is facilitated by endosome neutralization.

DISCUSSION

In this work, we examined the intracellular pathway of Onconase, an interestingly cytotoxic member of the RNase superfamily. Using different specific effectors, we found that Onco uses the well characterized AP-2/CME pathway for initial uptake. This finding seems difficult to reconcile with a previous study which indicated that Onco endocytosis is dynamin-independent (Haigis et al., 2003). Nevertheless, their conclusions were essentially drawn from cytotoxicity experiments using a HeLa cell line stably transfected with inducible dynamin-K44A dominant-negative mutant. Indeed, expression of mutant dynamin in this system did not protect cells against Onco (Haigis et al., 2003). We obtained the same results using this cell line (data not shown), but we realized that upon mutant dynamin induction, only ~1/3 of the cells were unable to endocytose Tf. This indicated that transgene expression was not homogenous in this cell line. Moreover, this expression leads to an increase in the pH of endocytic compartments by 0.4 to 0.7 pH units as measured using double-labeled fluorescent dextran (Bayer et al., 2001). In the light of our observations that Onco is taken up by CME (Figs 2,3,4) and that endosomal neutralisation enhances Onco toxicity (Fig.9A), it seems likely that two antagonistic effects are responsible for the absence of protection against Onco observed upon dynamin-K44A expression by these inducible and stably transfected HeLa cells. Indeed, although less toxin was endocytosed upon transgene expression, Onco encountered higher endosomal pH than in uninduced cells (Bayer et al., 2001), thereby facilitating its access to the cytosol.

Dynamin-K44A transient expression within the T cells we used for the toxicity assay prevented tracer uptake. We could therefore not examine whether endosomal pH is similarly increased within these transfected cells. Nevertheless, these dynamin-K44A transfected cells

were partly protected against Onco toxicity, essentially as efficiently as those transfected with a dominant negative construct of other major CME players such as Eps15 and intersectin (Fig.4).

On the basis of the effect of dominant negative Eps15, i.e. 50% inhibition in Onco toxicity, it can be concluded that more than 50% of Onco molecules that eventually reached the cytosol entered cells using CME. This value is likely an underestimate since, according to microscopic examination, Onco internalization only proceeded via CME (Fig.2).

Onco is then routed to the recycling compartment. It thus follows a quite unusual pathway for a tracer, which has only been documented for a few proteins such as transferrin (Yamashiro et al., 1984), and toxins, i.e. PE (Alami et al., 1998) and shiga toxin (Mallard et al., 1998; Wilcke et al., 2000). Indeed, other RNases such as RNase A and human pancreatic RNase variants were not addressed to recycling endosomes (as monitored using fluorescent transferrin), and the latter concentrated within late endosomes/lysosomes (Bosch et al., 2004; Haigis et al., 2003). Hence, regarding the handling by cells and compared to other members of the RNase superfamily, our results indicated that Onco shows two important specificities that might be related to its cytotoxicity. The first one is a much more efficient and rapid uptake (Bosch et al., 2004), and the second is this specific intracellular routing to the recycling compartment. Both characteristics are consistent with the existence of an Onco receptor. A previous study indeed identified saturable binding sites in glioma cells with a K_d ~6 x 10^{-8} M (Wu et al., 1993).

The use of TeNT-LC, that impairs ligand recycling from recycling endosomes (Galli et al., 1994; Wilcke et al., 2000) and increases Onco toxicity (Fig.8), underlined the role of this structure in the Onco intoxication process. This interpretation is in agreement with the differential effect of Tf coupling to Onco and RNase A (Rybak and Newton, 1999). When RNase A was coupled to Tf its cytotoxicity increased by~10,000 fold, likely as a result of more efficient uptake and routing to the recycling compartment. In contrast, conjugation of Onco to Tf only enhanced its cytotoxicity by 10-fold, probably reflecting an increase in internalization efficiency only.

The role of endosome acidification in Onco toxicity was previously examined using ammonium chloride to raise the endosomal pH (Haigis et al., 2003; Wu et al., 1993). Nevertheless, this drug alone is essentially not efficient for this purpose (Fig.9B) and the results obtained with Baf, that effectively neutralizes Tf-containing structures, showed that cells became much more sensitive to Onco under these conditions (Fig.9A). This was quite surprising, since conventional toxins translocating from endosomes to the cytosol usually rely on endosome acidification to trigger conformational changes that enable membrane insertion and translocation. This has been documented for diphtheria and anthrax toxin (Abrami et al., 2005; Beaumelle et al., 1992), PE (Méré et al., 2005) and HIV-1 Tat (Vendeville et al., 2004). It is therefore not clear why Onco requires both internalization and endosome neutralization to efficiently reach the cytosol. Since it does not seem to be able to translocate from the plasma

membrane, the ER or the Golgi (Haigis and Raines, 2003; Wu et al., 1993), Onco probably relies on an endosomal component to reach the cytosol. Our study indicated that this factor is likely concentrated within the receptor recycling compartment. Identification of the Onco receptor would undoubtedly help us to further understand the Onco entry process.

Acknowledgements

We are very grateful to A. Blangy (Montpellier), A. Benmerah, T. Galli, C. Lamaze and J. Salamero (Paris), J. Gruenberg (Geneva) and R.T. Raines (Madison, USA), for their kind gift of reagents. This work was supported by PICS between the CNRS (PICS N°3067) and the University of Girona (PICS2005-3, Generalitat de Catalunya) and by grants BMC2003-08485-CO2-02 and SGR2001-00196 from the Ministerio de Ciencia y Tecnología and Generalitat de Catalunya, respectively. MR and GT gratefully acknowledge their pre-doctoral fellowships from the Ministerio de Educación y Ciencia.

Abbreviations: Baf, bafilomycin A_1; CME, clathrin-mediated endocytosis; FACS, fluorescence-activated cell sorting; Lamp, lysosome-associated membrane protein; LBPA, lysobisphosphatidic acid; Onco, Onconase; Onco-Red, Onco-AlexaFluor 594; PE, Pseudomonas exotoxin; TeNT-LC, tetanus toxin light chain; Tf, transferrin.

REFERENCES

Abrami, L., Reig, N. and van der Goot, F. G. (2005). Anthrax toxin: the long and winding road that leads to the kill. *Trends Microbiol* **13**, 72-8.

Alami, M., Taupiac, M. P., Reggio, H., Bienvenue, A. and Beaumelle, B. (1998). Involvement of ATP-dependent Pseudomonas exotoxin translocation from a late recycling compartment in lymphocyte intoxication procedure. *Mol Biol Cell* **9**, 387-402.

Ardelt, B., Ardelt, W. and Darzynkiewicz, Z. (2003). Cytotoxic ribonucleases and RNA interference (RNAi). *Cell Cycle* **2**, 22-4.

Bayer, N., Schober, D., Huttinger, M., Blaas, D. and Fuchs, R. (2001). Inhibition of clathrin-dependent endocytosis has multiple effects on human rhinovirus serotype 2 cell entry. *J Biol Chem* **276**, 3952-62.

Beaumelle, B., Bensammar, L. and Bienvenue, A. (1992). Selective translocation of the A chain of diphtheria toxin across the membrane of purified endosomes. *J Biol Chem* **267**, 11525-31.

Beaumelle, B. and Hopkins, C. R. (1989). High-yield isolation of functionally competent endosomes from mouse lymphocytes. *Biochem J* **264**, 137-49.

Beintema, J. J. and Kleineidam, R. G. (1998). The ribonuclease A superfamily: general discussion. *Cell Mol Life Sci* **54**, 825-32.

Benmerah, A., Bayrou, M., Cerf-Bensussan, N. and Dautry-Varsat, A. (1999). Inhibition of clathrin-coated pit assembly by an Eps15 mutant. *J Cell Sci* **112**, 1303-11.

Boix, E., Wu, Y., Vasandani, V. M., Saxena, S. K., Ardelt, W., Ladner, J. and Youle, R. J. (1996). Role of the N terminus in RNase A homologues: differences in catalytic activity, ribonuclease inhibitor interaction and cytotoxicity. *J Mol Biol* **257**, 992-1007.

Bosch, M., Benito, A., Ribo, M., Puig, T., Beaumelle, B. and Vilanova, M. (2004). A nuclear localization sequence endows human pancreatic ribonuclease with cytotoxic activity. *Biochemistry* **43**, 2167-77.

Bucci, C., Thomsen, P., Nicoziani, P., McCarthy, J. and van Deurs, B. (2000). Rab7: a key to lysosome biogenesis. *Mol Biol Cell* **11**, 467-80.

Ceresa, B. P., Lotscher, M. and Schmid, S. L. (2001). Receptor and membrane recycling can occur with unaltered efficiency despite dramatic Rab5(q79l)-induced changes in endosome geometry. *J Biol Chem* **276**, 9649-54.

Conner, S. D. and Schmid, S. L. (2003). Regulated portals of entry into the cell. *Nature* **422**, 37-44.

Costanzi, J., Sidransky, D., Navon, A. and Goldsweig, H. (2005). Ribonucleases as a novel pro-apoptotic anticancer strategy: review of the preclinical and clinical data for ranpirnase. *Cancer Invest* **23**, 643-50.

Crider, B. P., Xie, X. S. and Stone, D. K. (1994). Bafilomycin inhibits proton flow through the H+ channel of vacuolar proton pumps. *J Biol Chem* **269**, 17379-17381.

Damke, H., Baba, T., Warnock, D. E. and Schmid, S. L. (1994). Induction of mutant dynamin specifically blocks endocytic coated vesicle formation. *J Cell Biol* **127**, 915-934.

Darzynkiewicz, Z., Carter, S. P., Mikulski, S. M., Ardelt, W. J. and Shogen, K. (1988). Cytostatic and cytotoxic effects of Pannon (P-30 Protein), a novel anticancer agent. *Cell Tissue Kinet* **21**, 169-82.

Dunn, K. W., Park, J., Semrad, C. E., Gelman, D. L., Shevell, T. and McGraw, T. E. (1994). Regulation of endocytic trafficking and acidification are independent of the cystic fibrosis transmembrane regulator. *J Biol Chem* **269**, 5336-45.

Favaretto, A. (2005). Overview on ongoing or planned clinical trials in Europe. *Lung Cancer* **49 Suppl 1**, S117-21.

Foti, M., Mangasarian, A., Piguet, V., Lew, D. P., Krause, K. H., Trono, D. and Carpentier, J. L. (1997). Nef-mediated clathrin-coated pit formation. *J Cell Biol* **139**, 37-47.

Galli, T., Chilcote, T., Mundigl, O., Binz, T., Niemann, H. and de Camili, P. (1994). Tetanus toxin-mediated cleavage of cellubrevin impairs exocytosis of transferrin receptor-containing vesicles in CHO cells. *J Cell Biol* **125**, 1015-1024.

Grabarek, J., Ardelt, B., Du, L. and Darzynkiewicz, Z. (2002). Activation of caspases and serine proteases during apoptosis induced by onconase (Ranpirnase). *Exp Cell Res* **278**, 61-71.

Gruenberg, J. and Maxfield, F. R. (1995). Membrane transport in the endocytic pathway. *Curr Opin Cell Biol* **7**, 552-563.

Haigis, M. C., Kurten, E. L. and Raines, R. T. (2003). Ribonuclease inhibitor as an intracellular sentry. *Nucleic Acids Res* **31**, 1024-32.

Haigis, M. C. and Raines, R. T. (2003). Secretory ribonucleases are internalized by a dynamin-independent endocytic pathway. *J Cell Sci* **116**, 313-24.

Henley, J. R., Krueger, E. W., Oswald, B. J. and McNiven, M. A. (1998). Dynamin-mediated internalization of caveolae. *J Cell Biol* **141**, 85-99.

Iordanov, M. S., Ryabinina, O. P., Wong, J., Dinh, T. H., Newton, D. L., Rybak, S. M. and Magun, B. E. (2000). Molecular determinants of apoptosis induced by the cytotoxic ribonuclease onconase: evidence for cytotoxic mechanisms different from inhibition of protein synthesis. *Cancer Res* **60**, 1983-94.

Lamaze, C., Dujeancourt, A., Baba, T., Lo, C. G., Benmerah, A. and Dautry-Varsat, A. (2001). Interleukin 2 receptors and detergent-resistant membrane domains define a clathrin-independent endocytic pathway. *Mol Cell* **7**, 661-71.

Leland, P., Schultz, L., Kim, B. and Raines, R. (1998). Ribonuclease A variants with potent cytotoxic activity. *Proc Natl Acad Sci U S A.* **95**, 10407-10412.

Mallard, F., Antony, C., Tenza, D., Salamero, J., Goud, B. and Johannes, L. (1998). Direct pathway from early/recycling endosomes to the Golgi apparatus revealed through the study of shiga toxin B-fragment transport. *J Cell Biol* **143**, 973-90.

Méré, J., Morlon-Guyot, J., Bonhoure, A., Chiche, L. and Beaumelle, B. (2005). Acid-triggered Membrane Insertion of Pseudomonas Exotoxin A Involves an Original Mechanism Based on pH-regulated Tryptophan Exposure. *J Biol Chem* **280**, 21194-201.

Mikulski, S. M., Ardelt, W., Shogen, K., Bernstein, E. H. and Menduke, H. (1990). Striking increase of survival of mice bearing M109 Madison carcinoma treated with a novel protein from amphibian embryos. *J Natl Cancer Inst* **82**, 151-3.

Mukhopadhyay, A., Barbieri, A. M., Funato, K., Roberts, R. and Stahl, P. D. (1997). Sequential actions of Rab5 and Rab7 regulate endocytosis in the Xenopus oocyte. *J Cell Biol* **136**, 1227-37.

Parton, R. G. and Richards, A. A. (2003). Lipid rafts and caveolae as portals for endocytosis: new insights and common mechanisms. *Traffic* **4**, 724-38.

Predescu, S. A., Predescu, D. N., Timblin, B. K., Stan, R. V. and Malik, A. B. (2003). Intersectin regulates fission and internalization of caveolae in endothelial cells. *Mol Biol Cell* **14**, 4997-5010.

Presley, J. F., Mayor, S., McGraw, T. E., Dunn, K. W. and Maxfield, F. R. (1997). Bafilomycin A1 treatment retards transferrin receptor recycling more than bulk membrane recycling. *J Biol Chem* **272**, 13929-36.

Proux-Gillardeaux, V., Gavard, J., Irinopoulou, T., Mege, R. M. and Galli, T. (2005). Tetanus neurotoxin-mediated cleavage of cellubrevin impairs epithelial cell migration and integrin-dependent cell adhesion. *Proc Natl Acad Sci U S A* **102**, 6362-7.

Ribo, M., Benito, A., Canals, A., Nogues, M. V., Cuchillo, C. M. and Vilanova, M. (2001). Purification of engineered human pancreatic ribonuclease. *Methods Enzymol* **341**, 221-34.

Ribo, M., Bosch, M., Torrent, G., Benito, A., Beaumelle, B. and Vilanova, M. (2004). Quantitative analysis, using MALDI-TOF mass spectrometry, of the N-terminal hydrolysis and cyclization reactions of the activation process of onconase. *Eur J Biochem* **271**, 1163-71.

Rosenfeld, J. L., Moore, R. H., Zimmer, K. P., Alpizar-Foster, E., Dai, W., Zarka, M. N. and Knoll, B. J. (2001). Lysosome proteins are redistributed during expression of a GTP-hydrolysis-defective rab5a. *J Cell Sci* **114**, 4499-508.

Rybak, S. M. and Newton, D. L. (1999). Natural and engineered cytotoxic ribonucleases: therapeutic potential. *Exp Cell Res* **253**, 325-35.

Sabharanjak, S., Sharma, P., Parton, R. G. and Mayor, S. (2002). GPI-anchored proteins are delivered to recycling endosomes via a distinct cdc42-regulated, clathrin-independent pinocytic pathway. *Dev Cell* **2**, 411-23.

Saxena, S. K., Sirdeshmukh, R., Ardelt, W., Mikulski, S. M., Shogen, K. and Youle, R. J. (2002). Entry into cells and selective degradation of tRNAs by a cytotoxic member of the RNase A family. *J Biol Chem* **277**, 15142-6.

Simpson, F., Hussain, N. K., Qualmann, B., Kelly, R. B., Kay, B. K., McPherson, P. S. and Schmid, S. L. (1999). SH3-domain-containing proteins function at distinct steps in clathrin-coated vesicle formation. *Nat Cell Biol* **1**, 119-24.

Sonnichsen, B., De Renzis, S., Nielsen, E., Rietdorf, J. and Zerial, M. (2000). Distinct membrane domains on endosomes in the recycling pathway visualized by multicolor imaging of Rab4, Rab5, and Rab11. *J Cell Biol* **149**, 901-14.

Stenmark, H., Parton, R. G., Steele-Mortimer, O., Lütcke, A., Gruenberg, J. and Zerial, M. (1994). Inhibition of rab5 GTPase activity stimulates membrane fusion in endocytosis. *Embo J* **13**, 1287-1296.

Traub, L. M. (2003). Sorting it out: AP-2 and alternate clathrin adaptors in endocytic cargo selection. *J Cell Biol* **163**, 203-8.

Vendeville, A., Rayne, F., Bonhoure, A., Bettache, N., Montcourrier, P. and Beaumelle, B. (2004). HIV-1 Tat enters T-cells using coated pits before translocating from acidified endosomes and eliciting biological responses. *Mol Biol Cell* **15**, 2347-2360.

Vitelli, R., Santillo, M., Lattero, D., Chiariello, M., Bifulco, M., Bruni, C. B. and Bucci, C. (1997). Role of the small GTPase Rab7 in the late endocytic pathway. *J Biol Chem* **272**, 4391-7.

Wilcke, M., Johannes, L., Galli, T., Mayau, V., Goud, B. and Salamero, J. (2000). Rab11 regulates the compartmentalization of early endosomes required for efficient transport from early endosomes to the trans-golgi network. *J Cell Biol* **151**, 1207-20.

Wu, Y., Mikulski, S. M., Ardelt, W., Rybak, S. M. and Youle, R. J. (1993). A cytotoxic ribonuclease. Study of the mechanism of onconase cytotoxicity. *J Biol Chem* **268**, 10686-93.

Yamashiro, D. J., Tycko, B., Fluss, S. R. and Maxfield, F. R. (1984). Segregation of transferrin to a midly acidic (pH 6.5) para-Golgi compartment in the recycling pathway. *Cell* **137**, 789-800.

FIGURE LEGENDS

Fig.1. Ribbon representation of the three-dimensional structure of Onco (PDB ID 1ONC) showing the location of the active site residues (green) and the Ser72Cys mutation (red), that was introduced for fluorescent labeling. This figure was drawn with PyMOL (http://pymol.sourceforge.net).

Fig.2. Onco is endocytosed by the clathrin-mediated pathway. Jurkat cells were transiently transfected with a vector coding for an EGFP-tagged protein (Eps15D3Δ2, Eps15Δ95/295 or intersectin SH3A), or with both an EGFP vector and another coding for dynamin II-WT or dynamin II-K44A. After 24 h, 250 nM Onco-Red and 100 nM Tf-Cy5 were added for 45 min. Cells were then washed, fixed and examined under a confocal microscope. Representative sections through the middle of the cell. Bar, 10 µm.

Fig.3. Onco is found within coated pits at the plasma membrane. Jurkat cells were labeled for 15 min at 37°C with Onco conjugated to 10 nm diameter colloidal gold. They were then cooled to 4°C, washed, fixed and processed for electronmicroscopic examination. Bar, 50 nm.

Fig.4. Inhibition of clathrin-mediated endocytosis protects cells against Onco-induced apoptosis. Jurkat cells were transfected with a vector coding for EGFP alone or EGFP-tagged proteins, as indicated. After 24 h, 6 µM Onco was added. Apoptosis was quantified 24 h later by monitoring Annexin-V-Cy5 binding to transfected cells by FACS. The results are expressed as mean ± s.e.m. of three separate experiments.

Fig.5. Onco intracellular pathway. HeLa cells were incubated for 45 min with Onco-Red and Tf-Cy5 (to label early endosomes). When indicated, cells were also labeled with dextran-FITC, a tracer which is addressed to lysosomes. Cells were then processed for immunodetection of markers for late endosome/lysosomes (Lamp-1, Lamp-2, Lamp-3 or LBPA), the ER (calnexin) or the TGN (TGN46), before mounting and observation under a confocal microscope. A, median optical sections; bar, 10 µm; images for Lamp-3 are not shown. B, colocalization quantitations; cells were labeled with Onco in the presence or absence of 100 nM bafilomycin (Baf), as indicated; the graph shows the percentage of Onco colocalisation with the indicated marker. Colocalization of two fluorescent Tf bearing different fluorochromes was not measured (ND).

Fig.6. Onco accumulates in recycling endosomes. HeLa cells were transiently transfected with EGFP-tagged Rab4, Rab5 or Rab11. After 24 h, Onco-Red and Tf-Cy5 were added for 45 min. Cells were then fixed and examined by confocal microscopy. Median optical sections; bar, 20 µm.

Fig.7. Onco uptake depends on Rab5. Jurkat cells were transfected with the indicated Rab5 or Rab7 expression vectors, together with EGFP. After 24 h, Onco-Red and Tf-Cy5 were added for 45 min before fixation and confocal microscopic examination. Bar, 10 µm.

Fig.8. Cellubrevin and Rab5 regulate Onco delivery to the cytosol. Jurkat cells were transfected with EGFP and either the wild type or a mutated version of Rab5, Rab7 or TeNT-LC, as indicated. After 24 h, 6 µM Onco was added. Cytotoxicity was measured after 24 h, on transfected cells, using Annexin-V-Cy5 labeling and FACS analysis.

Fig.9. Onco toxicity is enhanced by endosome neutralization. A, Cytotoxicity to HeLa and A431 cells. Cells were pre-incubated for 30 min with 0.25 µM monensin, 20 mM NH_4Cl (Amm Cl) or 100 nM bafilomycin (Baf), as indicated, before adding various concentrations of Onco. Cell viability was measured after 24 h (HeLa) or 36 h (A431). The results are expressed as the Onco concentration generating a growth inhibition of 50% (IC_{50}). Mean ± s.e.m. of at least three separate experiments. B, Endosomal pH measurements. A431 cells were labeled for 40 min with Fl-Tf-Rh before acquiring fluorescein and rhodamine fluorescence images using a confocal microscope. The Fl/ Rh intracellular intensity ratio was then used together with a calibration curve to determine the endosomal pH (see Materials and Methods for details).

Figure 1

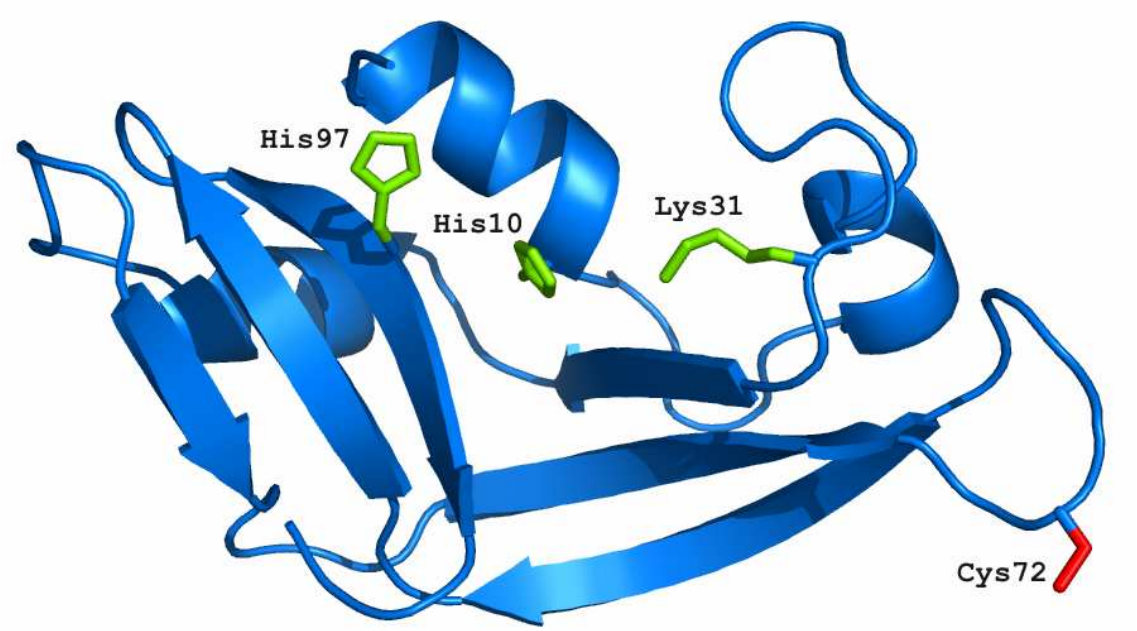

Fig.2, Rodriguez *et al*

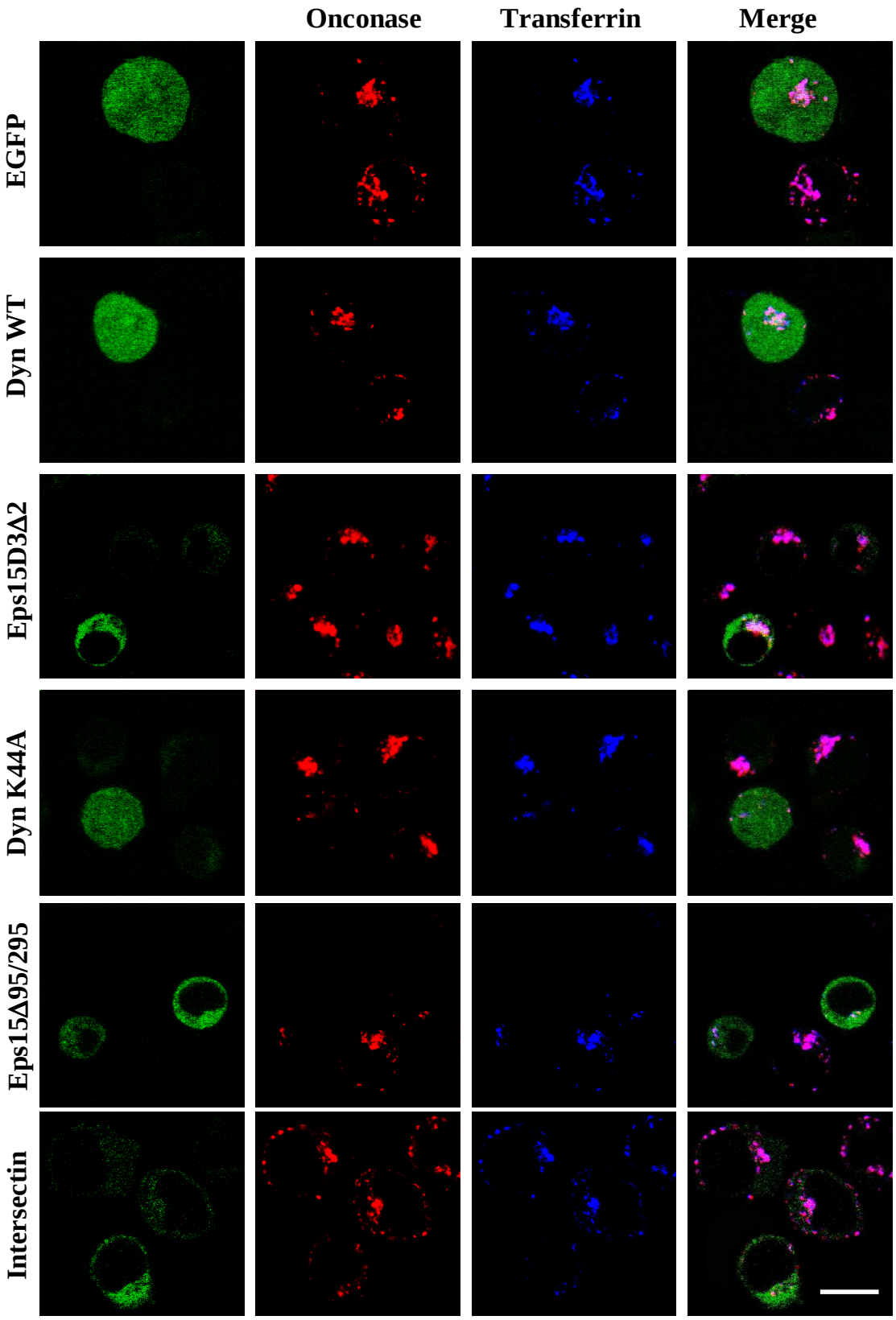

Fig.3, Rodriguez *et al*

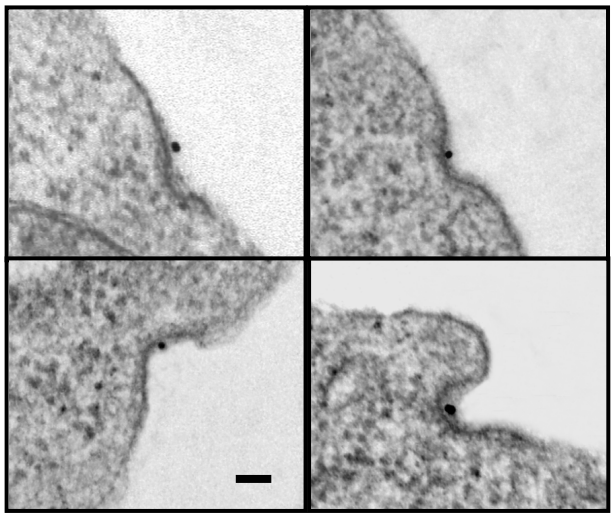

Fig.4, Rodriguez *et al*

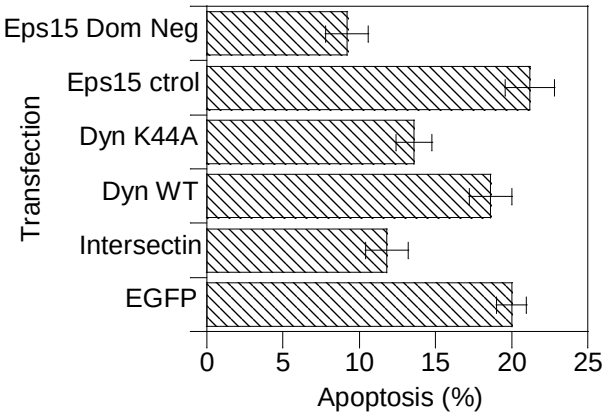

Fig.5A; Rodriguez *et al*

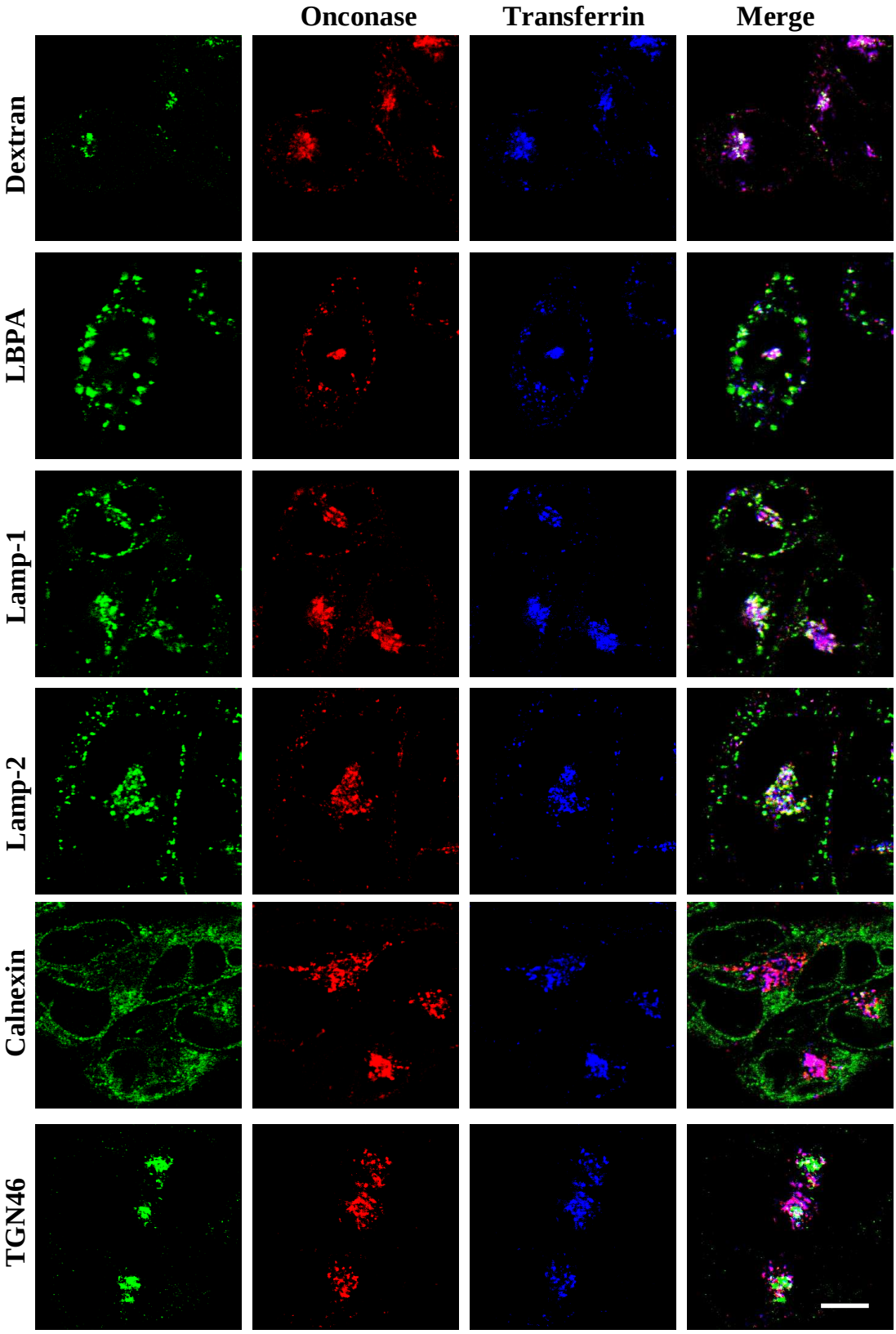

Fig.5B; Rodriguez *et al*

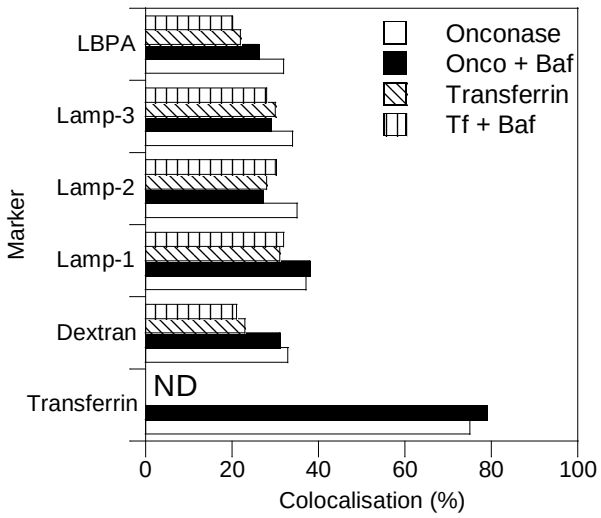

Fig.6; Rodriguez *et al*

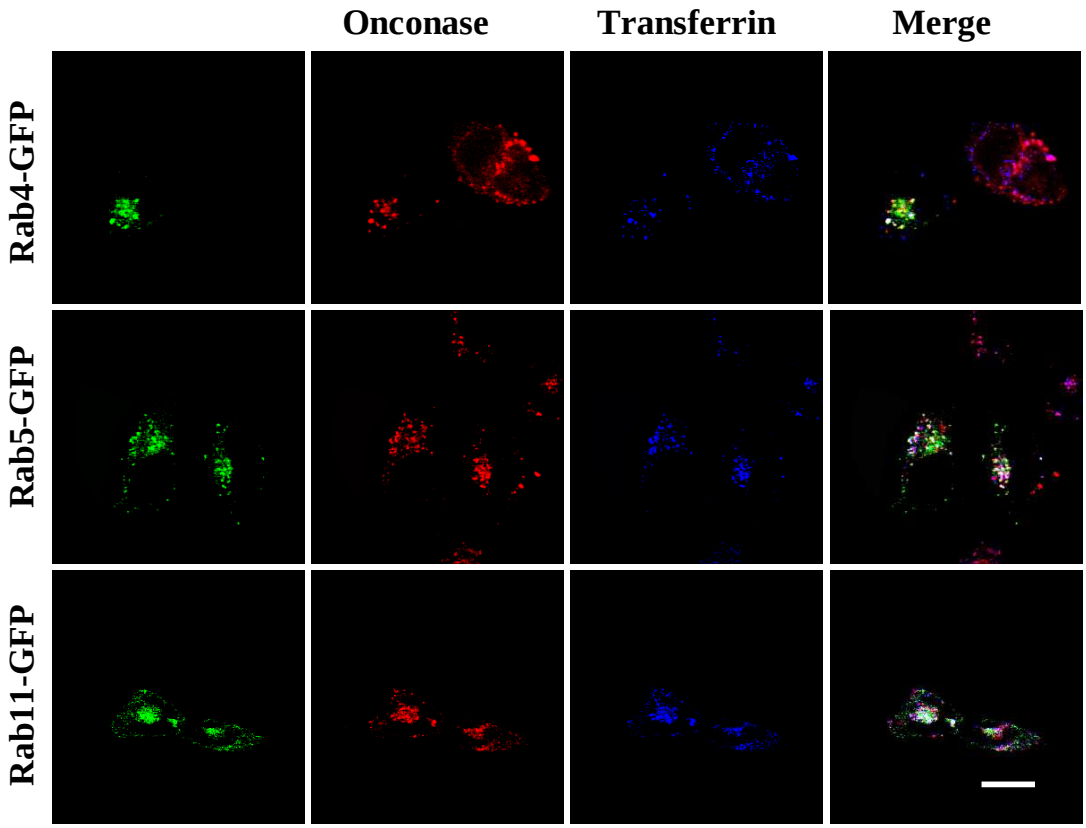

Fig.7; Rodriguez *et al*

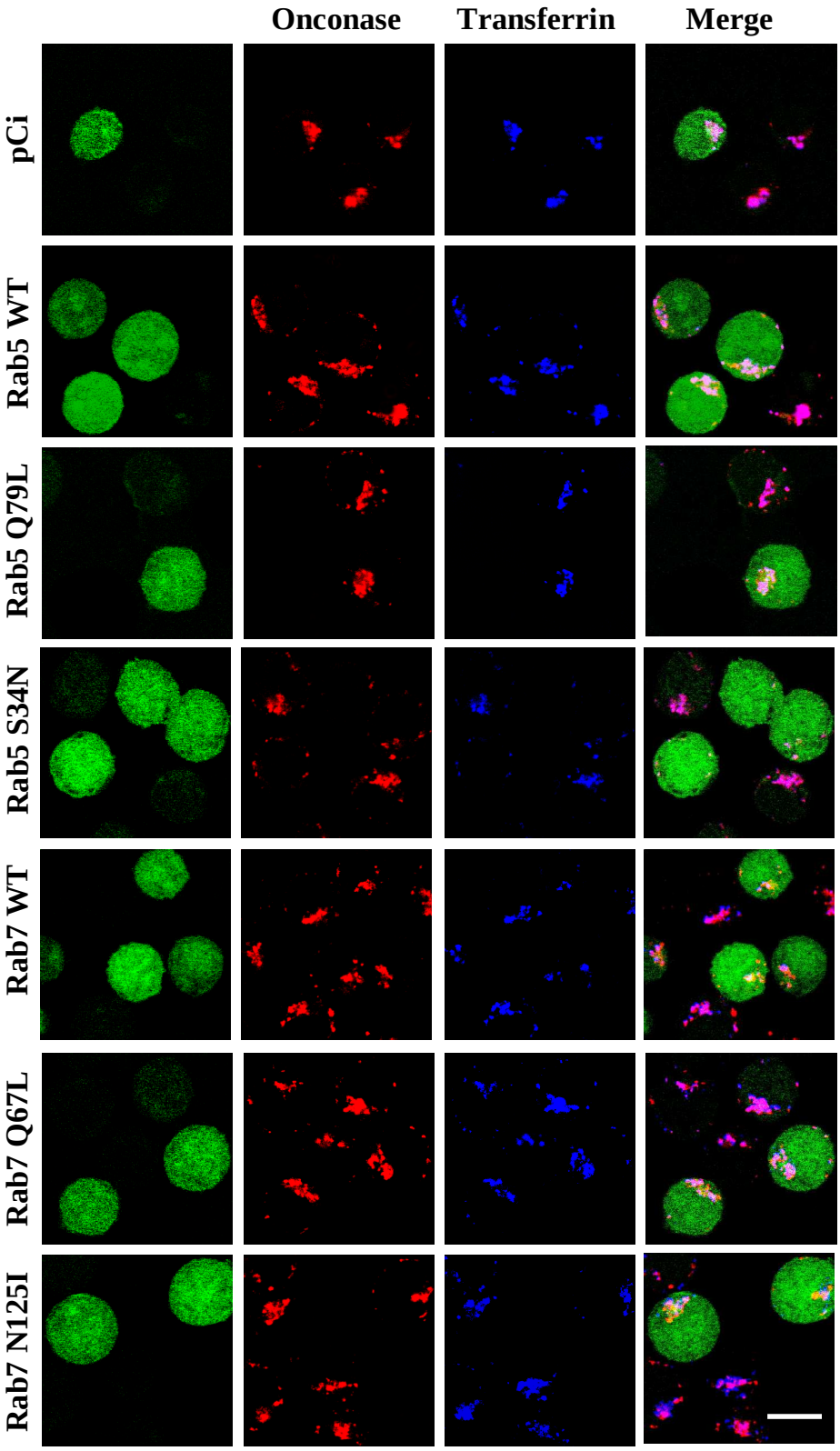

Fig.8; Rodriguez *et al*

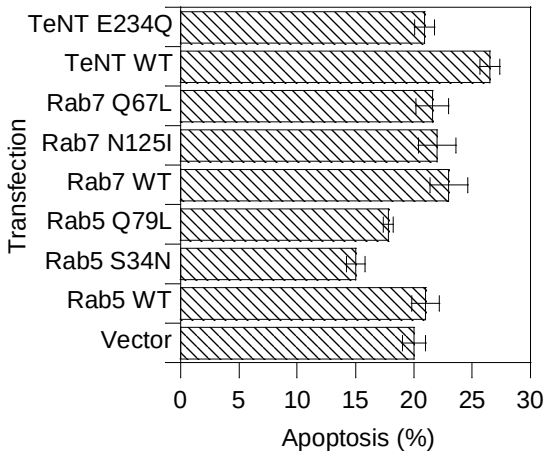

Fig.9A; Rodriguez *et al*

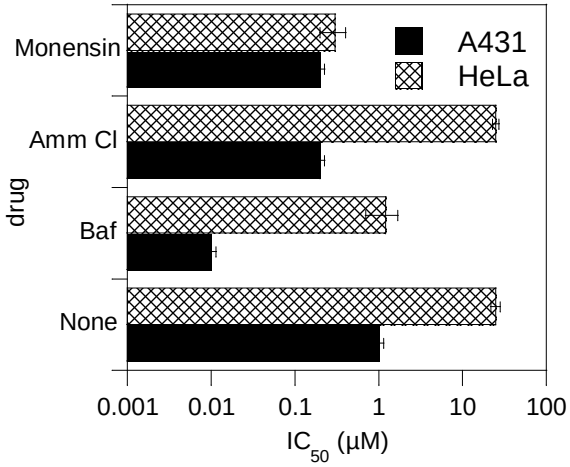

Fig.9B; Rodriguez *et al*

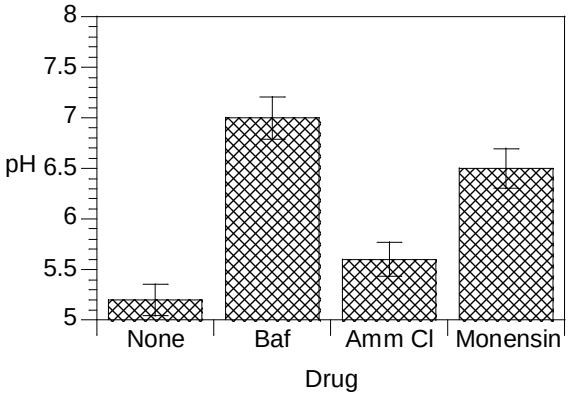

Capítol II:

A CYTOTOXIC RIBONUCLEASE VARIANT WITH A DISCONTINUOUS NUCLEAR LOCALIZATION SIGNAL CONSTITUTED BY BASIC RESIDUES SCATTERED OVER THREE AREAS OF THE MOLECULE

A CYTOTOXIC RIBONUCLEASE VARIANT WITH A DISCONTINUOUS NUCLEAR LOCALIZATION SIGNAL CONSTITUTED BY BASIC RESIDUES SCATTERED OVER THREE AREAS OF THE MOLECULE

M. Rodríguez[1], A. Benito[1], P. Tubert[1], J. Castro[1], M. Ribó[1], B. Beaumelle[2] and M. Vilanova[1]*

[1] Laboratori d'Enginyeria de Proteïnes, Departament de Biologia, Facultat de Ciències, Universitat de Girona, Campus de Montilivi, 17071 Girona, Spain. [2] UMR 5539 CNRS, Dept Biologie-Santé, Université Montpellier II, 34095 MONTPELLIER CEDEX 05, France

*To whom correspondence should be addressed. Fax: +34-972-418150. E-mail: maria.vilanova@udg.es

Running title: A new NLS spread over 90 residues of the protein.

Abbreviations: arm, armadillo motif; DTT dithiothreitol; GST, glutathione S-transferase; HP-RNase, human pancreatic-ribonuclease; IBB, importin β binding; IPTG, isopropylthiogalactoside; MALDI-TOF, matrix-assisted laser desorption/ionization time-of-flight; N1N2, N1N2 phosphoprotein; NLS, nuclear localization signal; PBS, phosphate-buffered saline; PCR, polymerase chain reaction; PMSF, phenylmethylsulfonylfluorid; Rb, human retinoblastoma protein.

SUMMARY

Nuclear import of proteins is determined by specific signals that allow them to bind to receptors that mediate their energy-dependent transport through the nuclear pore. These signals are termed nuclear localization signals and do not constitute a specific consensus sequence. Among them, the most characterized ones correspond to monopartite and bipartite nuclear localization signals, which interact with the importin α/ß heterodimer. We previously described a cytotoxic variant of human pancreatic-ribonuclease that is actively transported into the nucleus. Here we show that this protein interacts with importin α through different basic residues including Lys1 and the arginine clusters 31-33 and 89-91. Although these residues are scattered along the sequence, they are close in the three-dimensional structure of the protein and their topological disposition strongly resembles that of a classical bipartite nuclear localization signal.

Keywords: Human pancreatic ribonuclease, NLS, importin α, molecular recognition, protein-protein interactions, nuclear import.

INTRODUCTION

The nucleocytoplasmic transport of macromolecules occurs through nuclear pore complexes embedded within nuclear envelope. Nuclear proteins and RNAs are shuttled from their site of synthesis to their final destination by an active and selective mechanism that is mediated by signal-dependent binding to specific and saturable receptors[1]. These localization signals have been identified for several classes of cargo molecules. The first and best characterized nuclear targeting signals are the classical nuclear localization signals (NLS), which are composed of one or more clusters of basic amino acids[2] although they do not correspond to a specific consensus sequence. Identified NLSs are generally classified into two distinct groups termed monopartite NLSs, which contain a single cluster of basic amino acids, and bipartite NLSs, which contain two basic clusters separated by a linker of 10-12 non-conserved amino acids. In bipartite NLSs a larger downstream basic cluster resembles a monopartite NLS, but is not sufficient by itself and requires the smaller upstream cluster to target a protein to the nucleus. The spacer region is tolerant to mutations[3] and can also be replaced by 20 Ala residues[4]. Other sequence motifs, longer than these classical signals, have been described to facilitate the nuclear import of proteins. This is the case of the M9 sequence in hnRNP A1[5] and NLSs of ribosomal proteins, such as L23a[6] and L5[7]. In addition to linear NLSs, residues that come together upon folding into tertiary structure are postulated to contribute to nuclear import of histones[8].

The nuclear import of most cargo proteins that contain an NLS is mediated by a receptor, which is a heterodimer formed by importin α and importin ß[9]. Importin α contains both an NLS binding domain and an importin ß binding (IBB) domain. Importin ß is responsible for the translocation of the complex through the nuclear pore (for a review, see[10]). In the absence of importin ß, a segment of the IBB domain occupies the NLS binding site, thereby preventing NLS binding[11]. Importin α/ß heterodimer is not the sole nuclear import receptor and, for instance, more than ten different proteins that function as importins have been identified in yeast (for a review see[12]).

Importin α contains hydrophilic N- and C-terminal regions and a large central domain that consists of ten helical repeated modules known as armadillo (arm) motifs[13]. Each arm motif has an approximate triangular cross-section formed by three α-helices. The reported structures of the complex between importin α and different monopartite and

bipartite NLS peptides have provided the structural basis of the versatile specificity of this receptor[13;14;15;16]. The flexible arm repeats create a binding groove for both monopartite and bipartite NLSs. The NLS binding groove is lined by a regular array of conserved Asn and Trp residues that spatially accommodate the Lys and Arg residues from an NLS. These basic residues are also stabilized by acidic residues of the importin that line the binding pockets for each NLS residue. There are two binding pockets: a major one essentially occupied by monopartite NLSs and formed by Arm2 to Arm4; and a second or minor one, closer to the C-terminus, which can be occupied by the N-terminal portion of bipartite NLSs and essentially comprises Arm repeats 7 and 8. The array of Asn and Trp is interrupted by two conserved residues, Arg and Tyr, which correspond to a less defined region that specifically binds to the linker region of bipartite NLS[14;15;16;17]. Other NLS motifs interact with the major or minor sites and peptide binding occurs in alternative modes depending on the NLS[15;16].

We previously showed that the replacement of residues 89 and 90 by Arg in a variant of human pancreatic-ribonuclease (HP-RNase) confers to this protein (named PE5) the ability to be transported into the nucleus in an energy- and Ran-dependent manner[18]. Nevertheless, no conventional NLS could be identified in PE5. Here we report that PE5 contains an NLS composed of three basic regions that, although separated by more than 90 residues in the primary structure, cluster in the three-dimensional structure of the protein to reach a topological disposition equivalent to that of a bipartite NLS.

RESULTS

PE5 binds to importin α.

We previously showed that replacement of residues Gly89 and Ser90 by Arg in PM5 (a HP-RNase variant, which presents only five changes compared to wild-type enzyme[19]) enables this variant, namely PE5, to be efficiently transported into the nucleus by a mechanism that requires ATP and Ran[18]. These introduced Arg, together with the pre-existing Arg91, generated a basic cluster in an exposed loop of the protein (Figure 1). Classic monopartite and bipartite NLSs are defined by one or two stretches of basic amino acids. Since attempts to identify an NLS around this triplet of arginines using software PredictNLS[20] (http://cubic.bioc.columbia.edu/predictNLS) and PSORT II[21] (http://psort.nibb.ac.jp) were unsuccessful, we concluded that PE5 does not possess a conventional NLS. Nevertheless, it was possible that although PE5 did not own an NLS,

it was imported by a piggyback mechanism after binding to an NLS-containing partner (for a review of this mechanism see[10]). To examine this possibility, we tested whether PE5 was able to directly interact with a variant of importin α from *Xenopus laevis*[22] that lacks the IBB domain and is fused to GST (see material and methods for details). The IBB domain was deleted because, in the absence of importin β, part of the IBB domain occupies the major NLS binding site[11], thereby decreasing its affinity for NLSs[23]. We tested the interaction of Δ59-529Impα with PE5 in a GST-pull-down assay. Unspecific interaction to the affinity matrix was tested in a parallel experiment using GST. After loading the same amount of PE5 to each column, specifically retained proteins were eluted with reduced glutathione and identified in a zymogram. The same assay was performed using the parental enzyme, PM5, which lacks residues Arg89 and Arg90. As shown in Figure 2, PE5 binds to the Δ59-529Impα-GST but not to GST while PM5 neither binds to Δ59-529Impα-GST nor to GST.

The NLS of PE5 is constituted by residues scattered along the sequence.

Some proteins contain non-classical nuclear targeting signals that are longer than the two conventional motifs. For instance, it has been recently described[24] that the tumor suppressor protein Smad4 has an NLS located in its MH1 domain and that some of the basic residues that are necessary for NLS functionality are separated by more than 30 residues in the sequence. This protein is imported to the nucleus after binding to importin α/β heterodimer[24]. A molecular model of a fragment of the protein, which includes the basic residues important for the NLS functionality indicated that the disposition of these residues at the surface protein resembled that of an inverted bipartite NLS[24].

This kind of NLS is difficult to find in sequence databases so we investigated whether PE5 basic residues displayed a similar disposition. We compared the distribution and spacing of basic residues in Smad4 NLS, bipartite NLSs and PE5. To this end, three dimensional models of Smad4 and PE5 were generated using the Swissmodel software[25,26] (see materials and methods for details).

Comparison of PE5 and Smad4 models revealed that the residues required for NLS functionality in Smad4 share a similar disposition with two stretches of basic residues in PE5, namely residues Arg31 to Arg33 and residues Arg89 to Arg91 (Figure 3A). Indeed, the α carbon interatomic distances between both triplets of Arg in the PE5 model (Table I) and the distances between the residues involved in the NLS of Smad4

(Table II) are very similar. This is especially true if we compare the distances between residue 81 and residues 45, 46 and 48 of Smad4 with the distances between residue 32 and residues 89, 90 and 91 of PE5.

Comparison of the PE5 model and different bipartite NLSs[14;15;16] showed that the clusters of basic residues in the structure of bipartite NLSs are clearly at a greater distance than the two clusters of Arg in PE5. However, we found that Lys1 and residues 89-91 in the PE5 model are separated by the same distance as that found between both clusters in the bipartite NLS (see Figure 3B as example). In this case, the position of Arg33 in PE5 was nearly equivalent to that of Lys161 in the linker of nucleoplasmin NLS, whose side chain makes specific contacts with yeast importin α in a previously described structure[15].

To investigate the role of these residues in the nuclear import of PE5, we removed the positive charge of residues 1, 31, 32 and 33. These variants were constructed from PE5cys to allow protein labeling with a fluorophore. Lys1, Arg32 and Arg33 were replaced by Ala in the variants PE5-K1Acys, PE5-R32Acys and PE5-R33Acys, respectively. Arg31 and Arg32 were replaced by Glu to generate variants PE5-R31Ecys and PE5-R32Ecys. These latter variants, carrying more drastic mutations, were conceived to introduce electrostatic repulsion and test whether positions 31 and 32 made a contribution, even if minor, to importin α – RNase interaction.

We used digitonin permeabilized cells in a conventional nuclear import assay[27] to directly introduce the different fluorescently labelled variants into the cytosol and examine whether they were targeted to the nucleus. Digitonin is known to effectively permeabilize the plasma membrane but not the nuclear envelope[28]. The assay was performed in the presence of an ATP regenerating system. As expected[18], PE5 was efficiently imported into the nucleus within 12 minutes at 30ºC, whereas the parental variant PM5 was not imported (Figure 4A). None of the variants used to analyze the role of residues 31 to 33 were imported as efficiently as PE5cys but nuclear import was slightly more affected in the variants carrying a Glu (Figure 4B). Substitution of Lys1 by Ala completely abolished the transport of the RNase to the nucleus showing that Lys1 in PE5 is critical for nuclear import. To exclude the possibility that the mutations had destabilized the proteins we checked their thermal stability. Figure 5 shows the normalized thermal unfolding curves of each one of the variants. A decrease in the $T_{1/2}$ respective to PE5 was detected for all the variants, being the most affected PE5-R33Acys (3.9ºC) and PE5-K1Acys (6.1ºC). This decrease in thermal stability did not

affect the nuclear import assays since they were performed at 30ºC and at this temperature all the variants are 100% folded with the exception of K1A which is folded in a 90%.

DISCUSSION

Topogenic sequences are protein sequence determinants that specify the intracellular targeting of proteins[29] and are generally considered as more or less continuous sequences. In the case of NLSs, apart from the conventional monopartite and bipartite signals, there is high sequence diversity. Several alternate sequences have been described, and from the analysis of nuclear proteins it became apparent that many of them probably use other still unknown entry mechanisms or piggyback on cargo that does contain a NLS[12].

PE5 is a cytotoxic variant of HP-RNase, which carries a NLS, since it specifically binds to importin α (Figure 2) and is imported into the nucleus in an energy-and Ran-dependent manner[18]. The introduced Arg89 and Arg90 are necessary for nuclear transport[18]. Because the inserted residues, together with Arg91, create a cluster of three basic residues, we were surprised that the sequence of PE5 did not match any consensus sequence of conventional monopartite or bipartite NLS. Arg triplets are described in several nuclear proteins as a part of conventional RRRX NLSs. However, our results clearly show that none of the two investigated Arg triplets of PE5 act individually as a NLS. Other proteins that are imported into the nucleus and interact with an importin receptor through basic residues do not contain a conventional NLS. For example, the four human core histones are known to possess, within their globular domain, an NLS that seems to be based on the three-dimensional structure of the globular domain and that is constituted by residues that span along the sequence[8]. Nevertheless, core histones are transported to the nucleus by a mechanism independent of importin α[30;31]. Other proteins that are imported following binding to importin α also contain non-classical bipartite NLSs. The MH1 domain of the tumor suppressor protein Smad 4 is imported into the nucleus by the α/ß importin heterodimer. In this case, although the basic residues that conform the NLS are separated by more than 30 residues in the sequence[24], their three-dimensional disposition resembles an inverted classical bipartite NLS motif in which the smaller basic cluster is located downstream the larger basic cluster.

We examined whether the NLS of PE5 could be constituted by basic residues exposed at the surface of the protein, topologically arranged in a way that could mimic a bipartite NLS, or alternatively, mimic the NLS found in Smad4. We found residues that matched the space distribution of basic residues in both types of NLSs, and new variants of PE5 lacking the positive charges at these positions were constructed and their nuclear import tested. Our results indicate that PE5 nuclear import requires several basic residues located in three different regions of the sequence. It is interesting to note that it has been recently described[32] that the intracellular domain of ErbB-2 protein contains an NLS composed of three clusters of basic residues (^{655}KRRQQKIRKYTMRR). This NLS resembles a bipartite NLS in which a third cluster of basic residues is positioned in the linker region.

Four different structures of peptides reproducing three bipartite NLSs bound to truncated forms of yeast (*S. cerevisiae*) or mouse importin α have been described. They correspond to the NLSs of nucleoplasmin[14], *Xenopus laevis* N1N2 phosphoprotein (N1N2)[16] and retinoblastoma protein (Rb)[16] bound to mouse importin α, and nucleoplasmin[15] bound to yeast importin α. Residues interacting with the major binding pocket of importin α are denoted P_1 to P_5 whereas residues interacting with the minor one are denoted P'_1 to P'_3. The structural data, together with the accumulated knowledge on functional NLSs and mutagenesis studies allowed to define a bipartite NLS consensus sequence[16]. The most important residue for binding to importin α major site is located in P_2 (and preferentially corresponds to a Lys) but positions P_3 and P_5 also make an important energetic contribution to the binding (about two-thirds of P_2 contribution)[33]. In the minor site, the most important residue for binding is an Arg at position P'_2. The Cα interatomic distances between these positions are highly conserved in the different NLSs. Interestingly, P_2 to P'_2 and P_3 to P'_2 Cα interatomic distances are in close agreement with those found between residues Arg90-Lys1 and Arg89-Lys1 in the modelled structure of PE5 (Figure 6).

The region that links both basic clusters in a bipartite NLS is highly tolerant to mutations and can be artificially substituted by 20 Ala residues[4]. Nevertheless, functional and structural available data showed that this spacer makes multiple interactions with residues of arm5 and arm6 repeats of importin α in a species-dependent way. The linker residues mainly make main chain interactions with the side chains of conserved importin α residues, which line an important part of the surface groove. The side chain interactions of the linker residues are scarce. In the case of

nucleoplasmin NLS, they are completely absent when it is bound to mouse importin α and are limited to Lys161 side chain when complexed with yeast importin α[14;15]. The discrepancy has been attributed to structural differences between the two importins, *i.e.* the yeast protein structure appears slightly more "open" than the mouse importin[11]. Because basic clusters bind more tightly to the importins, the curvatures of the two proteins may be compensated by a different binding in the linker region[16]. The structure of the nucleoplasmin linker is more similar to that of Rb than that of N1N2[16]. In the case of Rb NLS, side chain interactions in the linker region are limited to Asn868 and Lys871 and in N1N2 NLS to Lys547[16]. Cα interatomic distances between Lys161 of nucleoplasmin, Asn868 of Rb and Lys547 of N1N2 NLSs and their respective P_2, P_3 and P'_2 binding pockets are shown in Figure 6. It is interesting to note that in the case of the nucleoplasmin and Rb these distances closely match those of residue Arg33 with Arg89, Arg90 and Lys1 in PE5, and that the deletion of any of these basic side chains generated a significant reduction of nuclear import efficiency.

The spatial distribution of the identified residues of PE5 involved in nuclear import is similar to the conformational organization of the residues that, in bipartite NLS, occupy most of the critical positions responsible for the interaction with importin α. We describe here a new class of discontinuous NLS consisting of three protein regions, which are scattered over 90 residues of the sequence. They nevertheless fold together in a conformation that is very close to that of a classical bipartite NLS. In PE5, some residues play analogous roles to those of the larger and smaller binding sites of bipartite NLS. In a bipartite NLS, the linker region seems to have two different functions. First, it is a spacer that separates the two clusters of basic sequences to a precise distance that allows their binding to importin α. Second, it also constitutes a region of the NLS that provides further interactions with the importin, thereby strengthening the binding of the complex[17]. The basic residues of PE5, which mimic the linker residues that more efficiently interact with importin α seem to fulfill both linker functions.

Discontinuous epitopes consist of stretches of residues that are not contiguous in the sequence but are brought together by the folding of the polypeptide chain. Analogously, the NLS of PE5 resembles a discontinuous bipartite NLS. These results have implications for the identification of NLS in nuclear proteins and provide a new example of the high versatility of importin α in recognizing a broad spectrum of signals.

MATERIALS AND METHODS

Construction of HP-RNase variants. Construction of PM5, PE5, PM5cys and PE5cys HP-RNase variants has been described elsewhere[18;19]. PM5 was obtained from wild type HP-RNase and incorporates the mutations Lys4 Ala, Lys6 Ala, Gln9 Glu, Asp16 Gly and Ser17 Asn[19]. PE5 was obtained from PM5 replacing Gly89 and Ser90 by Arg[18]. PM5cys and PE5cys were obtained from PM5 and PE5, respectively, and bear an additional Cys at the C-terminus of the protein[18]. PE5cys variants incorporating substitutions Lys1 Ala (PE5-K1Acys), Arg31 Glu (PE5-R31Ecys), Arg32 Ala (PE5-R32Acys), Arg32 Glu (PE5-R32Ecys) and Arg33 Ala (PE5-R33Acys) were constructed by site-directed mutagenesis following the strategy described elsewhere[34]. Oligonucleotides used for introducing mutations Lys1 Ala (PE5-K1Acys), Arg31 Glu (PE5-R31Ecys), Arg32 Ala (PE5-R32Acys), Arg32 Glu (PE5-R32Ecys) and Arg33 Ala (PE5-R33Acys) were: 5'-TAT ACA TAT GGC AGA ATC TGC TGC T-3'; 5'-CAT ATT TCG GCG CTC CAT CAT TTG ATT-3;, 5'-AGT CAT ATT TCG AGC CCT CAT CAT TTG-3; 5'-AGT CAT ATT TCG TTC CCT CAT CAT TTG-3; 5'-TTG AGT CAT ATT AGC GCG CCT CAT CAT-3', respectively). PCR products, corresponding to the whole mutated genes, were digested with *Sal*I and *Nde*I and inserted into plasmid pM5[19] from which the HP-RNase gene had been excised by digestion with the same enzymes. Screening was performed by restriction analysis and confirmed by sequence analysis at the Molecular Biology Facility of the Universitat de Girona.

Ribonuclease expression and purification. Expression and purification of the HP-RNase variants was carried out essentially as described[35]. Briefly, frozen pellets from 1 L of induced culture were resuspended in 30 ml of 50 mM Tris/HCl, 10 mM EDTA pH 8. Cells were lysed using a French Press and inclusion bodies were harvested by centrifugation. Pellets were then solubilized by resuspension in 10 ml of 6 M guanidinium chloride, 2 mM EDTA, 0.1 M Tris-acetate, pH 8.5. Reduced glutathione (GSH) was added to a final concentration of 0.1 M, the pH was adjusted to 8.5 with solid Tris, and the samples were incubated at room temperature for 2 h under nitrogen. Insoluble material was then removed by centrifugation. Solubilized protein was diluted dropwise into 0.5 M L-arginine, 1 mM oxidized glutathione, 2 mM EDTA, Tris-Acetate 0.1 M, pH 8.5, and then incubated at 10 ºC for at least 24 h. The pH was then lowered to 5 with acetic acid. The protein was concentrated by ultrafiltration and dialyzed against

50 mM sodium acetate, pH 5. Precipitated or insoluble material was eliminated by centrifugation and the refolded sample was then loaded onto a Mono-S HR 5/5 column (Amersham Biosciences). Recombinant HP-RNase variants were eluted with a linear gradient of 0-600 mM NaCl. Fractions containing pure ribonucleases were dialyzed against water, lyophilized and stored at -20 ºC.

Depending on the variant, a yield of 5 to 20 mg of protein per liter of culture was obtained. The molecular mass of each variant was confirmed by MALDI-TOF mass spectrometry using a Bruker-Biflex equipment in the Biocomputation and Protein Sequencing Facility of the Institut de Biotecnologia i Biomedicina of the Universitat Autònoma de Barcelona (Spain).

The protein concentration of each variant was determined by UV spectroscopy using an extinction coefficient of ε_{278}=8200 $M^{-1}cm^{-1}$, calculated using the method of Gill and von Hippel[36].

Construction of truncated importin α. The plasmid expressing the *Xenopus laevis* importin α[22] was kindly supplied by Dr. Dirk Görlich (ZMBH, Heidelberg). A truncated variant of this protein was constructed in order to remove an autoinhibitory segment in the IBB domain. This domain was identified by comparing the amino acid sequence of mouse and *Xenopus* importin α using the Blast Two Sequences program. The alignment showed that the sequence between residues 41 to 51 of *Xenopus* importin α was homologous to the autoinhibitory segment in the IBB domain of mouse importin α (spanning residues 44 to 54[11]). The DNA fragment of importin α gene, coding for residues 59 to 529, was amplified by PCR using two oligonucleotides that inserted at 3' and 5'ends a *Bam*HI and *Xho*I restriction sites, respectively. The fragment was digested with these enzymes and cloned into plasmid pGEX4T2 (Amersham Biosciences). The resulting truncated protein, namely Δ59-529Impα, is thereby fused to the C-terminus of glutathione S-transferase (GST).

Importin α binding assay. *E. coli* BL21 cells harbouring the plasmid encoding Δ59-529Impα, or pGEX4T2 in the control experiments, were grown at 30ºC in 2xYT medium containing 100 μg/ml ampicillin until an OD_{550} of 1.5 was reached. Protein expression was induced by adding IPTG to 1 mM. After 3-4 hours of further incubation, cells were collected by centrifugation, resuspended in binding buffer (50 mM Tris, 250 mM NaCl, 5 mM $MgCl_2$, 1 mM PMSF pH 7.5) and lysed with a French press. The sample was centrifuged in order to remove the cellular debris and the supernatant corresponding to 250 mL of culture (about 1 mg of truncated importin) was incubated

for 1.5 hours at 4ºC and 80 rpm with 250 µl of glutathione Sepharose 4B (Amersham Biosciences) previously equilibrated with binding buffer. The matrix was poured into a disposable column and extensively washed with binding buffer before applying 0.2 mg of an HP-RNase variant in binding buffer. Beads were then incubated for 2 h at 4ºC and 80 rpm, washed extensively with binding buffer until the OD_{280} dropped to zero and elution was performed with 2 mL of 50 mM Tris, 12 mM reduced glutathione . Fractions (250 µl) were diluted in SDS sample buffer and analyzed in a zymogram, essentially as described[37].

Protein labeling. The different variants incorporating a C-terminal Cys were reacted with Alexa Fluor® 594 C5 maleimide (Molecular Probes) at room temperature, essentially as recommended by the manufacturer. Before the reaction, a 10-fold molar excess of dithiothreitol (DTT) was added to the protein solution to reduce the disulfide bond formed during the purification process between the additional Cys present in the variants and a glutathione molecule. After 20 min, DTT was removed by desalting on a Sephadex G-25 column and a 20-fold molar excess of reactive dye (20 mM in PBS) was immediately added to the protein. The reaction was stopped after 2h by adding 1 mM reduced glutathione to consume the excess of thiol-reactive reagent. The conjugates were dialyzed against PBS at 4ºC, then filter-sterilized and stored at –20°C.

Nuclear import assays. Cytosolic fraction (~3 mg/ml) was purified from HeLa S3 cells as described[28] and stored at –80°C. Import reactions were performed at 30°C for 12 min using digitonin-permeabilized HeLa cells[27], cytosol, ~2 µg/ml of fluorescent substrate (Alexa Fluor 594-RNase) and an ATP regenerating system (1 mM ATP, 5mM phosphocreatine and 20 U/ml creatine phosphokinase)[38]. Cells were then washed and fixed by 3.7% paraformaldehyde. The nucleus was stained with 100 nM Sytox green (Molecular Probes) in PBS for 15 min before washing and mounting in 100 mM Tris-HCl, pH 8.5 containing 25% (v/v) glycerol, 10% Mowiol and 0.5 M 1,4-diazabicyclo-[2.2.2]octane. Cells were finally examined under a Leica confocal microscope using a 63x lens, a band-pass fluorescein filter for Sytox green and a long-pass 590 nm filter for Alexa Fluor 594. Bleed through from one channel to the other was negligible. Medial optical sections were recorded.

Protein modelling. *The structures of Smad4 and PE5 were modelled using the SwissModel and the SwissPDBViewer (v. 3.7) protein modelling program[25;26], which are both available from the ExPASy website (www.expasy.ch/spdbv). The sequence of Smad4 MH1 domain (only residues 19 to 142 were considered) and PE5 (residues 1 to*

128) were aligned superimposed using the SwissModel against the MH1 domain of Smad3[39] (pdb accession code 1HMD) and the HP-RNase variant PM7[40] (pdb accession code 1DZA), respectively. These proteins were selected on the basis of its high sequence conservation with Smad4 and PE5. The iterative Magic Fit function was used but the alignments were further optimized manually. The resulting models were analyzed using the What_Check verification tool[41] and minor problems were solved after subjecting the models to 500 steps of steepest descent energy minimization.

Determination of thermal stability by UV absorbance. The conformational stability of the HP-RNase variants was determined using UV absorbance spectroscopy to measure the change in environment of the aromatic residues during protein thermal unfolding. The protein was dissolved at 0.5 mg/ml in a 50 mM acetate pH 5.0 and the UV absorbance was monitored at 287 nm. The temperature was raised from 5 to 74ºC in 2-4ºC increments and the decrease in UV absorbance was registered after a 5 min equilibration at each temperature. Temperature-unfolding transitions curves were fitted to a two-state thermodynamic model combined with sloping linear functions for the native and denatured states, as described elsewhere[42].

ACKNOWLEDGEMENTS

This work was supported by grants from the *Ministerio de Ciencia y Tecnologia* (BMC2003-08485-CO2-02) and *Generalitat de Catalunya* (SGR2001-00196). We are also indebted to a PICS grant between the CNRS and the Universitat de Girona (PICS2005-3, Generalitat de Catalunya). M.R. and P.T. gratefully acknowledge pre-doctoral fellowships from MEC. J.C gratefully acknowledges a pre-doctoral fellowship from Universitat de Girona. We are very grateful to Dr. Dirk Görlich (Heidelberg) for providing us with the expression vector for *Xenopus laevis* importin α.

REFERENCES

1. Nakielny, S. & Dreyfuss, G. (1996). The hnRNP C proteins contain a nuclear retention sequence that can override nuclear export signals. *J Cell Biol* **134**, 1365-1373.
2. Dingwall, C. & Laskey, R. A. (1991). Nuclear targeting sequences--a consensus? *Trends Biochem Sci* **16**, 478-481.
3. Robbins, J., Dilworth, S. M., Laskey, R. A. & Dingwall, C. (1991). Two interdependent basic domains in nucleoplasmin nuclear targeting sequence: identification of a class of bipartite nuclear targeting sequence. *Cell* **64**, 615-623.
4. Makkerh, J. P., Dingwall, C. & Laskey, R. A. (1996). Comparative mutagenesis of nuclear localization signals reveals the importance of neutral and acidic amino acids. *Curr Biol* **6**, 1025-1027.
5. Pollard, V. W., Michael, W. M., Nakielny, S., Siomi, M. C., Wang, F. & Dreyfuss, G. (1996). A novel receptor-mediated nuclear protein import pathway. *Cell* **86**, 985-994.
6. Jakel, S. & Gorlich, D. (1998). Importin beta, transportin, RanBP5 and RanBP7 mediate nuclear import of ribosomal proteins in mammalian cells. *Embo J* **17**, 4491-4502.
7. Claussen, M., Rudt, F. & Pieler, T. (1999). Functional modules in ribosomal protein L5 for ribonucleoprotein complex formation and nucleocytoplasmic transport. *J Biol Chem* **274**, 33951-33958.
8. Baake, M., Doenecke, D. & Albig, W. (2001). Characterisation of nuclear localisation signals of the four human core histones. *J Cell Biochem* **81**, 333-346.
9. Gorlich, D., Kostka, S., Kraft, R., Dingwall, C., Laskey, R. A., Hartmann, E. & Prehn, S. (1995). Two different subunits of importin cooperate to recognize nuclear localization signals and bind them to the nuclear envelope. *Curr Biol* **5**, 383-392.
10. Mattaj, I. W. & Englmeier, L. (1998). Nucleocytoplasmic transport: the soluble phase. *Annu Rev Biochem* **67**, 265-306.
11. Kobe, B. (1999). Autoinhibition by an internal nuclear localization signal revealed by the crystal structure of mammalian importin alpha. *Nat Struct Biol* **6**, 388-397.

12. Macara, I. G. (2001). Transport into and out of the nucleus. *Microbiol Mol Biol Rev* **65**, 570-594.
13. Conti, E., Uy, M., Leighton, L., Blobel, G. & Kuriyan, J. (1998). Crystallographic analysis of the recognition of a nuclear localization signal by the nuclear import factor karyopherin alpha. *Cell* **94**, 193-204.
14. Fontes, M. R., Teh, T. & Kobe, B. (2000). Structural basis of recognition of monopartite and bipartite nuclear localization sequences by mammalian importin-alpha. *J Mol Biol* **297**, 1183-1194.
15. Conti, E. & Kuriyan, J. (2000). Crystallographic analysis of the specific yet versatile recognition of distinct nuclear localization signals by karyopherin alpha. *Structure* **8**, 329-338.
16. Fontes, M. R., Teh, T., Jans, D., Brinkworth, R. I. & Kobe, B. (2003). Structural basis for the specificity of bipartite nuclear localization sequence binding by importin-alpha. *J Biol Chem* **278**, 27981-27987.
17. Leung, S. W., Harreman, M. T., Hodel, M. R., Hodel, A. E. & Corbett, A. H. (2003). Dissection of the karyopherin alpha nuclear localization signal (NLS)-binding groove: functional requirements for NLS binding. *J Biol Chem* **278**, 41947-41953.
18. Bosch, M., Benito, A., Ribo, M., Puig, T., Beaumelle, B. & Vilanova, M. (2004). A nuclear localization sequence endows human pancreatic ribonuclease with cytotoxic activity. *Biochemistry* **43**, 2167-2177.
19. Canals, A., Ribo, M., Benito, A., Bosch, M., Mombelli, E. & Vilanova, M. (1999). Production of engineered human pancreatic ribonucleases, solving expression and purification problems, and enhancing thermostability. *Protein Expr Purif* **17**, 169-181.
20. Cokol, M., Nair, R. & Rost, B. (2000). Finding nuclear localization signals. *EMBO Rep* **1**, 411-415.
21. Nakai, K. & Horton, P. (1999). PSORT: a program for detecting sorting signals in proteins and predicting their subcellular localization. *Trends Biochem Sci* **24**, 34-36.
22. Gorlich, D., Prehn, S., Laskey, R. A. & Hartmann, E. (1994). Isolation of a protein that is essential for the first step of nuclear protein import. *Cell* **79**, 767-778.

23. Catimel, B., Teh, T., Fontes, M. R., Jennings, I. G., Jans, D. A., Howlett, G. J., Nice, E. C. & Kobe, B. (2001). Biophysical characterization of interactions involving importin-alpha during nuclear import. *J Biol Chem* **276**, 34189-34198.
24. Xiao, Z., Latek, R. & Lodish, H. F. (2003). An extended bipartite nuclear localization signal in Smad4 is required for its nuclear import and transcriptional activity. *Oncogene* **22**, 1057-1069.
25. Guex, N. & Peitsch, M. C. (1997). SWISS-MODEL and the Swiss-PdbViewer: an environment for comparative protein modeling. *Electrophoresis* **18**, 2714-2723.
26. Schwede, T., Kopp, J., Guex, N. & Peitsch, M. C. (2003). SWISS-MODEL: An automated protein homology-modeling server. *Nucleic Acids Res* **31**, 3381-3385.
27. Moore, M. S. & Blobel, G. (1992). The two steps of nuclear import, targeting to the nuclear envelope and translocation through the nuclear pore, require different cytosolic factors. *Cell* **69**, 939-950.
28. Kehlenbach, R. H., Dickmanns, A. & Gerace, L. (1998). Nucleocytoplasmic shuttling factors including Ran and CRM1 mediate nuclear export of NFAT In vitro. *J Cell Biol* **141**, 863-874.
29. Blobel, G. (1980). Intracellular protein topogenesis. *Proc Natl Acad Sci U S A* **77**, 1496-1500.
30. Baake, M., Bauerle, M., Doenecke, D. & Albig, W. (2001). Core histones and linker histones are imported into the nucleus by different pathways. *Eur J Cell Biol* **80**, 669-677.
31. Muhlhausser, P., Muller, E. C., Otto, A. & Kutay, U. (2001). Multiple pathways contribute to nuclear import of core histones. *EMBO Rep* **2**, 690-696.
32. Chen, Q. Q., Chen, X. Y., Jiang, Y. Y. & Liu, J. (2005). Identification of novel nuclear localization signal within the ErbB-2 protein. *Cell Res* **15**, 504-510.
33. Hodel, M. R., Corbett, A. H. & Hodel, A. E. (2001). Dissection of a nuclear localization signal. *J Biol Chem* **276**, 1317-25.
34. Juncosa-Ginesta, M., Pons, J., Planas, A. & Querol, E. (1994). Improved efficiency in site-directed mutagenesis by PCR using a Pyrococcus sp. GB-D polymerase. *Biotechniques* **16**, 820-823.
35. Ribo, M., Benito, A., Canals, A., Nogues, M. V., Cuchillo, C. M. & Vilanova, M. (2001). Purification of engineered human pancreatic ribonuclease. *Methods Enzymol* **341**, 221-234.

36. Gill, S. C. & von Hippel, P. H. (1989). Calculation of protein extinction coefficients from amino acid sequence data. *Anal Biochem* **182**, 319-326.

37. Bravo, J., Fernandez, E., Ribo, M., de Llorens, R. & Cuchillo, C. M. (1994). A versatile negative-staining ribonuclease zymogram. *Anal Biochem* **219**, 82-86.

38. Efthymiadis, A., Briggs, L. J. & Jans, D. A. (1998). The HIV-1 Tat nuclear localization sequence confers novel nuclear import properties. *J Biol Chem* **273**, 1623-1628.

39. Shi, Y., Wang, Y. F., Jayaraman, L., Yang, H., Massague, J. & Pavletich, N. P. (1998). Crystal structure of a Smad MH1 domain bound to DNA: insights on DNA binding in TGF-beta signaling. *Cell* **94**, 585-594.

40. Pous, J., Canals, A., Terzyan, S. S., Guasch, A., Benito, A., Ribo, M., Vilanova, M. & Coll, M. (2000). Three-dimensional structure of a human pancreatic ribonuclease variant, a step forward in the design of cytotoxic ribonucleases. *J Mol Biol* **303**, 49-60.

41. Hooft, R. W., Vriend, G., Sander, C. & Abola, E. E. (1996). Errors in protein structures. *Nature* **381**, 272.

42. Mozhaev, V. V., Heremans, K., Frank, J., Masson, P. & Balny, C. (1996). High pressure effects on protein structure and function. *Proteins* **24**, 81-91.

Table I: Cα interatomic distances between residues critical for the Smad4 binding to importin α in the modelled structure.

	Lys45	Lys46	Lys48
Arg81	16.49	15.10	20.43

Table II: Cα interatomic distances between candidate residues necessary for nuclear import of PE5 in the modelled structure.

	Arg89	Arg90	Arg91
Lys1	32.19	30.38	28.05
Arg31	16.53	13.71	12.99
Arg32	20.24	17.52	16.83
Arg33	20.23	18.00	17.10

FIGURE LEGENDS

Figure 1: Characteristics of PE5. (A) Amino acid sequence of PE5. The underlined residues (89 and 90) enabled nuclear import. Lys1, Arg31, Arg32 and Arg33 are shown in bold in the sequence. (B) Model structure of PE5 generated from the structure of the highly related variant PM7[40] (see materials and methods for details). Side chain of the exposed residues Arg89, Arg90 and Arg91 are shown. The figure has been drawn using the PyMol, DeLano Scientifics © program.

Figure 2: Importin α interacts with PE5 in a pull-down assay. *Xenopus laevis* truncated importin α-GST was immobilized on a Glutathione sepharose 4B and tested for PE5 and PM5 binding. Unspecific interaction of both proteins with the affinity matrix was tested by loading the same amount of each protein in an equal volume of GST loaded resin. After extensive washing, bound protein was eluted from the columns with reduced glutathione. Analysis of the starting material (loaded) and specifically bound fractions (eluted) was performed using a zymogram assay.

Figure 3: Comparison of the spatial distribution of the NLS of Smad4, nucleoplasmin and PE5. (A) Superposition of the model structures of PE5 (green) and Smad4 MH1 domain (pink). Basic residues important for the nuclear import of PE5 are colored in blue whereas the basic residues of the extended NLS of Smad4 are colored in cyan. (B) Overlapping of the model structure of PE5 (green) and the structure of the nucleoplasmin NLS[14] (pdb accession code 1EJY) (violet). Basic residues critical for ensuring the nuclear localization of PE5 are coloured in blue whereas the basic residues of the extended NLS of nucleoplasmin are coloured in cyan. The figures have been constructed using the program SwissPDBViewer program[25].

Figure 4: Analysis of PE5 residues critical for the nuclear import. (A) HeLa cells were permeabilized with digitonin before adding cytosol and the indicated fluorescent RNase variant (red). Import reactions were performed for 12 min at 30 °C, before fixation and nuclei labelling with Sytox green (green). Cells were then mounted for viewing under a confocal microscope, and medial optical sections were recorded. Bar, 20 µm. (B) Quantification of nuclear import efficiency. The ratio N / (N +C) was

calculated after measuring signal intensity in the nucleus (N) and in the entire cell (N +C) using the ImageQuant Software (Amersham Biosciences).

Figure 5: Normalized thermal unfolding curves for the HP-RNase variants. (■)PE5-R32Acys, (▽) PE5-R32Ecys, (**▼)** PE5-R31Ecys, **(△)** PE5-R33Acys, **(▲)** PE5-K1Acys**.** The $T_{1/2}$ values are 47.7, 45.6, 45.8, 42.3 and 39.6ºC for PE5-R32Acys, PE5-R32Ecys, PE5-R31Ecys**,** PE5-R33Acys**,** PE5-K1Acys, respectively.

Figure 6: The topological distribution of critical residues of the PE5 NLS mimics that of the bipartite NLS. Cα interatomic distances between the selected residues of PE5 (red) compared with those of P_2, P_3, P'_2 and the residue of the linker (L) performing most of the side chain interactions with importin α (black) in different bipartite NLSs. (A) Retinoblastoma protein bipartite NLS[16] (pdb: 1PJM) P_2 corresponds to Lys874, P_3 to Lys875, P'_2 to Arg862 and L to Asn868. (B) N1N2 phosphoprotein bipartite NLS[16] (pdb: 1PJN) P_2 corresponds to Lys551, P_3 to Lys552, P'_2 to Arg538 and L to Lys547. (C) Nucleoplasmin bipartite NLS bound to yeast importin α[15] (pdb: 1EE5). (D) Nucleoplasmin bipartite NLS bound to mouse importin α[14] (pdb: 1EJY). In C and D P_2 corresponds to Lys167, P_3 to Lys168, P'_2 to Arg156 and L to Lys161.

Figure 1

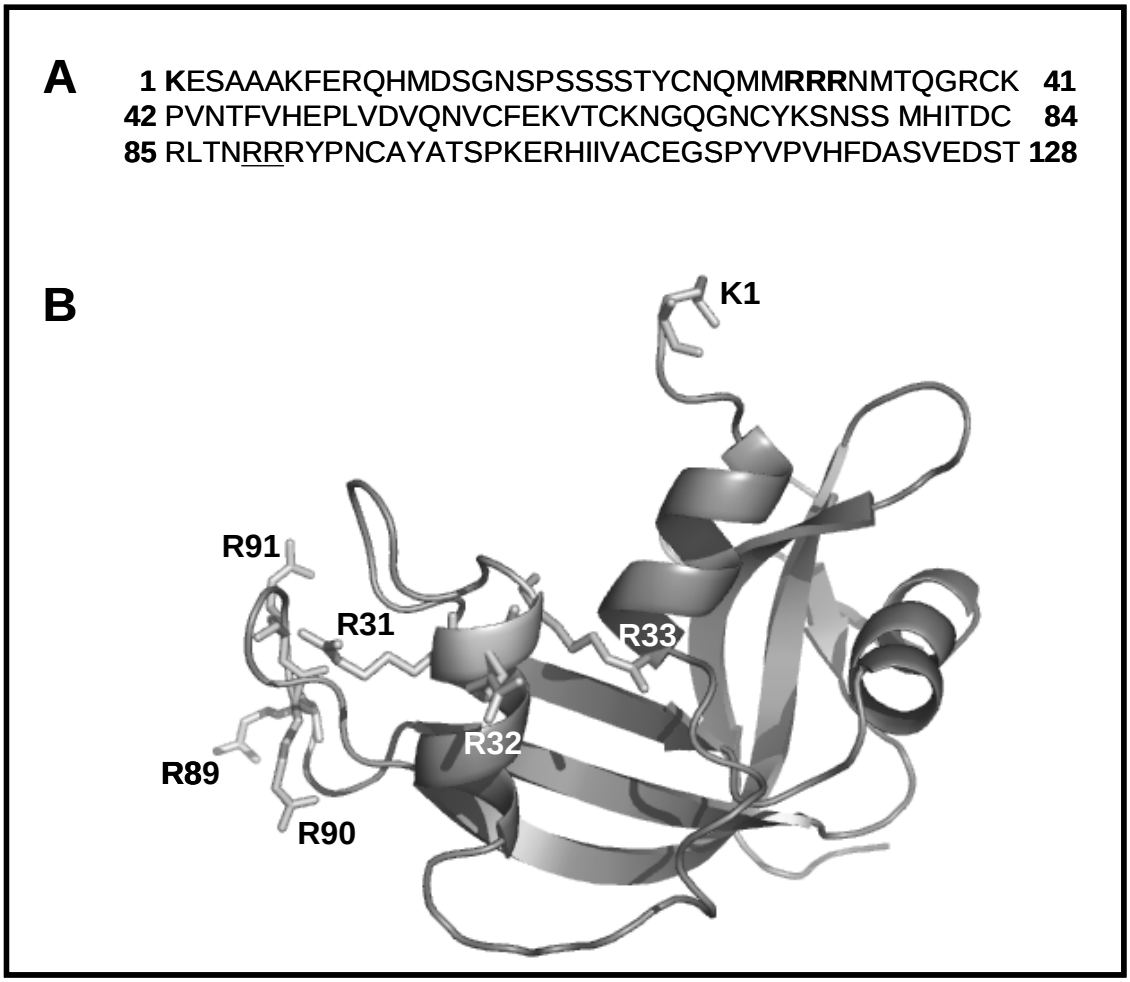
A
1 KESAAAKFERQHMDSGNSPSSSSTYCNQMMRRRNMTQGRCK 41
42 PVNTFVHEPLVDVQNVCFEKVTCKNGQGNCYKSNSS MHITDC 84
85 RLTNRRRYPNCAYATSPKERHIIVACEGSPYVPVHFDASVEDST 128
B
K1
R91
R31
R33
R32
R89
R90

Figure 2

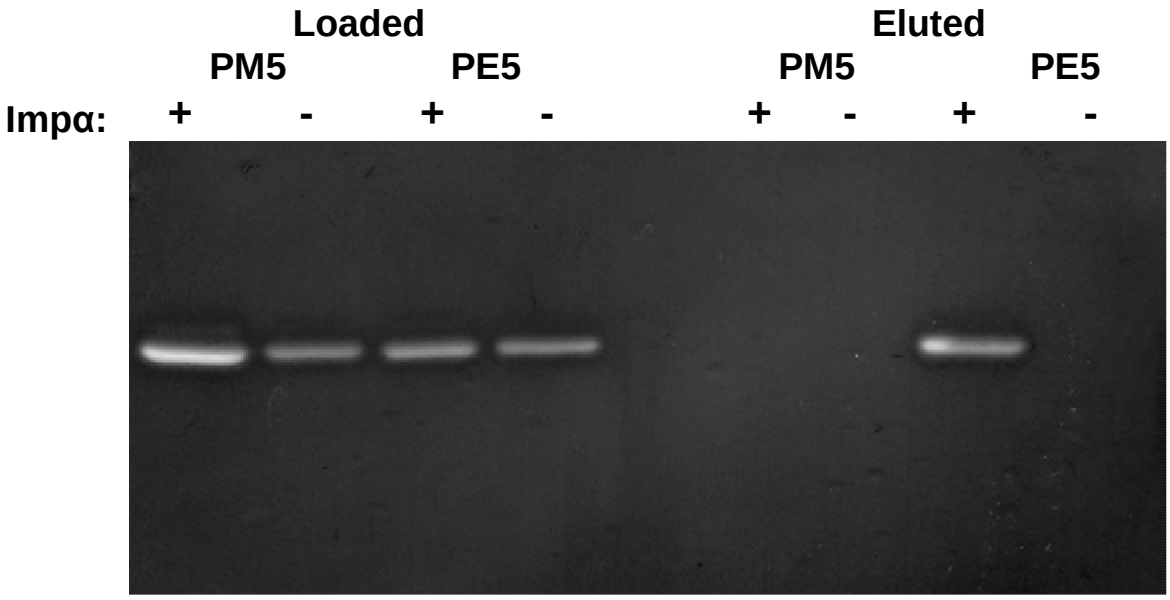

Figure 3

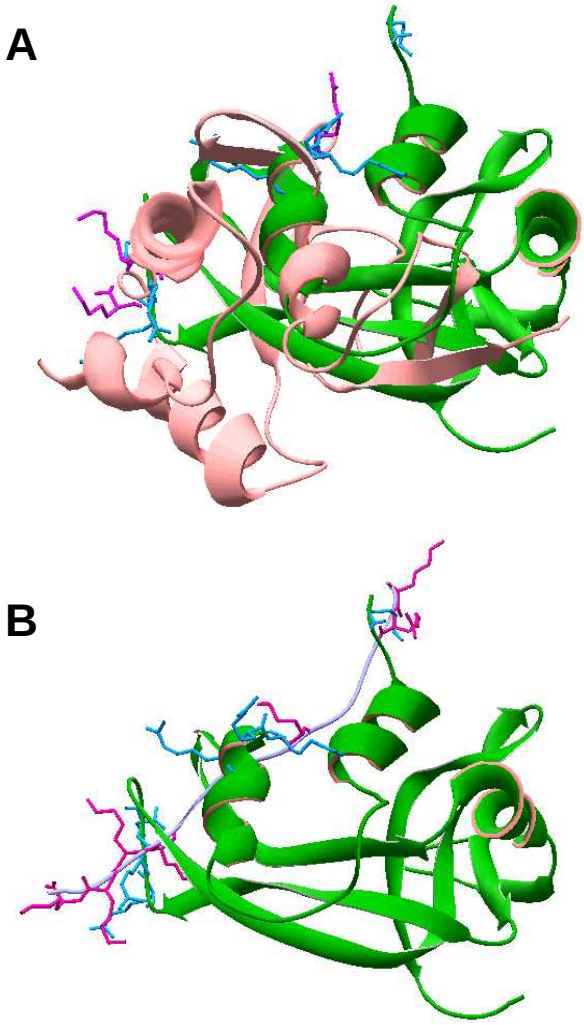

Figure 4

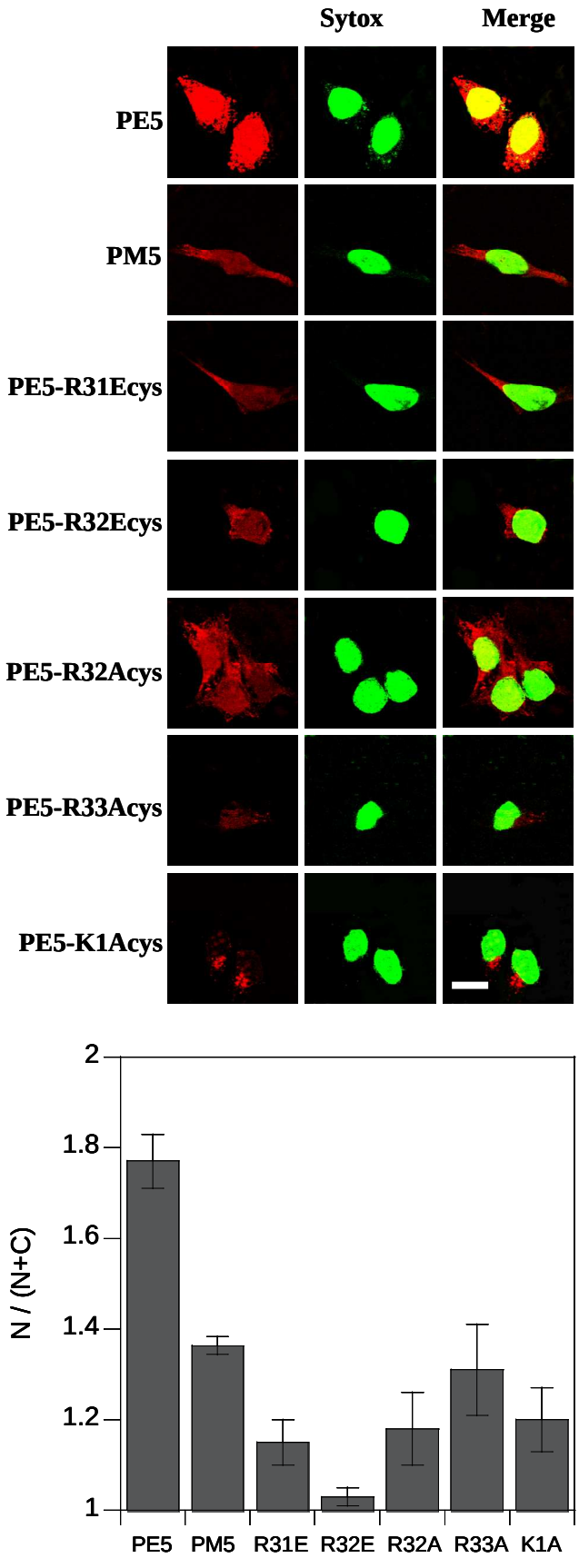
Sytox
Merge
PE5
PM5
PE5-R31Ecys
PE5-R32Ecys
PE5-R32Acys
PE5-R33Acys
PE5-K1Acys
N / (N+C)
2
1.8
1.6
1.4
1.2
1
PE5
PM5
R31E
R32E
R32A
R33A
K1A

Figure 5

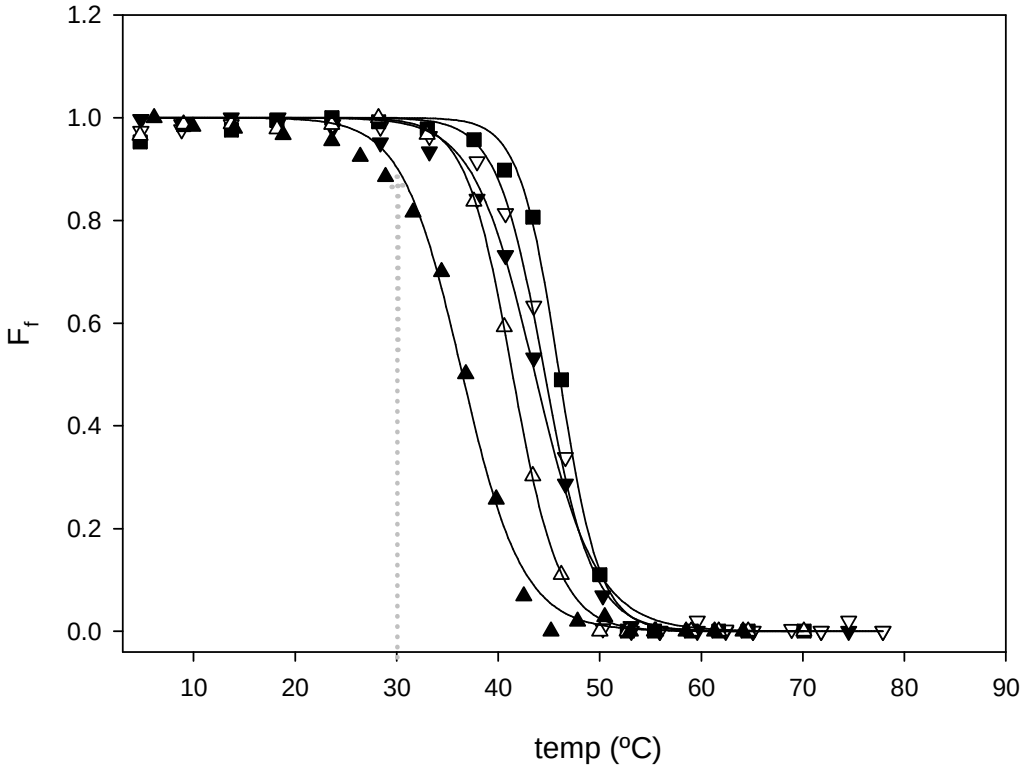

Figure 6

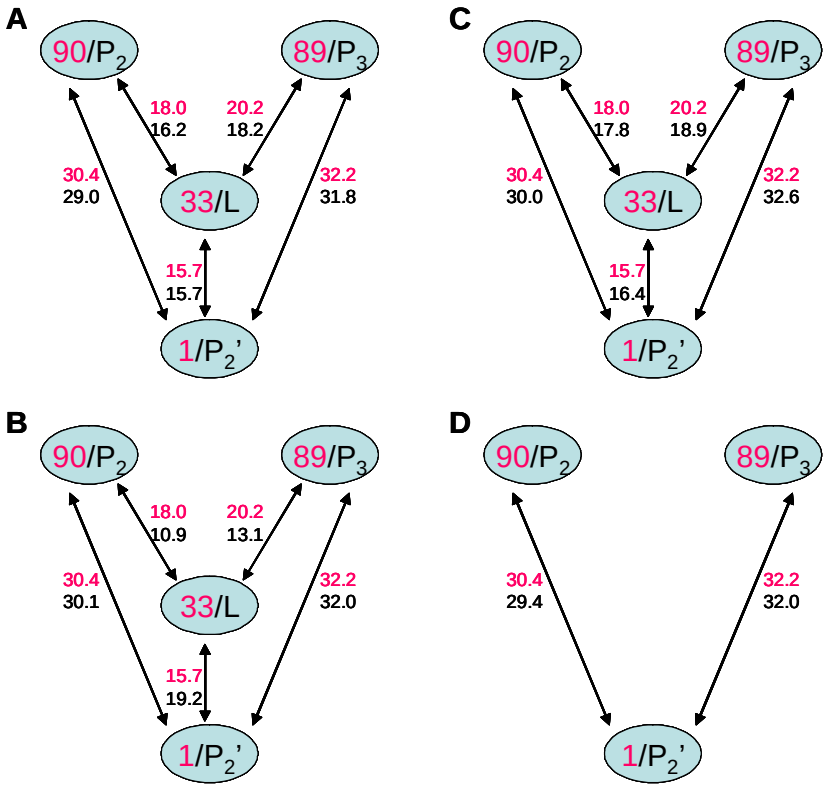
A
90/P2
89/P3
18.0
16.2
20.2
18.2
30.4
29.0
32.2
31.8
33/L
15.7
15.7
1/P2'
C
90/P2
89/P3
18.0
17.8
20.2
18.9
30.4
30.0
32.2
32.6
33/L
15.7
16.4
1/P2'
B
90/P2
89/P3
18.0
10.9
20.2
13.1
30.4
30.1
32.2
32.0
33/L
15.7
19.2
1/P2'
D
90/P2
89/P3
30.4
29.4
32.2
32.0
1/P2'

Capítol III:

CHARACTERIZATION OF THE DIMERIZATION PROCESS OF A DOMAIN-SWAPPED DIMERIC VARIANT OF HUMAN PANCREATIC RIBONUCLEASE

CHARACTERIZATION OF THE DIMERIZATION PROCESS OF A DOMAIN-SWAPPED DIMERIC VARIANT OF HUMAN PANCREATIC RIBONUCLEASE

Montserrat Rodríguez, Antoni Benito, Marc Ribó and Maria Vilanova

Laboratori d'Enginyeria de Proteïnes, Departament de Biologia, Facultat de Ciències, Universitat de Girona, Campus de Montilivi s/n 17071 Girona (Spain).

Running title: Mechanism of dimerization of an HP-RNase variant

Subdivision: protein structure and chemistry

Corresponding author: Dr. Maria Vilanova. Laboratori d'Enginyeria de Proteïnes, Departament de Biologia, Facultat de Ciències, Universitat de Girona, Campus de Montilivi s/n 17071 Girona (Spain). Telephone: 34-972-418-173 Fax: 34-972-418-150. E-mail: maria.vilanova@udg.es

***Keywords*: HP-RNase, dimerization, domain-swapping, oligomers, protein engineering**

Abbreviations: HP-RNase, human pancreatic ribonuclease; MPM8, monomeric form of PM8; DPM8, dimeric form of PM8; BS-RNase, bovine seminal ribonuclease; RNase A, bovine pancreatic ribonuclease A; DVS, divinyl sulfone; $T_{1/2}$ midpoint of thermal denaturation; DSC, differential scanning calorimetry.

Enzymes: Human pancreatic ribonuclease (EC: 3.1.27.5).

SUMMARY

It has been previously reported that the structure of a human pancreatic ribonuclease variant, namely PM8, constitutes a dimer by the exchange of an amino terminal domain, although in an aqueous solution it is found mainly as a monomer. First, we investigated the solution conditions that favour the dimerization of this variant. At 29ºC in a 20% ethanol buffer a significant fraction of the protein is found in a dimeric form without the appearance of higher oligomers. This dimer was isolated by size exclusion chromatography and the dimerization process was studied. The dissociation constant of this dimeric form is 5 mM at 29ºC. Analysis of the dependence of the dimerization process on the temperature shows that unlike bovine pancreatic ribonuclease, a decrease in the temperature shifts the monomer-dimer equilibrium to the latter form. We also show that a previous dissociation of the exchangeable domain from the main protein body does not take place before the dimerization process. Our results suggest a model for the dimerization of PM8 that is different to that postulated for the dimerization of the homologous bovine pancreatic ribonuclease. In this model, first an open interface is formed and then intersubunit interactions stabilize the hinge loop in a conformation that completely displaces the equilibrium between non-swapped and swapped dimers to the latter one.

INTRODUCTION

Three-dimensional domain swapping is a process by which two or more identical protein molecules exchange an identical structural element (often referred as a “tail” or a “domain”) to form an intertwined oligomer [1]. The exchanged domain may correspond to an entire tertiary globular domain or simply to a single element of secondary structure (for a review, see [2], [3]). Since the swapped domain is positioned in the partner subunit in the same conformation as it would adopt in its proper subunit, the resulting oligomers are composed of subunits that have the same structure as the original monomer with the exception of the “hinge loop” that connects the tail with the rest of the structure (often referred to as the “body”). The interface between domains present in both the monomer and the domain-swapped dimer is called the closed interface, whereas the interface found only in the oligomer is called the open interface [1].

Three-dimensional domain swapping has been proposed as a mechanism to explain the evolution from monomeric to oligomeric proteins and in recent years has attracted much interest since it has been implicated in the mechanism of amyloid formation [4, 5, 6]. The structural determinants that lead a polypeptide chain to be folded in an oligomeric state are difficult to identify because they are diverse and subtle. Structural analysis of domain-swapped dimers and their monomeric homologues together with protein engineering, kinetic and thermodynamic analysis of oligomer formation are required to understand these determinants. In turn, this knowledge would help in the design of new proteins from existing monomers. Although an increasing number of structures of domain-swapped dimers are already available (for a review, see [2]), experimental data on the thermodynamics and the mechanism of domain swapping have until recently been almost entirely qualitative [7]. This was primarily due to domain swapped oligomers often being metastable (once formed, they take a long time to convert back to the more stable monomer), thereby rendering any quantitative analysis unfeasible and, secondly, to required tractable model systems in which monomers and domain swapped forms can be isolated and studied in solution.

We have previously shown that the crystal structure of an engineered human pancreatic ribonuclease (HP-RNase) variant named PM8 is constituted by a new kind of domain swapped dimer (Figure 1A) based on the interchange of N-terminal domains (residues 1 to 15) between the two protomers through a linker peptide spanning residues 16 to 22

[8]. PM8 is a HP-RNase variant in which the sequence of the N-terminal domain has been substituted by that of bovine seminal ribonuclease (BS-RNase) and Pro101 has been substituted by Gln [9]. There are five changes in the sequence of the N-terminal domain of PM8 related to HP-RNase, which correspond to Arg4 Ala, Lys6 Ala, Gln9 Glu, Asp16 Gly and Ser17 Asn. The oligomeric structure was unexpected since in solution, at different pH and protein concentration values, most PM8 molecules exist in the monomeric form (MPM8). Nevertheless, the presence of a few dimeric or oligomeric forms was confirmed by non-denaturing PAGE [8]. This observation suggests that while equilibrium between the monomeric and dimeric forms exists, it is displaced to the monomeric form in aqueous solutions. The analysis of the structure indicated that the interactions found along the open interface of the PM8 dimer (DPM8), partially consisting of two electrostatic interactions, were too weak to ensure a significant population of dimeric forms in an aqueous solution. On the other hand, these interactions could be more favoured in the crystal due to the low dielectric constant of the precipitant solution.

BS-RNase and bovine pancreatic ribonuclease A (RNase A) are two homologous enzymes that are also able to dimerize by interchanging an N-terminal domain and have been extensively characterised (reviewed in [10, 11]). RNase A can form two kinds of domain-swapped dimers, one interchanging an N-terminal domain (minor dimer) and the other interchanging a C-terminal domain (major dimer). It has recently been described that an engineered variant of RNase A forms amyloid-like fibrils with three-dimensional domain-swapped and native-like structures [6]. Two kinds of dimers can also be found for BS-RNase, both maintained by two intersubunit disulfides but only one interchanging the N-terminal domains [12]. There are no significant differences between the closed interfaces of the N-terminally swapped RNase dimers that have been published to date [8, 13, 14] but there are variations in the overall quaternary structure that are a consequence of the interactions taking place along the open interface. These differences are illustrated in Figure 1. In domain-swapped BS-RNase, the open interface is formed by the two hinge loops and the following α-helices. The helix-helix interactions are not present in DPM8, which presents an additional contribution to the open interface through a partial symmetric pairing of β-strands. This pairing produces two salt bridges between Glu103 of one chain and Arg104 of the second chain and *vice versa*. Both residues are located along the open interface in β-strand 5. A more efficient

asymmetric pairing of the two β-strands is achieved in the N-terminal exchanged dimer of RNase A [14], which is stabilized by several interchain hydrogen bonds.

Comparison of the N-terminal sequences of DPM8, BS-RNase and RNase A shows that the interchanged domain is highly conserved but that important differences can be found in the hinge loop, in which residues 16 to 20 correspond to STSAA for RNase A and to GNSPS for BS-RNase and PM8. The structures of monomeric RNase A [15], BS-RNase [16, 17] and monomeric HP-RNase variant PM7 (PM5 carrying the substitution Pro50Ser) [18] have also been described in addition to their N-terminal-swapped counterpart dimers [8, 13, 14]. It is interesting to remark that while the hinge loop could be defined in the crystal of the three types of dimers and in that of RNase A monomer, it was fully disordered in carboxymethylated monomeric BS-RNase [16] and in PM7 [18]. Moreover, the dimeric unswapped form of BS-RNase also presents a rather pronounced flexibility in the hinge region [19].

Here, the study of the dimerization process of PM8, offers new clues about the structural determinants that are responsible for the dimerization of the RNases.

RESULTS

Screening of solvent and temperature conditions that favour the formation of dimeric PM8. In solution, there is equilibrium between MPM8 and DPM8 [8]. Both the temperature and the solvent dielectric constant were tested as variables that could displace this equilibrium to the dimeric form. Temperatures ranging from 10 to 37ºC were tested in combination with buffers containing increasing concentrations of ethanol, from 0 to 25%. Initially, the presence of the oligomeric forms was monitored by a cathodic non-denaturing PAGE. Analysis of the different gels (data not shown) revealed that at 10ºC the oligomeric forms were detectable only after 72 h of incubation but that at higher temperatures their presence was apparent between 24 to 48h. In addition, a concentration of 10 to 20% of ethanol in the incubation buffer shifted the equilibrium to the oligomeric forms. However, since it was difficult in the non-denaturing PAGE to discriminate and quantify the different species, the oligomerization process was alternatively analysed by size exclusion chromatography selecting those conditions that, by non-denaturing PAGE, were more promising for the dimer/oligomer formation (i.e. 20% ethanol). This technique allowed to clearly discriminate between the different forms and to quantify them. Under the conditions assayed (50 mM MOPS, 50 mM

NaCl, 20% ethanol pH6.7), the only oligomeric form of PM8 found in the chromatograms eluted in a symmetrical peak with an elution volume corresponding to a dimer (see Figure 2 A).

Once the size exclusion chromatography conditions were set up, the effect of temperature on dimer formation was quantitatively assayed. MPM8 (10 mg/ml) was incubated at 25, 29 and 37ºC in the previously described buffer and the amount of monomer and dimer were evaluated at different incubation times. As can be seen in Figure 3-A, as temperature increases, the equilibrium is reached at shorter incubation times, whereas the percentage of DPM8 at equilibrium, estimated from the asymptotic values obtained by fitting the data points to a hyperbolic curve, decreases (Figure 3-B). A temperature of 42ºC was also tested but, in contrast with the other incubation temperatures, a very significant aggregation of the sample was observed.

Dissociation constant of dimeric PM8. The stability of DPM8 was investigated. 70% of the purified DPM8 remained in the dimeric form when incubated for 90h at 4ºC. Since at low temperatures the equilibrium is shifted to the dimeric form, this result indicated that the dimer was not highly metastable and that a dissociation constant value (*K*d) could be measured. The *K*d of the dimer at 29ºC was calculated by measuring the ratio between the MPM8 and DPM8 forms at different protein concentrations which ranged from 0.1 to 1.3 mM. The plot of $[MPM8]^2$ versus [DPM8] (Figure 4) gives a linear curve (r=0.982) with a slope of 5 mM corresponding to the *K*d of DPM8.

Thermal unfolding of monomeric PM8. It was possible that, in the presence of ethanol, PM8 was partially unfolded, even at the lowest temperature assayed. This possibility was examined by following the thermal-unfolding process of MPM8 in the presence of 20% ethanol by monitoring the change in absorbance at 287 nm (Figure 5A). As has been previously described for other HP-RNase variants [20], the unfolding process of MPM8 is reversible and fits well into a two-state model, its $T_{1/2}$ being 48.1ºC under the solvent conditions used. The transition to the unfolded state did not begin until the temperature reached 39-40ºC, which is higher than the assayed temperatures for the oligomerization process. No minor transition could be observed before 39ºC.

Alternatively, unfolding of PM8 in 20% ethanol was investigated by differential scanning calorimetry (DSC). As expected, only one transition was observed (Figure 5B) which again indicates that PM8 begins to unfold when the temperature reaches 39ºC. The $T_{1/2}$ of PM8 measured by DSC corresponded to 47.5ºC.

Study of the swapping mechanism in a variant of PM8 with a stabilised open interface. When DPM8 is isolated, two equilibrium processes occur, i.e.: the interchange of swapped domains and the monomerization of the dimer, and the latter process precludes the study of the former. In order to study the swapping mechanism during the dimerization of PM8, we constructed a new variant in which the open interface was stabilized enough to allow the dimerization to take place independently of the swapping. To this end, the open interface of PM8 was engineered by introducing a Cys residue that would allow the binding of the protomers by means of a disulfide bridge. Analysis of the structure of DPM8 showed that residues Glu103 in both subunits are located in β-strand 5 with the lateral chains facing each other in the open interface (Figure 6) and that the interatomic distance between Cα of both residues is of 7,83 Å. As this value is close to the average for the eight cysteine residues in PM8 (5, 6 Å), we choose to mutate this residue to Cys to create an intersubunit disulfide bond. The residue Lys102 was also considered because the Cα interatomic distance is even closer, but it was rejected since their lateral chains face in opposite senses in the structure (Figure 6).

The resulting protein, namely PM8E103C, was expressed and purified yielding a monomeric protein, as analysed by size exclusion chromatography, with the additional cysteine blocked by a glutathione molecule, as analyzed by MALDI-TOF (data not shown). Monomers were reduced with DTT in order to remove the glutathione molecule and incubated overnight at 10ºC in 50 mM Tris/acetate pH 8.5. After centrifugation to eliminate insoluble material, the dimeric protein was purified in a G75 size exclusion column. In contrast to PM8, the chromatogram showed the existence of different oligomeric forms that could not be resolved, the maximum of the peak being compatible with an oligomer of six subunits (Figure 2B). These aggregates could be due to the presence in the sample of residual molecules of PM8E103C presenting a reduced intrasubunit disulfide bond as a consequence of the treatment with DTT. These molecules could form alternative oligomers that could act as a nucleation centre. At a concentration between 2 to 2.5 mg/ml of PM8E103C the yield of dimer corresponded to 32% of the initial protein amount. The presence of 20% ethanol in the incubation buffer was also assayed but it resulted in a drastic formation of aggregates even at a low protein concentration.

To check the possibility that the open interface was different after the cysteine was introduced, steady-state kinetic parameters for the hydrolysis of cytidine 2',3'-cyclic

monophosphate were calculated for both monomeric and dimeric forms of PM8 and PM8E103C at 25ºC. The change in the catalytic efficiency upon dimerization, calculated from the ratio between the catalytic efficiency of dimer related to monomer, was not significantly different between PM8 (0.468) and PM8E103C (0.400).

The degree of swapping between the protomers in the purified covalent dimer was analysed by crosslinking His12 and His119 of both active sites with divinyl sulfone (DVS) [21]. If the active site of the dimer is composite, with His-12 coming from one subunit and His-119 coming from the other, the cross-link should covalently join the two subunits even under denaturing conditions. If the active site is not composite, cross-linking would link two histidines from the same subunit, yielding monomers rather than dimers under reducing conditions. Different incubation times with DVS were assessed in order to optimise the reaction. After more than 75 h of incubation with DVS, a single band of 27,000 Da was observed in a reductive SDS-PAGE (Figure 7) indicating that nearly 100% of the dimer was interchanging the N-terminal moiety. This result is in agreement with the fact that in the crystallographic structure of PM8 all the molecules were domain-swapped [8]. The absence of non-swapped dimers indicates that, when PM8E103C is in the dimeric conformation, the N-terminal domain of one subunit is settled more stably over the other subunit.

DISCUSSION

As has been previously pointed out, the HP-RNase variant named PM8 exists in solution mainly in the monomeric form. In this work we have found solution conditions favouring its dimerization. The dimer form has been isolated by size exclusion chromatography and elutes as a single symmetrical peak. It has been described that when RNase A is transiently subjected to unfolding conditions like lyophilisation from 40% acetic acid solutions [22] or heating to 60-70ºC in the presence of 20-40% ethanol [23], two types of domain-swapped dimers can be formed by the interchange of either C- or N-terminal domains [23]. These two dimers can be detected as independent peaks in a size exclusion chromatography [22], and this fact suggests that the symmetrical peak found for DPM8 (Figure 2A) may correspond to a unique type of dimer which can be assigned to the N-terminal-swapped dimer whose structure was previously described [8]. RNase A swapping through the N-terminal domain occurs at milder denaturing conditions than those of the C-terminal domain [23]. Therefore, from our results it

cannot be ruled out that PM8 may form alternative oligomers involving a C-terminal swapping whether more drastic conditions were used.

The dimerization equilibrium of PM8 has a *K*d of 5 mM. This value is 50 times lower than the value estimated for HP-RNase [24] but it is very similar to that found for the dimerization of RNase A at 37ºC and pH 6.5 in aqueous solution (*K*d = 2.7 mM) [25]. In these conditions, the RNase A dimer formed is very unstable and, in contrast to PM8, it cannot be isolated. Under more drastic conditions (i.e. 40% trifluoroethanol, 200mg/ml of protein) a metastable N-swapped dimer of RNase A is formed even at 30ºC, although the yield obtained at this temperature is very low [23].

PM8 can be considered a good model to study the swapping of the RNases for two reasons: i) dimer and monomer forms can interconvert and can be easily isolated and ii) simple models for the swapping can be constructed since only one species of dimer is found in the solvent conditions described here.

When the effect of the temperature on the PM8 dimerization was analysed, it was found that the amount of dimer at equilibrium rose as the temperature decreased (Figure 3). The effect of the temperature on the oligomerization is dependent on the protein studied, and there are examples of proteins, like β-lactoglobulin (which forms a non-swapped dimer), for which the decrease of temperature also promotes dimer formation [26]. However, this result was unexpected. Although HP-RNase and RNase A are highly homologous, it is described that the amount of RNase A dimer formed (either N- or C-swapped) increases as temperature is raised [23]. In this case, this dependence has been explained by a major unfolding and mobility of the swapped domain favoured by the temperature. In a first step, the RNase A folded monomer would be transiently subjected to an unfolding process that would favour the dissociation of the tail from the body, favouring the domain swapping from one subunit to another in a second refolding step, especially at high protein concentrations (Figure 8A). The data presented here for PM8 suggest that it does not dimerize following an analogous mechanism. A possible explanation for the opposite effects of temperature on the N-terminal swapping could be that the dimerization rate-limiting step for RNase A would correspond to the “opening” of the monomer, while for PM8 the dimerization rate-limiting step would correspond to the stabilisation of the open interface.

The temperature-unfolding process of PM8 in presence of 20% ethanol (Figure 5) does not begin until the temperature reaches 39-40ºC, which is higher than the temperatures at which the oligomerization process has been observed without aggregation. This fact

has important implications for the understanding of the PM8 dimerization process since it shows that dimerization takes place before the swapping occurs. We reject that significant dissociation of the N-terminal domain takes place at temperatures lower than the temperature at which the unfolding of the protein begins for the following reasons: 1) only a main transition is observed in the unfolding curve followed by UV absorbance and in the DSC thermogram (Figure 5); 2) His12 catalytic residue is located at the N-terminal exchanged domain, so a decrease of the enzymatic activity of the protein would be expected if this domain was dissociated. We have observed that the enzymatic activity (cytidine 2',3'-cyclic monophosphate hydrolysis) of PM8, at temperatures ranging from 22 to 36ºC, is not altered by the presence of 20% ethanol in the reaction buffer (data not shown); and 3) for RNase S (an RNase A whose peptide bond between residues 20 and 21 has been cleaved), evidence has been provided that the mechanism of thermal unfolding involves body and tail unfolding prior to their dissociation [27]. Taken together, the results show that for PM8, disruption of the N-terminal domain from the rest of the protein during thermal denaturation would also require a substantial unfolding of the whole protein and thus a previous dissociation of the N-terminal domain from the rest of the protein would not be required prior to the dimerization of PM8.

Although PM8 could be a good model to study the swapping process, it has the limitation that its analysis does not discern between the formation of the open interface and the swapping of the tails. For this reason a PM8 variant in which the open interface was stabilised by a disulfide bond was produced to specifically study the degree of swapping in this dimer. In this covalent variant, nearly all the molecules have exchanged the N-terminal domain (Figure 7).

The comparison of the structures of PM7 (a very related monomeric HP-RNase variant) and DPM8, together with the results presented here suggest a model for the dimerization of PM8 in which different residues of the open interface as well as of the hinge loop are directly involved. Analysis of both structures show that in the monomer, the hinge loop is fully disordered whereas in the dimer it adopts a 3_{10} helix conformation which is stabilized by multiple-centred hydrogen bonds established between the two subunits. We postulate that dimerization would occur in a two step process (Figure 8B). First, interaction between monomers would create an open interface that would be stabilised, almost in part, by two salt bridges established between Glu103 residues of one subunit and Arg104 residues of the other [8]. In this

dimer, the relative positions of the two subunits would prepare the molecule for the swapping of the N-terminal domain while, in the hinge loop, Gly16 would provide the necessary degree of freedom for the change of conformation. In a second step, the domain swapping process would be driven by the intersubunit stabilisation of the disordered hinge loops in a conformation that would favour the interchange. Stabilisation of hinge loops would behave as a driving belt for the swapping of the N-terminal domains. In the dimeric structure of PM8, the two Pro19 residues are stacked between the side chains of residues Gln101 and Tyr25 of the other subunit. In addition, Gln101, absent in PM7, establishes three hydrogen bonds with residue Ser20 of both subunits. Finally, the hinge loop is stabilised by multiple-centred hydrogen bonds in a 3_{10} helix conformation. This model of dimerization could be analogous to that proposed for BS-RNase for which experimental data indicate that the non-swapped M=M dimer is formed first and the interchange of the N-terminal domains occurs successively [28]. It is worth mentioning that PM8 share the same N-terminal sequence as BS-RNase and that, again, the hinge loop could be defined in the crystal structure of domain swapped BS-RNase [16, 17] but it was fully disordered in carboxymethylated monomeric BS-RNase [16] and in the dimeric unswapped form of BS-RNase [19].

It is also interesting to remark that while in BS-RNase only 70% of the molecules are domain-swapped [11], nearly all the dimeric PM8E103C interchange the N-terminal domains. Since both dimeric RNases are covalently bound, the equilibrium ratio between the two isomers would be related to the stabilisation of the hinge loops. The hinge loop in DPM8 is more structured than in BS-RNase (Figure 1). DPM8 is the only known dimeric RNase in which both hinge loops form a helical structure. Indeed, whereas in the crystal structure of DPM8 the hinge loop clearly appeared as a well-ordered region, all studies on domain-swapped BS-RNase report a poor definition of the hinge region around Pro19.

Our results suggest a model for the mechanism of dimerization of PM8 that is different to the one postulated for the dimerization of RNase A. This model explains how the exchange of the swapped domain between two folded identical subunits can take place at physiological conditions. In this model, intersubunit interactions between residues located at the hinge peptide and at the open interface stabilize the hinge loop in a conformation that completely displaces the equilibrium between non-swapped and swapped dimers to the latter one.

EXPERIMENTAL PROCEDURES

Construction of PM8E103C

PM8E103C, a variant of PM8 carrying the substitution of Glu103 by Cys, was constructed using the QuikChange site-directed mutagenesis kit (Stratagene, La Jolla, CA, USA) following the instructions of the manufacturer.

Ribonuclease expression and purification

HP-RNase variants were expressed in BL21 (DE3) cells (Novagen, Madison, WI, USA) using the T7 expression system and the recombinant proteins were purified essentially as described in [29]. The molecular mass of each variant was confirmed by MALDI-TOF mass spectrometry using Bruker-Biflex (Billerica, MA, USA) equipment in the Biocomputation and Protein Sequencing Facility of the Institut de Biotecnologia i Biomedicina of the Universitat Autònoma de Barcelona (Spain).

The protein concentration of PM8 and PM8E103C was determined by UV spectroscopy using the extinction coefficient of ε_{278}=8200 $M^{-1}cm^{-1}$ [30].

Production of dimeric PM8E103C

Purified monomeric PM8E103C presented one molecule of glutathione bound to Cys103 residue. One ml at 2.5 mg/ml of monomer in 100mM Tris/acetate, 1.7mM DTT, pH 8.5 was incubated for 30 min at room temperature. In these conditions only the intermolecular disulfide bond with glutathione is reduced. The protein was dialysed overnight against 50mM Tris/acetate, pH 8.5 at 10ºC, and a 1:1000 volume of glacial acetic was added to the sample. The dimeric form was then purified by size exclusion chromatography at a flow of 0.4 ml/min using a G75 HR 10/30 column (Amersham Biosciences, Piscataway, NJ, USA) equilibrated with 200 mM sodium acetate pH 5.0.

Detection of oligomeric forms in solution by cathodic non-denaturing PAGE

Pure samples of PM8 were analysed by cathodic gel electrophoresis under non-denaturing conditions consisting of a β-alanine/acetic acid buffer (pH 4.0), according to the method of Reisfeld [31]. Polyacrylamide (7.5%) was used and gels were run at 20 mA for 1 hr at 4ºC. 10 μg of protein at a 10 mg/ml concentration was loaded onto a nondenaturing gel.

Kinetics of formation of PM8 dimeric form and *K*d calculations

To follow the dimerization of PM8, 10 mg/ml MPM8 samples (0.7 mM) were incubated in 50 mM MOPS, 50 mM NaCl, 20% ethanol pH6.7 at different temperatures. At given times, aliquots were withdrawn, and the mixtures were immediately chromatographed at a flow of 0.4 ml/min on an analytical Sephadex G75 HR 10/30 column (Amersham Biosciences, Piscataway, NJ, USA) equilibrated with 200 mM sodium phosphate pH 6.7. To calculate the dissociation constant of PM8 at 29ºC MPM8 samples were incubated in 50 mM MOPS, 50 mM NaCl, 20% ethanol at concentrations ranging from 0.1 to 1.3 mM. After 100 hours, aliquots were withdrawn, and the mixtures were immediately chromatographed at a flow of 0.4 ml/min on an analytical Sephadex G75 HR 10/30 column. No protein aggregation was observed in any of these experiments and the concentrations of monomer and dimer were evaluated quantitatively in each case by integrating the peaks of dimer and monomer, respectively. Given the equilibrium M +M $\leftrightarrow$D, the *K*d can be calculated from the slope of a plot of M^2 concentration versus D concentration.

Assessment of the extent of the domain-swapping

The degree of N-terminal domain swap was investigated following the protocol described by Ciglic and colleagues [21]. Only when the dimer is N-terminal swapped, does each histidine in the active sites belong to a different protomer with the consequent crosslinking of the subunits. Briefly, PM8E103C (14 µg, 1 nM/subunit) in 100 mM sodium acetate, pH 5.0 (100 µL) and DVS (1µL 10% solution in ethanol, 1 µM) were incubated at 30°C. This is about a 1000-fold excess of sulfone per subunit of the protein. Aliquots were withdrawn over a period of 150 h and the reaction was quenched by adding 2-mercaptoethanol (final concentration 200 mM) and incubating for 15-30 min at room temperature. The samples were loaded on a reducing SDS-PAGE and bands were revealed by Coomassie Blue staining.

Determination of thermal stability by UV absorbance

The conformational stability of MPM8 was determined using UV absorbance spectroscopy to measure the change in environment of the aromatic residues during protein thermal unfolding. The protein was dissolved at 0.5 mg/ml in a 50 mM acetate pH 5.0, 20% ethanol and the UV absorbance was monitored at 287 nm. The temperature was raised from 5 to 74ºC in 2-4ºC increments and the decrease in UV absorbance was

registered after a 5 min equilibration at each temperature. Temperature-unfolding transitions curves were fitted to a two-state thermodynamic model combined with sloping linear functions for the native and denatured states, as described elsewhere [32].

Differential Scanning Calorimetry

DSC experiments were carried out on a MicroCal MC2 instrument (MicroCal Inc., Studio City, CA, USA) operating at a heating rate of 1.5 ºC/min within the range 10 - 80ºC. A nitrogen pressure of 1.7 atm was kept during scans to avoid sample evaporation at high temperatures. 1.33 ml of solution was introduced into the sample cell at a final protein concentration of 2 mg/ml. The reversibility of the thermal transitions was checked by reheating the samples immediately after cooling at 6ºC. Data were processed with the Origin^{TM} software supplied by MicroCal Inc. Each thermogram was corrected by subtracting buffer thermograms (50 mM acetate pH 5.0, 20% ethanol) acquired in the same conditions as the sample and by subtracting the chemical baseline using the method of Takahashi and Sturtevant [33].

Enzymatic activity measurements

Hydrolysis of cytidine 2',3'-cyclic monophosphate (Sigma Chemicals, St. Louis, MO, USA) was carried out as described in [34] in a sodium acetate buffer pH 5.5 in the presence and absence of 20% ethanol at the temperatures indicated in the text.

ACKNOWLEDGEMENTS

This work was supported by grants BMC2003-08485-CO2-02 from the *Ministerio de Educación y Ciencia* (MEC), Spain and SGR01-00196 from DGR, *Generalitat de Catalunya.* M.R. gratefully acknowledges a pre-doctoral fellowship grant from MEC. We are also indebted to Fundació M. F. de Roviralta, Barcelona, Spain, for equipment-purchasing grants. We thank Josep Cladera, Víctor Buzón and Elodia Serrano (Universitat Autònoma de Barcelona, Spain) for valuable help in carrying out the DSC experiment.

REFERENCES

1. Bennett MJ, Schlunegger MP & Eisenberg D (1995) 3D domain swapping: a mechanism for oligomer assembly. *Protein Sci* **4**, 2455-2468.

2. Liu Y & Eisenberg D (2002) 3D domain swapping: as domains continue to swap. *Protein Sci* **11**, 1285-1299.

3. Newcomer ME (2002) Protein folding and three-dimensional domain swapping: a strained relationship? *Curr Opin Struct Biol* **12**, 48-53.

4. Staniforth RA, Giannini S, Higgins LD, Conroy MJ, Hounslow AM, Jerala R, Craven CJ & Waltho JP (2001) Three-dimensional domain swapping in the folded and molten-globule states of cystatins, an amyloid-forming structural superfamily. *Embo J* **20**, 4774-4781.

5. Janowski R, Kozak M, Jankowska E, Grzonka Z, Grubb A, Abrahamson M & Jaskolski M (2001) Human cystatin C, an amyloidogenic protein, dimerizes through three-dimensional domain swapping. *Nat Struct Biol* **8**, 316-320.

6. Sambashivan S, Liu, Y., Sawaya, M.R., Gingery, M., Eisenberg, D. (2005) Amyloid-like fibrils of ribonuclease A with three-dimensional domain-swapped and native-like structure. *Nature* **437**, 266-269.

7. Rousseau F, Schymkowitz JW & Itzhaki LS (2003) The unfolding story of three-dimensional domain swapping. *Structure (Camb)* **11**, 243-251.

8. Canals A, Pous J, Guasch A, Benito A, Ribo M, Vilanova M & Coll M (2001) The structure of an engineered domain-swapped ribonuclease dimer and its implications for the evolution of proteins toward oligomerization. *Structure (Camb)* **9**, 967-976.

9. Canals A, Ribo M, Benito A, Bosch M, Mombelli E & Vilanova M (1999) Production of engineered human pancreatic ribonucleases, solving expression and purification problems, and enhancing thermostability. *Protein Expr Purif* **17**, 169-181.

10. Libonati M & Gotte G (2004) Oligomerization of bovine ribonuclease A: structural and functional features of its multimers. *Biochem J* **380**, 311-327.

11. D'Alessio G, Di Donato, A., Mazzarella, L., and Piccoli, R. (1997) *Seminal Ribonuclease: The importance of diversity*, edn. Academic Press, New York.

12. Piccoli R, Tamburrini M, Piccialli G, Di Donato A, Parente A & D'Alessio G (1992) The dual-mode quaternary structure of seminal RNase. *Proc Natl Acad Sci U S A* **89**, 1870-1874.

13. Mazzarella L, Capasso S, Demasi D, Di Lorenzo G, Mattia CA & Zagari A (1993) Bovine seminal ribonuclease: structure at 1.9 A resolution. *Acta Crystallogr D Biol Crystallogr* **49**, 389-402.

14. Liu Y, Hart PJ, Schlunegger MP & Eisenberg D (1998) The crystal structure of a 3D domain-swapped dimer of RNase A at a 2.1-A resolution. *Proc Natl Acad Sci U S A* **95**, 3437-3442.

15. Wlodawer A, Svensson LA, Sjolin L & Gilliland GL (1988) Structure of phosphate-free ribonuclease A refined at 1.26 A. *Biochemistry* **27**, 2705-2717.

16. Sica F, Di Fiore A, Zagari A & Mazzarella L (2003) The unswapped chain of bovine seminal ribonuclease: Crystal structure of the free and liganded monomeric derivative. *Proteins* **52**, 263-271.

17. Avitabile F, Alfano C, Spadaccini R, Crescenzi O, D'Ursi AM, D'Alessio G, Tancredi T & Picone D (2003) The swapping of terminal arms in ribonucleases: comparison of the solution structure of monomeric bovine seminal and pancreatic ribonucleases. *Biochemistry* **42**, 8704-8711.

18. Pous J, Canals A, Terzyan SS, Guasch A, Benito A, Ribo M, Vilanova M & Coll M (2000) Three-dimensional structure of a human pancreatic ribonuclease variant, a step forward in the design of cytotoxic ribonucleases. *J Mol Biol* **303**, 49-60.

19. Berisio R, Sica F, De Lorenzo C, Di Fiore A, Piccoli R, Zagari A & Mazzarella L (2003) Crystal structure of the dimeric unswapped form of bovine seminal ribonuclease. *FEBS Lett* **554**, 105-110.

20. Benito A, Bosch M, Torrent G, Ribo M & Vilanova M (2002) Stabilization of human pancreatic ribonuclease through mutation at its N-terminal edge. *Protein Eng* **15**, 887-893.

21. Ciglic MI, Jackson PJ, Raillard SA, Haugg M, Jermann TM, Opitz JG, Trabesinger-Ruf N & Benner SA (1998) Origin of dimeric structure in the ribonuclease superfamily. *Biochemistry* **37**, 4008-4022.

22. Gotte G, Bertoldi M & Libonati M (1999) Structural versatility of bovine ribonuclease A. Distinct conformers of trimeric and tetrameric aggregates of the enzyme. *Eur J Biochem* **265**, 680-687.

23. Gotte G, Vottariello F & Libonati M (2003) Thermal aggregation of ribonuclease A. A contribution to the understanding of the role of 3D domain swapping in protein aggregation. *J Biol Chem* **278**, 10763-10769.

24. Russo N, Antignani A & D'Alessio G (2000) In vitro evolution of a dimeric variant of human pancreatic ribonuclease. *Biochemistry* **39**, 3585-3591.

25. Park C & Raines RT (2000) Dimer formation by a "monomeric" protein. *Protein Sci* **9**, 2026-2033.

26. Aymard P, Durand D & Nicolai T (1996) The effect of temperature and ionic strength on the dimerisation of beta-lactoglobulin. *Int J Biol Macromol* **19**, 213-221.

27. Stelea SD & Keiderling TA (2002) Pretransitional structural changes in the thermal denaturation of ribonuclease S and S protein. *Biophys J* **83**, 2259-2269.

28. D'Alessio G (1995) Oligomer evolution in action? *Nat Struct Biol* **2**, 11-13.

29. Ribo M, Benito A, Canals A, Nogues MV, Cuchillo CM & Vilanova M (2001) Purification of engineered human pancreatic ribonuclease. *Methods Enzymol* **341**, 221-234.

30. Bosch M, Benito A, Ribo M, Puig T, Beaumelle B & Vilanova M (2004) A nuclear localization sequence endows human pancreatic ribonuclease with cytotoxic activity. *Biochemistry* **43**, 2167-2177.

31. Reisfeld RA, Lewis UJ & Williams DE. (1962) *Disk electrophoresis of basic proteins and peptides on polyacrylamide gels*, edn.

32. Mozhaev VV, Heremans K, Frank J, Masson P & Balny C (1996) High pressure effects on protein structure and function. *Proteins* **24**, 81-91.

33. Takahashi K & Sturtevant JM (1981) Thermal denaturation of streptomyces subtilisin inhibitor, subtilisin BPN', and the inhibitor-subtilisin complex. *Biochemistry* **20**, 6185-6190.

34. Boix E, Nogues MV, Schein CH, Benner SA & Cuchillo CM (1994) Reverse transphosphorylation by ribonuclease A needs an intact p2-binding site. Point mutations at Lys-7 and Arg-10 alter the catalytic properties of the enzyme. *J Biol Chem* **269**, 2529-2534.

35. Koradi R, Billeter M & Wuthrich K (1996) MOLMOL: a program for display and analysis of macromolecular structures. *J Mol Graph* **14**, 51-55, 29-32.

FIGURE LEGENDS

Figure 1. *Dimeric ribonucleases exchanging an N-terminal domain differ in the open interfaces*. Ribbon representation of the structures of (A) PM8 (pdb accession code 1H8X), (B) RNase A minor dimer (pdb accession code 1A2W) and (C) BS-RNase domain-swapped dimer (pdb accession code 1BSR). Secondary structure elements forming the open interface are labelled in the figures as β5 (strand β5) α2 (α –helix 2) and HL (hinge loop). Details of the main structural differences between these dimers are given in the text. Figures have been drawn using the MOLMOL program [35].

Figure 2. *Chromatographic characterisation of PM8 and PM8E103C oligomers*. Size exclusion profiles of PM8 (A) and PM8E103C (B) eluted from a G75 HR10/30 column. Peaks corresponding to monomeric (m), dimeric (d) and oligomeric (o) are indicated.

Figure 3. *Kinetic analysis of the dimerization of PM8*. A) Aliquots of MPM8 **(0.7 mM)** were incubated for different times at 25ºC (□), 29ºC (△) and 37ºC (▽). The percentage of the dimeric form as a function of the incubation time is reported for each temperature. B) Percentage of DPM8 at equilibrium versus incubation temperature.

Figure 4. *Measurement of the dissociation constant of PM8*. Samples of PM8 at concentrations ranging between 0.1 and 1.3 mM were equilibrated at 29ºC for 160 h and analysed by size exclusion to measure the fractions of monomer and dimer. In the plot of $[MPM8]^2$ versus [DPM8] (r=0.982), *K*d is given by the slope.

Figure 5. *Thermal stability of PM8 in the presence of 20% ethanol*. A) Temperature-unfolding curve of PM8 (0.5 mg/ml dissolved 50 mM acetate, 20% ethanol pH 5.0) followed by monitoring the changes in absorbance at 287 nm when increasing temperature. B) DSC thermogram of PM8 (2 mg/ml dissolved in 50 mM acetate, 20% ethanol pH 5.0) between 10 and 80ºC. Thermogram was corrected from instrumental and chemical baselines. Cp^{ex} express the partial heat capacity of the protein relative to the heat capacity of the protein in the native state.

Figure 6. *Analysis of the open interface of DPM8*. Ribbon representation of the domain-swapped crystallographic structure of PM8 showing the position and interatomic

distances between the alpha carbons of residues 102, 103 and 104 of each subunit. The figure has been drawn using the MOLMOL program [35].

Figure 7. *Assessment of the degree of swapping of the N-terminal domain in PM8E103C.* SDS-PAGE analysis under reducing conditions of the DVS crosslinking reaction of PM8E103C at different times of incubation (indicated at the top of each lane) at 30ºC. Relative positions of each molecular weight marker are detailed in the figure. The two bands found at the relative position of the dimer can be assigned to molecules crosslinked by one or two molecules of DVS.

Figure 8. *Scheme for the putative mechanism of domain-swapping dimerization of RNase A and PM8.* For RNase A (A), the protein is subjected to conditions which favour the dissociation of the exchanged domain from the rest of the protein and, when unfolding conditions are removed, the domain-swapping can occur, especially at high protein concentrations. For PM8 (B), in a first step the protein dimerizes, creating an open interface, in which the hinge loops are highly disordered. At this point interactions within subunits would stabilise the hinge loop in a conformation that would favour the domain swapping. The relative positions of the subunits in the figure do not reflect the actual position in the dimer structure. In both dimers, the open interface is formed by residues belonging to the body and the hinge loop.

Figure 1

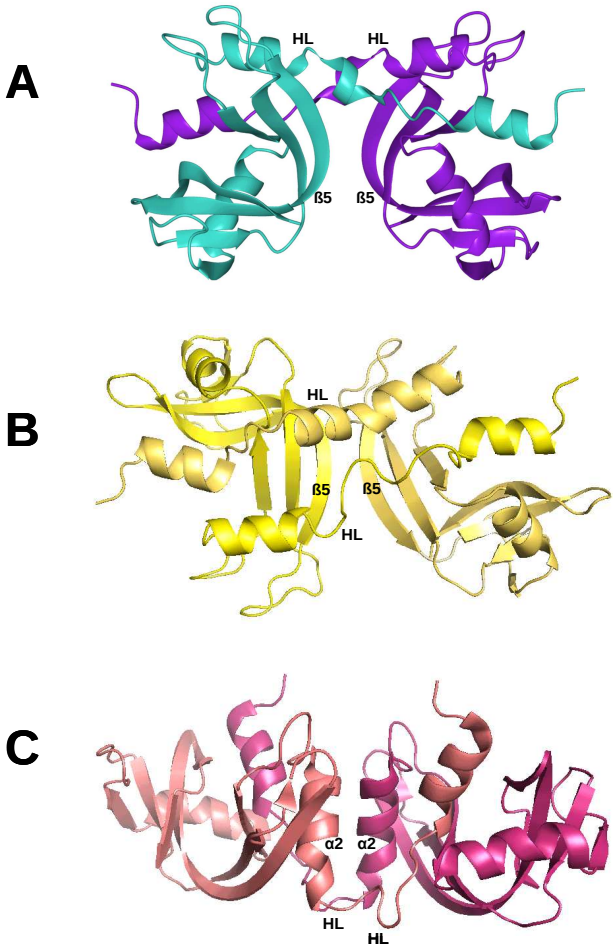

Figure 2

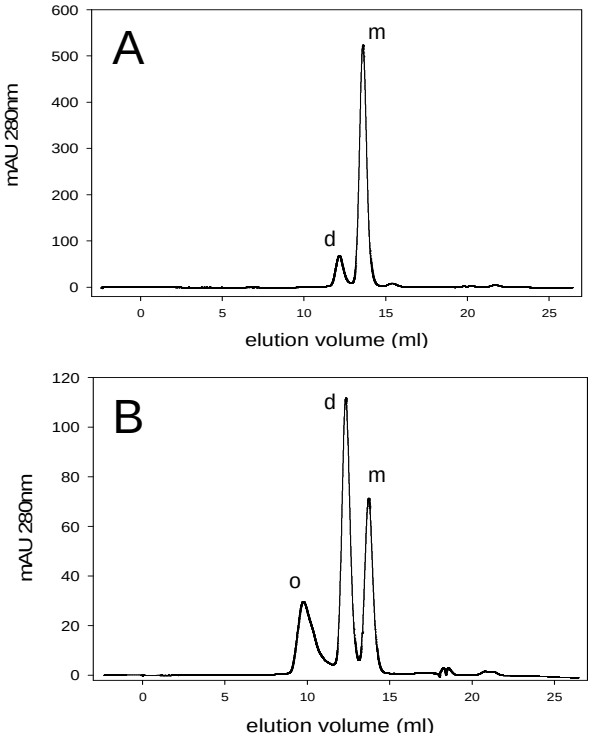
A
m
d
mAU 280nm
elution volume (ml)
B
d
m
o
mAU 280nm
elution volume (ml)

Figure 3

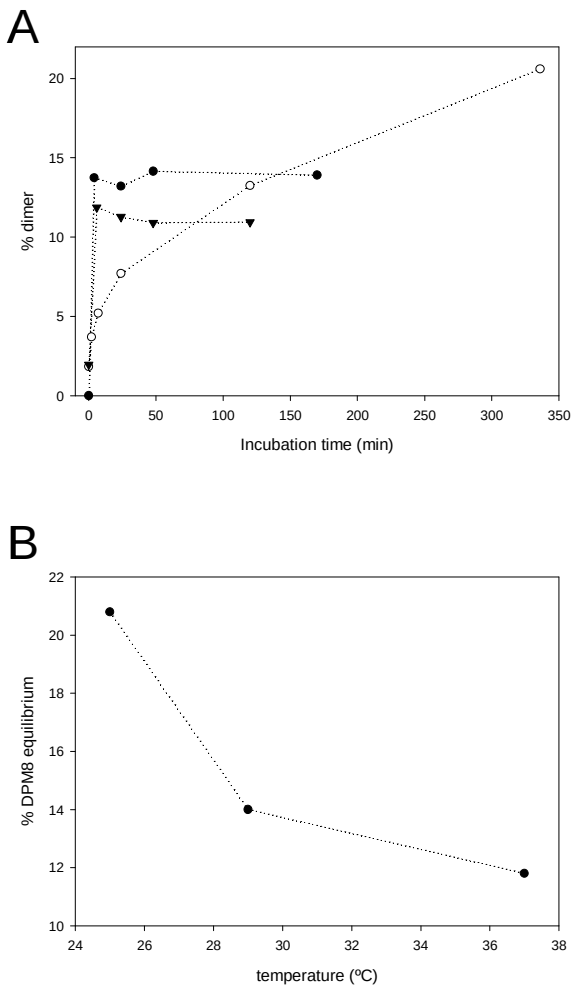
A
% dimer
Incubation time (min)
0
5
10
15
20
0
50
100
150
200
250
300
350
B
% DPM8 equilibrium
temperature (ºC)
10
12
14
16
18
20
22
24
26
28
30
32
34
36
38

Figure 4

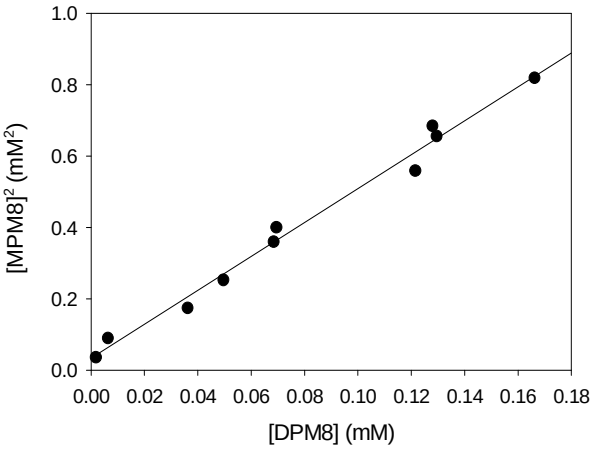
1.0
0.8
0.6
0.4
0.2
0.0
[MPM8]2 (mM2)
0.00 0.02 0.04 0.06 0.08 0.10 0.12 0.14 0.16 0.18
[DPM8] (mM)

Figure 5

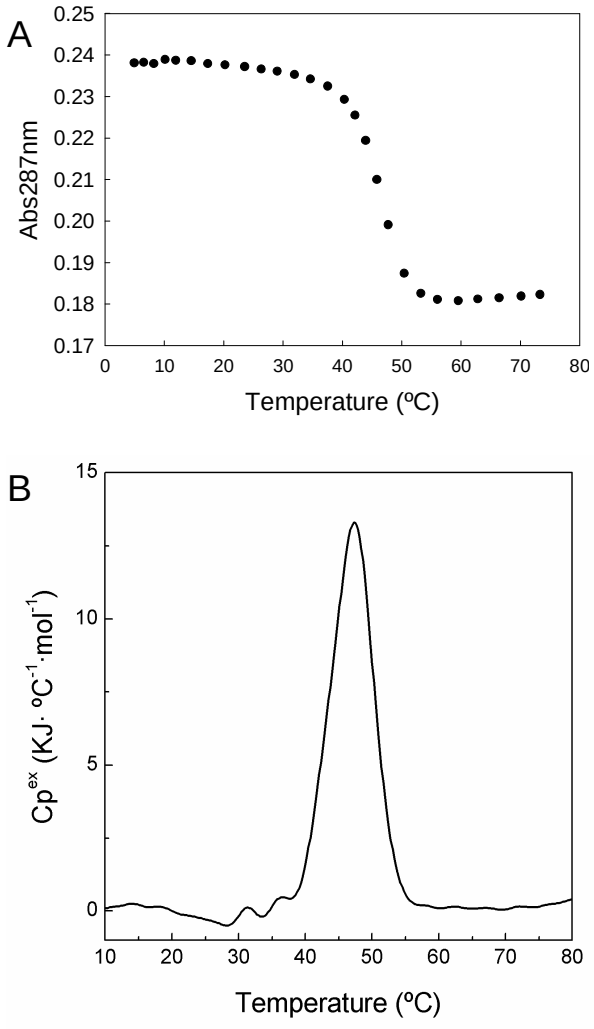

Figure 6

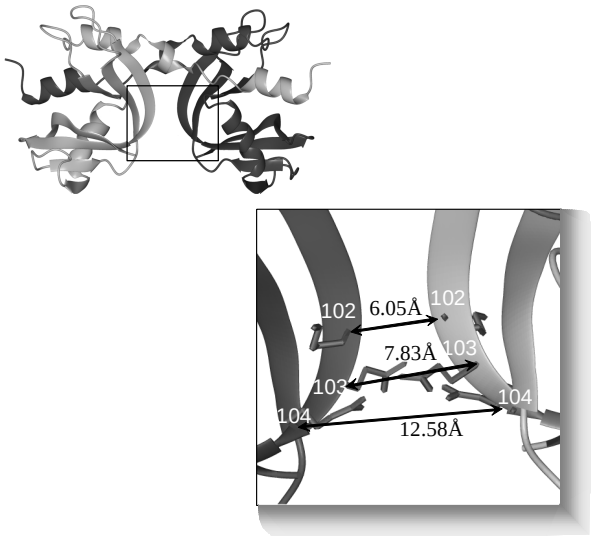

Figure 7

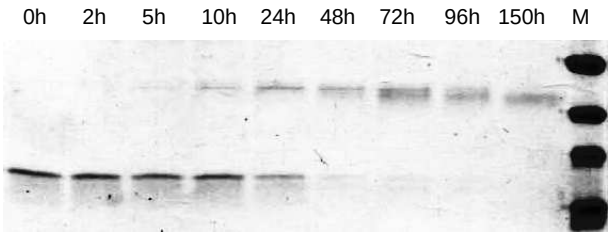

Figure 8

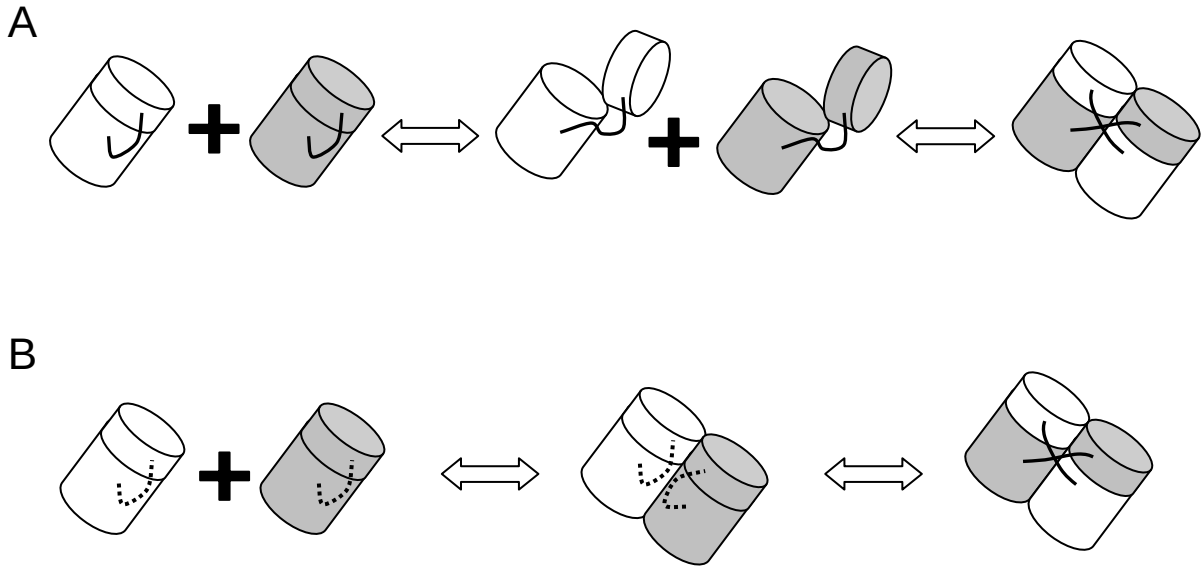

Capítol IV:

HUMAN PANCREATIC RIBONUCLEASE CLEAVES POLYMERIC SUBSTRATES WITH A MARKED ENDONUCLEASE PREFERENCE COMPARED TO RIBONUCLEASE A

HUMAN PANCREATIC RIBONUCLEASE CLEAVES POLYMERIC SUBSTRATES WITH A MARKED ENDONUCLEASE PREFERENCE COMPARED TO RIBONUCLEASE A

Rodríguez, M.[a], Moussaoui, M.[b], Benito, A.[a], Cuchillo, C.M.[b], Nogués, M.V.[b] and Vilanova, M.[a]

[a] Laboratori d'Enginyeria de Proteïnes, Departament de Biologia, Facultat de Ciències, Universitat de Girona, Campus de Montilivi s/n 17071 Girona (Spain).

[b] Departament de Bioquímica i Bologia Molecular, Facultat de Ciències, Universitat Autònoma de Barcelona E-08193 Bellaterra (Spain)

ABSTRACT. Analysis of the pattern of oligonucleotide formation by HP-RNase shows that the enzyme does not act randomly and follows a more endonucleolytic pattern when compared to RNase A. The enzyme prefers the binding and cleavage of longer substrate molecules, especially when the phosphodiester bond broken is 9-11 nucleotides apart from at least one of the ends of the substrate molecule. Deletion of two positives charges on the N-terminus (R4A and K6A) modifies this pattern of external/internal phosphodiester bond cleavage preference, leading to a more exonucleolytic enzyme. These residues may reinforce the strength of phosphate binding to p_2 or, alternatively, constitute a p_3 phosphate binding subsite. Addition of positive charges (R89 and R90) on the protein surface increases interaction between protein and substrate, thereby resulting in a increase in the length of digestion products using poly(C) as substrate. Finally, we show that the interaction of a dimeric variant of HP-RNase with its substrate in one of the active sites probably induces a conformational change on the enzyme that precludes the binding of the substrate on the other active site.

Abreviations: C>p, cytidine 2',3'-cyclic phosphate; (Cp)nC>p, an oligocytidylic acid of n+1 residues ending in a cytidine 2',3'-cyclic phosphate; DPM8E103C, dimeric form of PM8E103C; HPLC, high pressure liquid chromatography; HP-RNase, human pancreatic ribonuclease; MPM8E103C, monomeric form of PM8E103C; poly(C), polycytidylic acid; RNase A, bovine pancreatic ribonuclease A; DTT, 1,4-dithiothreitol; MALDI-TOF-MS, matrix-assisted laser desorption/ionization time-of-flight mass spectroscopy; ECP, eosinophil cationic protein.

INTRODUCTION

Human pancreatic ribonuclease (HP-RNase; EC 3.1.27.5) is a protein of 128 residues that catalyzes the cleavage of RNA on the 3'-side of pirimidine bases. This enzyme is considered the homologue of bovine pancreatic ribonuclease (RNase A) in humans [Beintema et al., 1984]. They present a high sequence similarity (70% identity), both operate at an optimal pH of 8.0, show a marked preference for poly(C) over poly(U) and hydrolyze 2',3'-cyclic phosphate nucleotides [Sorrentino, 1998]. The nucleotide on the 3' position of the broken phophodiester bond must be a pyrimidine, with cytidine being preferred over uridine. For RNase A, the base in the nucleotide on the 5' position of the broken bond is also important in defining its efficiency, the preference being A>G>C>U [Witzel and Barnard, 1962]. The cleavage mechanism of the phosphodiester bond by RNase A takes place in two independent processes and it has been examined in detail [Cuchillo et al., 1993; Thompson et al., 1994]. In the first step there is a transphosphorylation reaction from the 5' position of one nucleotide to the 2' position of the adjacent nucleotide with the formation of a 2',3'-cyclic phosphate. In the second step the 2',3'-cyclic phosphate is hydrolysed to a 3'-nucleotide. There is a lag in the formation of the final product of the reaction, and no 3'-nucleotide appears until all the 3', 5'-phosphodiester bonds have been converted to mononucleotide 2',3'-cyclic phosphate. Because the catalytic residues are completely conserved and share a common topological distribution, the catalytic mechanism is likely to be the same as HP-RNase.

In addition to the catalytic centre, several binding subsites that contribute to the binding of the polymeric substrates in RNase A have been characterized by means of structural and kinetic approaches [for a review, see Cuchillo et al., 1997]. All these residues are also conserved in the HP-RNase sequence. The phosphate group of the phosphodiester bond to be cleaved by the enzyme is placed at the catalytic subsite designed as p_1, while the pyrimidine nucleoside binding site located at the 3' position of the cleaved bond is denoted as B_1R_1. Residues involved in the recognition of the purine nucleoside at the 5' position of the cleaved bond are designed as B_2R_2. Finally, other phosphate-binding subsites have been proposed, in addition to the active site. Among them, the best characterized are p_0 (Lys 66) and p_2 (Lys 7 and Arg 10) which bind adjacent phosphates to the one placed at p_1, in the 5' and 3' directions, respectively. Other phosphate-binding subsites, such as p_{-1} that includes Arg 85 [Fontecilla-Camps et al., 1994; Fisher

et al., 1998], and other subsites located at the surface of the protein have also been considered.

Although catalytic and substrate-binding subsite residues are conserved between RNase A and HP-RNase, the latter enzyme displays more basic residues on its surface and this fact has been related to additional catalytic activities. HP-RNase presents a great catalytic versatility, and under physiological salt conditions it can degrade both single- and double-stranded RNA as well as poly (A) [Sorrentino and Libonati, 1997; Sorrentino 1998; Libonati and Sorrentino, 2001, Sorrentino et al., 2003]. According to a mechanism proposed by Sorrentino and Libonati [Sorrentino and Libonati, 1997], the degradation of dsRNA by HP-RNase is based on the number and location of positive charges displayed by the RNase molecule in its interaction with the polyanionic double helical substrate [Libonati and Sorrentino, 2001].

The preference for cleavage of phosphodiester bonds in the polymeric substrates has been studied for RNase A and human eosinophil cationic protein (ECP) [Moussaoui et al., 1996]. It has been shown that these proteins do not act randomly. ECP shows a marked preference for exonucleolytic cleavage. RNase A has no special preference for endonucleolytic or exonucleolytic cleavage but shows a preference for the longer substrate molecules and for the release of fragments containing 6-8 nucleotide units [Moussaoui et al., 1996]. The differences between both enzymes have been related to the disappearance of p_2 and B_2 subsites in the ECP [Boix et al, 1999]. Kinetic studies of variants of RNase A have shown that the p_0 binding subsite contributes to the exonucleolytic preference, whereas p_2 binding subsite is involved directly in the endonucleolytic pattern [Cuchillo et al., 2002].

In the present work, we have studied the catalytic properties and the cleavage preference of HP-RNase using different substrates. We have found that although all the residues belonging to the characterized subsites are conserved in HP-RNase, this enzyme shows a marked preference for an endonucleolytic cleavage respective to RNase A. In addition, we show that other basic residues contribute to the catalytic preference of HP-RNase. Finally, we have also characterized the catalytic properties of a dimeric variant of HP-RNase. In this variant, the interaction of one active site with the substrate probably induces the inactivation of the active site of the other subunit.

MATERIALS AND METHODS

Materials. Bovine pancreatic ribonuclease A, (Poly(C)), C>p and HEPES were obtained from Sigma (St. Louis, MO). Exclusion size column G75 HR 10/30 was from Amersham Biosciences (Sweden) and reversed-phase Nova-Pak C_{18} column (4 µm, 3.9 x 150 mm) was from Waters (Milford, MA). Acetonitrile (HPLC grade) was obtained from Carlo Erba (Milan, Italy). All other reagents were of analytical grade. Milli-Q water (Millipore Corp., Milford, MA) was used for the preparation of HPLC solutions. HPLC separations were performed with a modular HPLC chromatograph from Waters Corp. (Mildford, MA). Steady state kinetics were carried out with a UV-visible Spectrophotometer Cary 100 Bio (Varian, Australia).

HP-RNases variants. Construction and production of HP-RNase and its variants PM5, PE5 and PM8E103C, have been described elsewhere [Canals et al., 1999; Bosch et al., 2004; Rodríguez et al., 2006]. PM5 was obtained from wild type HP-RNase with the mutations Arg4 Ala, Lys6 Ala, Gln9 Glu, Asp16 Gly and Ser17 Asn [Canals et al., 1999]. PE5 was obtained from PM5 replacing residues 89 and 90 by Arg [Bosch et al., 2004]. PM8E103C is a variant of PM5 carrying the mutations Pro101 Gln and Glu103 Cys [Rodríguez et al., 2006]. The precise location of the substitutions is indicated for PM5 and PE5 in Figure 1A and for PM8E103C in Figure 1B.

Ribonuclease purification. Wild-type HP-RNase and its variants (PM5, PE5 and PM8E103C) were purified as previously described [Ribó et al., 2001]. Purified monomeric PM8E103C (MPM8E103C) presents one molecule of glutathione bound to Cys103 residue. For the purification of the dimeric form of PM8E103C (DPM8E103C), 1 ml of the monomeric form (MPM8E103C) at 2.5 mg/ml in 100 mM Tris/acetate, 1.7 mM DTT, pH 8.5 was incubated for 30 min at room temperature. In these conditions only the intermolecular disulfide bond with glutathione is reduced. The protein was dialysed overnight against 50 mM Tris/acetate, pH 8.5 at 10ºC, and a 1:1000 volume of glacial acetic acid was added to the sample. The dimeric form was then purified by size-exclusion chromatography at a flow of 0.4 ml/min using a G75 HR 10/30 column equilibrated with 200 mM sodium acetate pH 5.0.

Digestion of poly(C) by HP-RNase and its variants. 50 µl of poly (C) 2.5 mg/ml in 15 mM HEPES-KOH (pH 7.5) were incubated at 25 ºC with enzyme, whose concentration ranged between 20 to 30 nM depending on the variant. At different time intervals, between 0 to 30 min, the products of the reaction were analyzed as previously described [Moussaoui et al., 1996 and Cuchillo et al., 2002]. Briefly, reversed-phase Nova-Pak C_{18} HPLC column was washed for 20 min with Milli-Q water and equilibrated for 20 min with solvent A (10% (w/v) ammonium acetate and 1% (v/v) acetonitrile in water). 50 µl of the reaction mixture were injected at 1 ml/min and elution was performed with an initial 10 min wash and a 50 min linear gradient from 100% solvent A to 10% solvent A plus 90% solvent B (10% (w/v) ammonium acetate and 11% (v/v) acetonitrile in water). After each run, the system was washed for 5 min with water containing 1% acetonitrile. Slight differences in the retention times of oligonucleotides can be produced depending on the equilibration time of the column. Eluted products were monitored following absorbance at 260 nm (Fig. 2) and were quantified by integrating the chromatographic peaks as described in [Cuchillo et al., 2002]. The elution positions of the oligonucleotides were deduced according to the method of McFarland and Borer (1979) and Moussaui et al. (1996).

Preparation of tetracytidylic acid [$(Cp)_3C>p$] from poly(C) digestion. The tetracytidylic acid used as a substrate was obtained by RNase A digestion of a poly(C) solution. In a typical experiment, 500µl of a 10 mg/ml poly(C) solution in a 15 mM HEPES-KOH (pH 7.5) were digested with 1 nM RNase A at 25 ºC for 15 min. The reaction products were separated as described before. The fractions corresponding to the tetracytidylic acid from several chromatographic runs were pooled, freeze-dried, and kept al -20ºC until use. The identity of each product was corroborated by MALDI-TOF MS analysis of the individual peak.

Analysis of products from the cleavage of tetracytidylic acid by HP-RNases. All assays were performed in 15 mM HEPES-KOH buffer (pH 7.5) at 25ºC, the substrate solution used had an absorbance ($A_{260\ nm}$) close to 0.1, and the enzyme concentration used was between 40 to 60 nM depending on the variant used. The enzyme concentration was selected in such way that a progress curve covering the depletion of at least 20 % of the initial substrate could be obtained. The enzyme solution was made immediately before the assay to avoid denaturation. Tetracytidylic acid incubated with either HP-RNase or

specific variants, and the rate of formation of products at different digestion times was analyzed by means of reversed-phase HPLC. The column was washed for 20 min with Milli-Q water and equilibrated for 20 min with solvent A (10% (w/v) ammonium acetate and 0.3% (v/v) acetonitrile in water). Then, 50 µl of the reaction mixture was injected into the column and elution was performed with an initial 10 min wash and a 40 min linear gradient from 100% solvent A to 10% solvent A plus 90% solvent B (10% (w/v) ammonium acetate and 5% (v/v) acetonitrile in water). Given the time taken for each assay (~ 30 min) and to avoid degradation owing to contamination effects associated with continuous freezing and thawing, aliquots of the substrate stock solution were kept frozen in Eppendorf tubes and only thawed immediately before use. The tetracytidylic acid subproducts concentration was calculated by using ε_{260}: 7845 M^{-1} cm^{-1} for C>p, 15175 M^{-1} cm^{-1} for CpC>p, 20745 M^{-1} cm^{-1} for $(Cp)_2C>p$ and 28683 M^{-1} cm^{-1} for $(Cp)_3C>p$ [Cuchillo et al., 2002].

Determination of steady-state kinetic parameters. The kinetic parameters for the cleavage of poly(C) and the hydrolysis of C>p by wild type and HP-RNase variants were spectrophotometrically determined as described elsewhere [Moussaoui et al., 1998]. All reactions were carried out in 0.2 M sodium acetate, pH 5.5, at 25 ºC. For C>p, the concentration of enzyme was 0.1 µM and the concentration range of C>p was from 0.15 to 3 mM. The activity was measured by recording the increase in absorbance at 296 nm using 1-cm path length quartz cells. For assays with poly(C), the enzyme concentration was 5 nM, the concentration range of poly(C) was from 0.01 to 3 mg/ml, and the decrease in absorbance at 294 nm was monitored using 0.2-cm path length quartz cells. Steady-state kinetic parameters were obtained by nonlinear regression analysis using the program GraFit v.5 [Leatherbarrow, 2001]. The values in table 1 are the averages of two determinations, with a standard error of less than 10%.

RESULTS AND DISCUSSION

1. Analysis of exonucleolytic and endonucleolytic activities of HP-RNase.

We have studied the cleavage preference of polymeric substrates by HP-RNase. First, we analyzed the pattern of products generated by the HP-RNase cleavage of poly(C) at different incubation times in a reversed-phase column. The poly(C) used as substrate is a high molecular mass polymer; however, it eluted as a single fraction from the reversed-phase HPLC column (data not shown), indicating that oligonucleotides were not present in the sample at the initial conditions.

Figure 2-A shows the elution profile obtained by reversed-phase HPLC of the cleavage products of poly(C) when only 50% of the substrate remained as a high molecular polymer. An analysis of the distribution of the oligonucleotides below 15 bases at different percentages of undigested poly(C) is shown in Figure 3. The elution position of the small nucleotides was deduced from the pattern obtained after a long time of incubation (100 min), when no high molecular mass poly(C) was left, and corresponded to that previously described for the RNase A cleavage [Moussaoui et al. 1996, Cuchillo et al., 2002]. Analysis of the chromatograms at different percentages of poly(C) digestion indicated that the enzyme does not act in a random fashion. Although at the beginning of the reaction only polynucleotide fragments are formed (data not shown), shortly thereafter a clear trend toward the formation of oligocytidylic acids with a size of about 9-11 residues is observed. These results suggest that the enzyme prefers binding and cleavage of long substrates and that to be preferentially cleaved by the enzyme the phosphodiester bond has to be some nine-eleven nucleotides apart from at least one of the ends of the molecule. In contrast, RNase A accumulates fragments containing 6-8 nucleotides [Moussaoui *et al*., 1996]. The difference in the length of the accumulated intermediate oligonucleotides between both proteins can be due to the presence of a greater number of positive charges in HP-RNase than in RNase A, which can interact with the substrate. As expected, the chromatograms show that the enzyme possesses an endonucleolytic activity, but the appearance of mononucleotides also indicates that this enzyme possesses an exonucleolytic activity.

Characterization of the poly(C) breakdown is complicated by the complexity of the molecule and by the fact that most products of the reaction are also substrates, although with different specificities. It has been shown that the exo- or endonucleolytic activity of RNase A can be characterized by analyzing the products formed from the cleavage of

tetracytidylic acid at different time reactions [Cuchillo et al., 2002]. The tetranucleotide is the smallest substrate that can be used for this analysis. The cleavage of an external bond of the tetranucleotide (exonucleolytic cleavage) adjacent to either the 5'- or 3'-terminal nucleotide creates a trinucleotide plus a mononucleotide, whereas the cleavage of central bond (i.e. endonucleolytic cleavage) gives rise to two dinucleotides (Figure 4-A). Figure 4-B shows a chromatographic pattern for tetracytidylic acid digestion by HP-RNase when approximately 50% of substrate has been digested. From this chromatogram, it is apparent that there is an even accumulation of both the trinucleotide and dinucleotide, indicating that HP-RNase acts on the substrate with no preference for the phosphodiester bond broken. However, visual inspection of the chromatogram by itself is non-conclusive because two molecules of CpC>p are formed for each central bond broken instead of one, as is the case for $(Cp)_2C>p$ derived from the breaking of an external bond. On the other hand, the molar extinction coefficients of the species are different. These effects, together with the effect of a different diffusion according to the retention time, clearly influence the actual height and broadness of the peaks. Therefore, rigorous quantification is mandatory for meaningful results as discussed in Cuchillo et al. (2002). According to this work, the endonucleolytic to exonucleolytic cleavage preference has to be determined from the ratio of product formation at the beginning of the reaction when only the tetranucleotide is present (0% digested). This is because the formation of the dinucleotide at later stages of the reaction would not be the result of the endonucleolytic cleavage of the original tetranucleotide but the result of the exonucleolytic cleavage from intermediate trinucleotide product.

The extrapolation to zero time of the ratios was performed graphically with the program GraFit v. 5 [Leatherbarrow, 2001] (Figure 5-A). The exonucleolytic versus endonucleolytic activity of HP-RNase, as determined from the ratios of the products at zero time, was around 1.35 (Table 1). Although this result indicates that the enzyme shows no clear preference for any bond, the comparison with RNase A (in which extrapolation to zero digestion time gives a value of 2.15) indicates that the human protein has a more endonucleolytic activity than RNase A. This preference change could be related to the specific function of both enzymes. Unlike RNase A, which basically displays a digestive function of exogenous RNA in the ruminant [Barnard, 1969], the function of HP-RNase is not clear but it has been related to vascular homeostasis [Landré et al., 2002] and to the induction of dendritic cell maturation [Yang et al., 2004].

It has been previously described that the non-catalytic subsites p_2 and p_0 of RNase A influence its cleavage pattern of polymeric substrates [Moussaoui et al, 1996]. A comparison of the primary sequence of HP-RNase and RNase A shows that all the residues belonging to any characterized non-catalytic subsite in RNase A are conserved in the sequence of HP-RNase. We have previously reported the structure of an HP-RNase variant named PM7 [Pous et al. 2000] in which five residues of the N-terminal region were substituted by the corresponding residues of the bovine seminal RNase (BS-RNase) and, in addition, a Pro to Ser mutation was introduced at position 50. When comparing this structure with that of RNase A, only small differences were found, restricted to the position of Lys66 (p_0), both at its main and side-chains (Figure 6A). Curiously, the exo- vs. endonucleolytic activity of HP-RNase is similar to that of the Lys66Gln RNase A, variant which presents the p_0 subsite abolished (for this RNase A variant extrapolation to zero digestion time gives a values of 1.4 (Table 1)).

The comparison of the primary sequences of HP-RNase and RNase A reveals the presence of a high number of additional basic residues at the N-terminus of the human enzyme (Figure 6B). In addition, for RNase A, it has been reported that the deletion of basic residues in this region belonging to p_2 renders this enzyme more exonucleolytic [Moussaoui et al., 1996; Cuchillo et al., 2002]. We therefore asked whether the additional basic residues in HP-RNase could increase its endonucleolytic activity. For this, we characterized the cleavage pattern of PM5, a variant of HP-RNase that lacks the basic residues Arg4 and Lys6, which have been substituted by Ala, and that also incorporates the substitutions Gln9Glu, Asp16Gly and Ser17Asn.

2. Substitution of basic residues located near p_2 in HP-RNase changes its cleavage preference for tetracytidylic acid.

Analysis of the products obtained after the cleavage of the tetranucleotide by PM5 showed that this enzyme presents a completely different pattern when compared with HP-RNase (Table 1, Figure 5B). PM5 shifts its preference for the cleavage of external bonds, and its ratio between exonucleolytic versus endonucleolytic activities resembles that of RNase A (Table 1). This change of preference is similar to that reported in an RNase A variant lacking the basic side chains of residues 7 and 10 proposed as belonging to p_2 [Cuchillo *et al*., 2002]. That is, the ratio of external/internal bonds broken relative to the parental enzyme is of 2.15 for PM5 and of 2.29 for Lys7Gln/Arg10Gln-RNase A (Table 1). Given the polyanionic nature of the RNase

substrate, it is likely that the residues of HP-RNase responsible for this change of preference may be Arg4 and Lys6, especially the latter because it is the only changed residue whose side chain faces the catalytic cleft of the enzyme (Figure 1).

Considering that the tetranucleotide phosphates can only bind in the enzyme at positions $p_{-1}p_0p_1p_2$ and $p_1p_2p_3p_4$ giving rise to an exonucleolytic cleavage and at positions $p_0p_1p_2p_3$ with endonucleolytic cleavage, these basic residues could constitute part of p_3 or alternatively, reinforce the binding of the substrate in p_2. Different arguments can reinforce both hypotheses. On the one hand, and from a theoretical point of view, if Arg4 and Lys6 were reinforcing p_2, an equal increase of the three binding possibilities could be expected, giving rise to a more exonucleolytic pattern. On the contrary, if Arg4 and Lys6 constituted p_3, they would not affect the binding to $p_{-1}p_0p_1p_2$ and then a more endonucleolytic pattern could be expected. On the other hand, however, when steady state kinetic parameters of PM5 and HP-RNase were compared (Table 2), the data obtained seem to indicate that the positive charges of Arg4 and Lys6 in HP-RNase do not constitute a phosphate-binding subsite. As can be seen in Table 2, k_{cat} values for C>p and poly(C) and the K_m for C>p are not modified, whereas the K_m for poly(C) is slightly higher than in the native enzyme. These differences are very small when they are compared with the effects of deleting a phosphate binding subsite in the RNase A. Deletion of p_{-1}, p_0 or p_2 increases the K_m for poly(C) of the resulting variants by 16, 2.5 and 3.5 times respectively [Nogués et al., 1998; Fisher et al., 1998]. Also, PM5 shows a digestion pattern of poly(C) similar to that of HP-RNase (Figure 2-A and B), including the accumulation of an oligonucleotide of 9-11 nucleotides. It could be argued that if Arg4 and Lys6 constituted a phosphate binding subsite, a decrease in the size of the oligonucleotide accumulated would be expected in PM5. A molecular model for the binding of a tetranucleotide to the HP-RNase could help to discriminate between both hypotheses.

3. Introduction of basic residues at positions 89 and 90 create a new phosphate-binding site.

When comparing the electrostatic surface of HP-RNase, PM5 and RNase A, where the catalytic cleft is located, the human enzyme contains more basic residues than the bovine enzyme, whereas on the opposite face they are not actually different (Figure 7). Since HP-RNase is able to bind larger nucleotides than RNase A, we wondered whether the addition of positive charges on the face of the enzyme where the active site clef is

located could increase the anchoring points of the RNA. PE5 is an HP-RNase variant [Bosch et al., 2004] carrying the substitutions Gly89Arg and Ser90Arg which increase the basicity of the molecule at the active site cleft (Figure 7).

The profile of poly(C) digestion by PE5 shows a pattern resembling that of the wild-type enzyme but with the accumulation of larger oligonucleotides (approximately between 13-15 residues in length) (Figure 2C). When the ratio of exo- to endonucleolytic activities was determined, no significant differences were encountered with respect to the parental enzyme (Table 1). This result was expected because this variant presents the same N-terminal changes as the parental enzyme (PM5) and the phosphate binding sites for this substrate are restricted to subsites between p_{-1} and $p_{4,}$ as discussed above.

The steady state kinetic parameters of PE5 were determined for C>p and poly(C). No significant differences were found for the k_{cat} for poly(C) and C>p respective to PM5 (Table 1). K_m values were not modified for the C>p substrate, but a slight decrease in the K_m for poly(C) was obtained, which could indicate a strengthened binding of the polymeric substrate

4. Characterization of the catalytic properties of the dimeric form of PM8E103C

DPM8E103C is a domain-swapped dimeric variant of PM5 that has been stabilized through a disulfide bond between both subunits [Rodríguez et al., 2006]. It has been described that other dimeric ribonucleases possess special catalytic properties [Piccoli and D'Alessio, 1984; Di Donato et al., 1987]; therefore we decided to characterize the catalytic properties of this variant. Stabilization through a disulfide bond between the two subunits assured that during the assays the ribonuclease did not become a monomer.

The steady-state kinetic parameters of DPM8E103C and those of its monomeric form are shown in Table 2. The k_{cat} of the dimeric form was around 35% lower than that of the monomeric form for both C>p and poly(C). However, when considering the catalytic activity of the molecule per mole of active site, the dimeric form showed a two to three-fold decrease in the catalytic activity with respect to the monomeric form. This result could be interpreted in two ways: either both active centres have about half the catalytic activity of the monomer; or one active centre is not functional. The K_m for C>p of both, monomer and dimer, was slightly lower to that of PM5 but, when poly(C) was assayed, a 4-fold increase of the K_m was observed upon dimerization (Table 2). This

result could be interpreted in the sense that when a substrate molecule is placed in one subunit of the dimer, it interferes with the binding of a second substrate molecule to the other subunit.

Figure 5D represents the exonuclease versus endonuclease activity of DPM8E103C determined from the ratio of tetranucleotide digestion products at the beginning of the reaction. As expected, the preference for external versus internal bond cleavage was analogous to that of PM5 because both variants possess the same N-terminus. We then analyzed the pattern of products generated by the cleavage of poly(C) catalyzed by DPM8E103C. At short incubation times the products of the cleavage of poly(C) by this dimeric ribonuclease mainly corresponded to very long oligonucleotides (not shown), suggesting that this enzyme prefers to bind and cleave long substrates. Figure 2-D shows the elution profile obtained after the cleavage of poly(C) when only 50% of the substrate remained as a high molecular polymer. In these conditions an accumulation of oligonucleotides of both 9-11 and over 25 bases in length were obtained. We interpret the accumulation of this longer oligonucleotide by an increase in positive charges per molecule as a consequence of the dimeric structure. In a dimer where one subunit remains inactive, the molecule has many more basic residues per active site. These basic residues could act as new interaction centres for anchoring the substrate on the protein surface. If the strength of the binding was high, the cleaved product could remain bound to the enzyme through the non-catalytic binding subsites leading to an uncompetitive inhibition that could account for the dramatic difference in the K_m for the polymeric substrate when compared to the monomeric enzyme.

Finally, it has been previously reported that domain-swapped dimeric BS-RNase displays non-hyperbolic kinetics when concentrations over 4 mM of C>p are used [Piccoli and D'Alessio, 1984]. We also tested whether DPM8E103C displayed an allosteric behaviour a high concentration of C>p. Figure 8 shows the catalytic activity of both monomeric and dimeric forms of PM8E103C at C>p concentrations up to 10 mM. Results show that both forms behaved equivalently on this substrate and therefore the dimerization of the human enzyme does not seem to endow it with allosteric properties.

REFERENCES

Barnard, E.A. (1969) Biological function of pancreatic ribonuclease, *Nature* **221**: 340-344.

Beintema, J.J., Wietzes, P., Weickmann, J.L. and Glitz, D.G. (1984) The amino acid sequence of human pancreatic ribonuclease. *Anal. Biochem.* **136**: 48-64.

Boix, E., Nikolovski, Z., Moiseyev, G.P., Rosenberg, H.,, Cuchillo, C.M. and Nogués, M.V. (1999) Kinetic and product distribution analysis of human eosinophil cationic protein indicates a subsite arrangement that favors exonuclease-type activity. *J. Biol. Chem.* **274**: 15605-15614.

Bosch, M., Benito, A., Ribó, M., Puig, T., Beaumelle, B. and Vilanova, M. (2004) A nuclear localization sequence endows human pancreatic ribonuclease with cytotoxic activity. *Biochemistry* **43**: 2167-2177.

Canals, A., Ribó, M., Benito, A., Bosch, M., Mombelli, E. and Vilanova, M. (1999) Production of engineered human pancreatic ribonucleases, solving expression and purification problems, and enhancing thermostability. *Protein Expr. Purif.* **17**: 169-181.

Cuchillo, C.M., Parés, X., Guasch, A., Barman, T., Travers, F. and Nogués, M.V. (1993) The role of 2',3'-cyclic phosphodiesters in the bovine pancreatic ribonuclease A catalysed cleavage of RNA: intermediates or products? *FEBS Lett.* **333**: 207-210.

Cuchillo, C. M., Vilanova, M. and Nogués, M.V. (1997) Pancreatic ribonucleases. In *"Ribonucleases: Structures and Functions"* 272-304, D'Alessio G. and Riordan J. F. (eds), Academic Press, San Diego.

Cuchillo, C.M., Moussaoui, M., Barman, T., Travers, F. and Nogués, M.V. (2002) The exo-or endonucleolytic preference of bovine pancreatic ribonuclease A depends on its subsites structure and on the substrate size. *Protein Sci.* **11**: 117-128.

Di Donato A, Piccoli R, D'Alessio G. (1987) Co-operativity in seminal ribonuclease function: binding studies. *Biochem J.*, **241**, 435-440.

Fisher, B.M., Grilley, J.E. and Raines, R.T. (1998) A new remote subsite in ribonuclease A. *J. Biol. Chem.* **273**: 34134-34138.

Fontecilla-Camps, J.C., de Llorens, R., le Du, M.H. and Cuchillo, C.M. (1994) Crystal structure of ribonuclease Ad(ApTpApApG) complex. Direct evidence for extended substrat recognition. *J.Biol. Chem.* **269**: 21526-21531.

Guex, N. & Peitsch, M. C. (1997). SWISS-MODEL and the Swiss-PdbViewer: an environment for comparative protein modeling. *Electrophoresis* **18**, 2714-2723

Leatherbarrow R.J. (2001) GraFit Version 5. Erithacus Software Ltd., Hortley, U.K.

Landré JB, Hewett PW, Olivot JM, Friedl P, Ko Y, Sachinidis A, Moenner M. (2002) Human endothelial cells selectively express large amounts of pancreatic-type ribonuclease (RNase 1). *J Cell Biochem.*, **86,** 540-552.

Libonati, M. and Sorrentino, S. (2001) Degradation of double-stranded RNA by mammalian pancreatic-type ribonucleases. *Methods Enzymol* **341**: 139-151.

McFarland, G.D. and Borer, P. (1979) Separation of oligo-RNA by reverse-phase HPLC. *Nucleic Acids Res.* **7**: 1067-1079.

Moussaoui, M., Guasch, A., Boix, E., Cuchillo, C.M. and Nogués, M.V. (1996) The role of non-catalytic binding subsites in the endonuclease activity of bovine pancreatic ribonuclease A. *J. Biol. Chem.* **271**: 4687-4692.

Moussaoui, M., Nogués, M.V., Guasch, A., Barman, T., Travers, F. and Cuchillo, C.M (1998) The subsites structure of bovine pancreatic ribonuclease A accounts for the abnormal kinetic behavior with cytidine 2',3'-cyclic phosphate. *J. Biol. Chem.* **40**: 25565-25572.

Nogués, M.V., Moussaoui, M., Boix, E., Vilanova, M., Ribó, M. and Cuchillo, C.M. (1998) The contribution of noncatalytic phosphate-binding subsites to the mechanism of bovine pancreatic ribonucleases A. *Cell. Mol. Life Sci*. **54**: 766-774.

Piccoli, R. and D'Alessio, G. (1984) relationship between nonhyperbolic kinetics and dimeric structure in ribonucleases. *J Biol Chem*, **259**, 693-695.

Pous J, Canals A, Terzyan SS, Guasch A, Benito A, Ribo M, Vilanova M, Coll M. (2000) Three-dimensional structure of a human pancreatic ribonuclease variant, a step forward in the design of cytotoxic ribonucleases. *J Mol Biol.*, **303**, 49-60.

Ribó, M., Benito, A., Canals, A., Nogués, M.V., Cuchillo, C.M. and Vilanova, M. (2001) Purification of engineered human pancreatic ribonuclease. *Methods Enzymol*, **341**: 221-234.

Rodríguez, M., Benito, A., Ribó, M., Vilanova, M. (2006) Characterization of the dimerization process of a domain-swapped dimeric variant of human pancreatic ribonuclease. *FEBS J.*, **273**, 1166-1176.

Sorrentino, S. (1998) Human extracellular ribonucleases: multiplicity, molecular diversity and catalytic properties of the major RNases types. *Cell Mol Life Sci* **54**: 785-794.

Sorrentino, S. and Libonati, M. (1997) Structure-function relationships in human ribonucleases: main distinctive features of the major RNase types. *FEBS Lett* **404**: 1-5.

Sorrentino, S., Nadeo, M., Russo, M. A. and D'Alessio, G. (2003) Degradation of double-stranded RNA by human pancreatic ribonuclease: crucial role of noncatalytic basic amino acid residues. *Biochemistry* **42**: 10182-10190.

Thompson, J.E., Venegas, F.D. and Raines, R.T. (1994) Energetics of catalysis by ribonucleases: Fate of the 2',3'-cyclic phosphodiester intermediate. *Biochemistry* **33**: 7408-7414.

Witzel. H., Barnard, E.A. (1962) Mechanism and binding sites in the ribonucleases reaction. II. Kinetic studies on the reaction. *Biochem. Biophys. Res. Commun.* **7**: 295-299.

Yang D., Chen Q., Rosenberg H.F., Rybak S.M., Newton D.L., Wang Z.Y., Fu Q., Tchernev V.T., Wang M., Schweitzer B., Kingsmore S.F., Patel D.D., Oppenheim J.J., Howard O.M. (2004) Human ribonuclease A superfamily members, eosinophil-derived neurotoxin and pancreatic ribonuclease, induce dendritic cell maturation and activation. *J Immunol.*, **173:** 6134-6142.

Table 1. *Exonucleolytic / endonucleolytic activity values for wild-type HP-RNase, RNase A and their variants.*

Variant	Exo/endo	Activity ratio with respect to parental enzyme [a]
HP-RNase	1.35	---
PM5	2.90	2.15
PE5	2.35	0.81
DPM8	2.7	1.07
RNase A[b]	2.15	---
RNase A K66Q[b]	1.38	0.64
RNase A K7Q/R10Q[b]	4.94	2.29

[a] For PM5 the parental enzyme is HP-RNase. For the rest of the HP-RNase variants the parental enzyme is PM5. For RNase A variants, the parental enzyme is RNase A.
[b] Data obtained from Cuchillo et al., 2002.

Table 2. *Steady state kinetic parameters for the hydrolysis of cytidine 2',3'-cyclic monophosphate and the cleavage of poly(C) by HP-RNase and its variants.* Assays were performed at 25 ºC in 0.2 M sodium acetate buffer, pH 5.5. The poly(C) substrate was heterogeneous, with a relative molecular mass range, as determined by electrophoresis or spectroscopy, of 260,000-1,200,000 (information provided by Sigma). K_m for poly(C) was calculated using the lowest M_r value as the basis for the calculation.

	C>p			Poly(C)		
Protein	K_m µM	k_{cat} s^{-1}	k_{cat}/K_m %	K_m mg/ml	k_{cat} s^{-1}	k_{cat}/K_m %
HP-RNase	440±40	0.36±0.003	100	0.34±0.08	13.3±0.6	100
PM5	435±55	0.45±0,03	126	0.47±0.03	16±1	108
PE5	490±50	0.45±0.001	112	0.26±0.03	8.8±0.5	105
MPM8E103C	405±5.0	0.5±0.1	150	0.36±0.03	14±0.5	120
DPM8E103C	352±18	0.35±0.005	121	1.22±0.08	8.76±0.6	22.3

FIGURE LEGENDS

Figure 1

Localization of the amino acid changes introduced in the HP-RNase variants. A) Ribbon representation of the structure of the monomeric HP-RNase variant PM7 (Pous *et al*., 1999). The side chain of the residues replaced both in PM5 and PE5 (R4A, K6A, Q9E, D16G, S17N) are shown in red and the side chain of the residues replaced only in PE5 (G89R, S90R) are shown in green. B) Ribbon representation of the structure of the dimeric HP-RNase variant PM8 (Canals *et al*., 2001). Side chain of residue 103 replaced in PM8E103C is shown in red. Figures have been drawn using the PyMol, DeLano Scientifics© program.

Figure 2

Analysis by reversed-phase HPLC of the products obtained from digestion of poly(C) by HP-RNase (A), PM5 (B), PE5 (C), DPM8E103C (D) at 50% of poly(C) digestion. The elution conditions are described in Materials and Methods. Note that in each chromatogram the best scale on the ordinate is used.

Figure 3

Comparison of (Cp)nC>p (n = 0-14) formation from poly(C) cleavage by HP-RNase when 80, 50 and 20% of the polymeric substrate remains undigested. Area percent has been determined from the area of the corresponding peak eluted from the Nova-Pak C_{18} column. Note that in each graphic the best scale on the ordinate is used.

Figure 4

*Analysis of the endonucleolytic versus exonucleolytic activity using tetracitidylic acid digestion. (*A) Distribution of products formed by the initial cleavage of tetracytidylic acid when exonucleolytic (left) or endonucleolytic (right) activities are considered. Arrows indicate the phosphodiester bond that can be cleaved in each possibility, giving rise to the products indicated. (B) Elution profile on a reversed-phase HPLC column of the products of tetracytidylic acid $(Cp)_3C>p$ after digestion by HP-RNase when about 50% of the substrate has been digested.

Figure 5

Exonucleolytic versus endonucleolytic activity of wild type HP-RNase, PM5, PE5 and DPM8E103C for the cleavage of the tetranucleotide $(Cp)_3C>p$ substrate. The value was determined from the ratio of trinucleotide concentration versus one half of dinucleotide concentration at zero time. Exonucleolytic versus endonucleolytic activity of the different RNases at different percentage of tetranucleotide digestion is presented together with the linear correlation between both parameters: HP-RNase (A), PM5 (B), PE5 (C) and DPM8E103C (D). The extrapolation of the ratio to zero time was determined with the program GraFit v. 5 (Leatherbarrow, 2001) and indicates the preference of the enzymes on the intact substrate. The ratio decreases over time because the trinucleotide produced at the initial stages of the reaction is used later as a substrate by the enzyme producing more dinucleotide.

Figure 6

Comparison of the residues belonging to the phosphate-binding sites in HP-RNase and RNase A. (A) Stereoview of HP-RNase. The residues of the active centre and those that are described as belonging to the phosphate-binding sites (green) are superimposed with those of RNase A in yellow (pdb accession number: 7rsa [Wlodaver et al]), and RNase A complexed with d(ApTpApA) in orange (pdb accession number: 1rcn [Fontecilla-Camps et al., 1994]). (B) Sequence comparison between HP-RNase and RNase A. Basic and acidic residues are shown in blue and red, respectively.

Figure 7

Electrostatic surfaces of RNase A, PM5, wild-type HP-RNase and PE5. Left column shows the active site clef side. Right column shows the opposite side of the molecule. The positives charges are in blue and negatives charges are in red. Surfaces calculated using the program SwissPDBViewer [Guex and Peitsch, 1997].

Figure 8

Saturation curves with C>p as substrate of monomeric (○) and dimeric (●) PM8E103C.

Figure 1

A

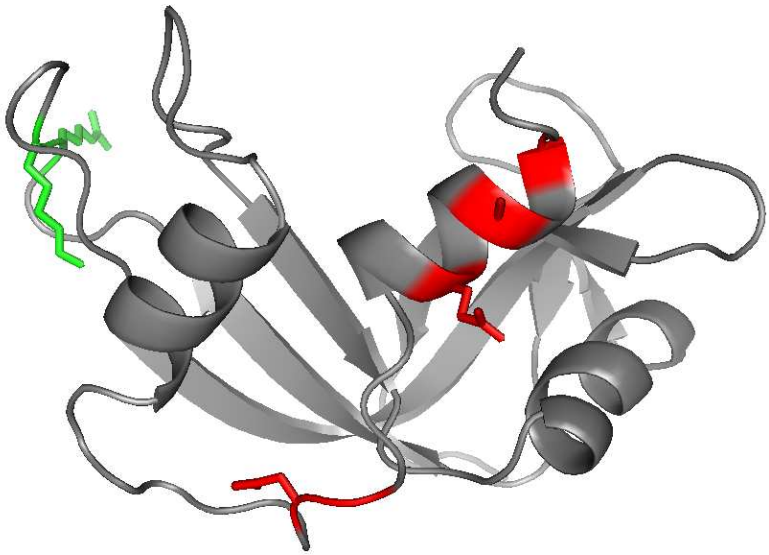

B

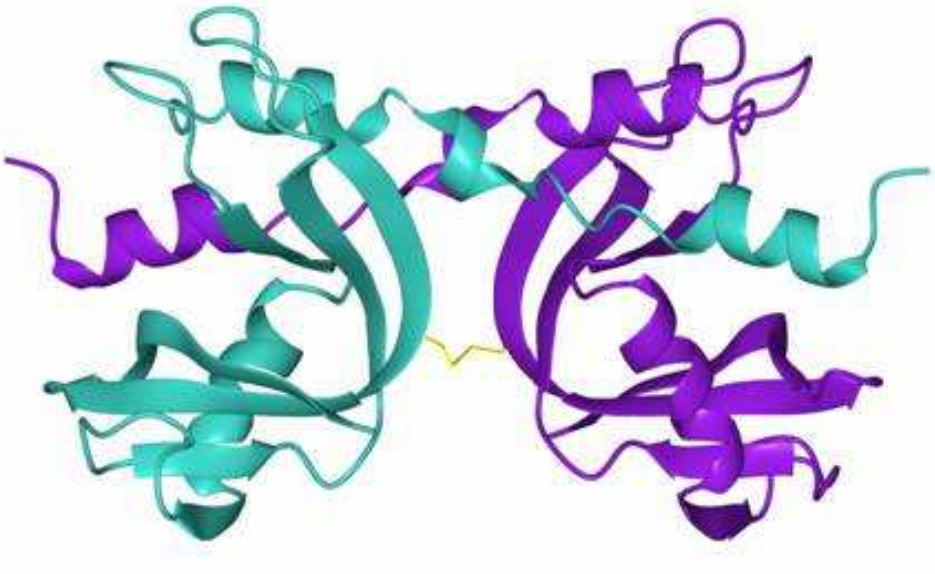

Figure 2

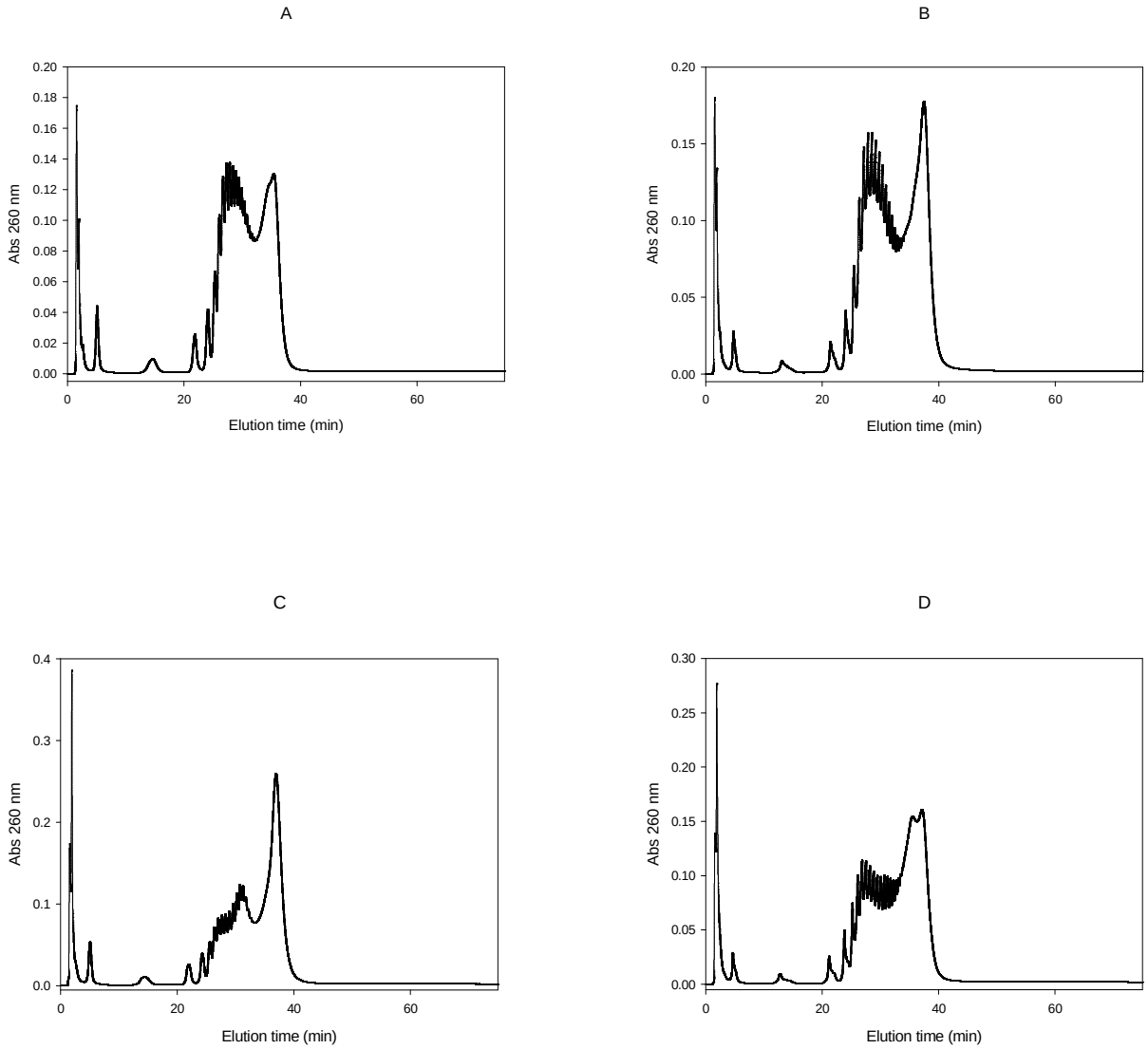

Figure 3

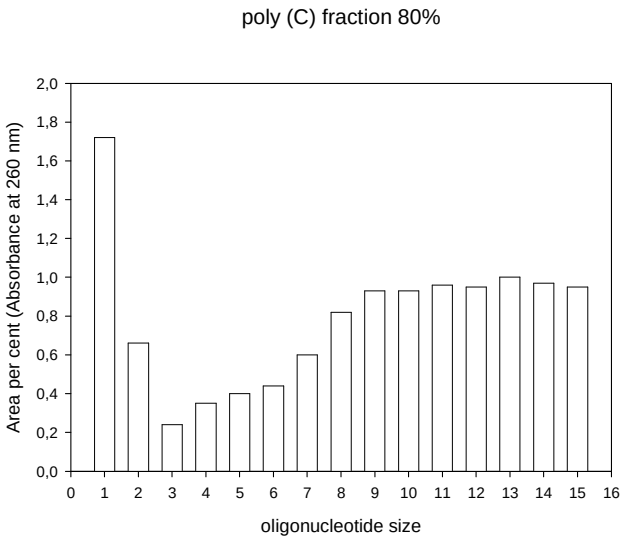
poly (C) fraction 80%
Area per cent (Absorbance at 260 nm)
oligonucleotide size

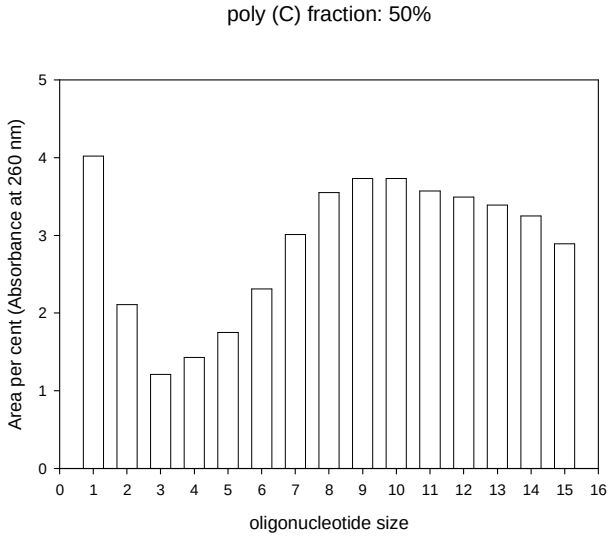
poly (C) fraction: 50%
Area per cent (Absorbance at 260 nm)
oligonucleotide size

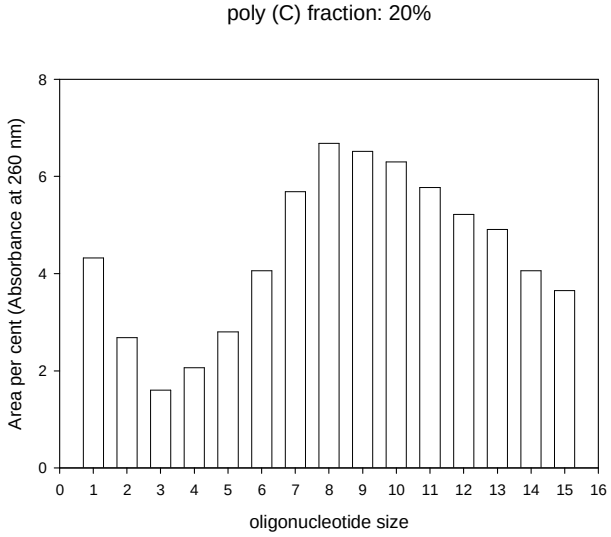
poly (C) fraction: 20%
Area per cent (Absorbance at 260 nm)
oligonucleotide size

Figure 4

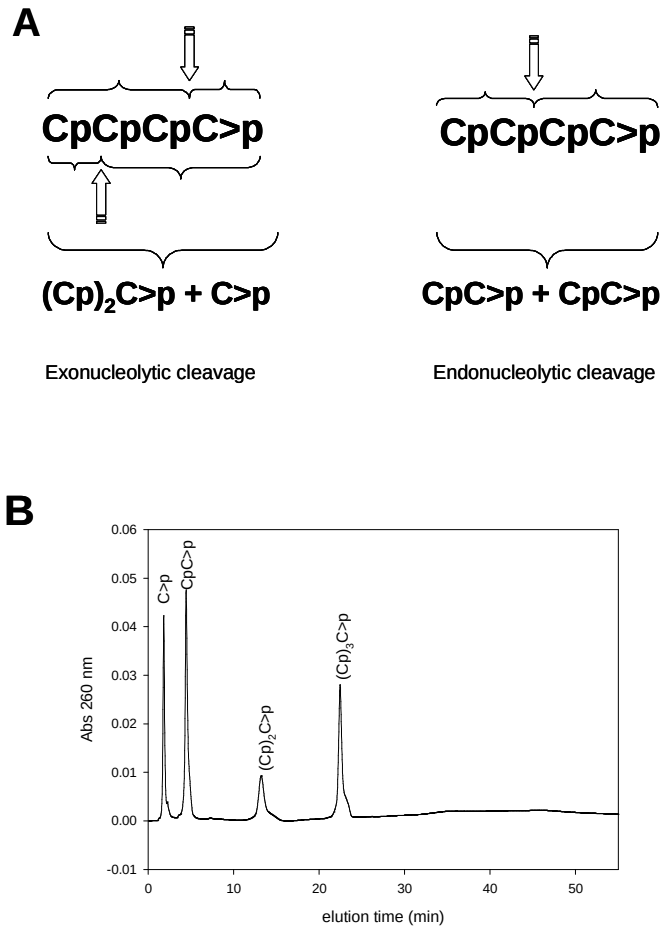
A
CpCpCpC>p
(Cp)2C>p + C>p
Exonucleolytic cleavage
CpCpCpC>p
CpC>p + CpC>p
Endonucleolytic cleavage
B
Abs 260 nm
elution time (min)
C>p
CpC>p
(Cp)2C>p
(Cp)3C>p
0.06
0.05
0.04
0.03
0.02
0.01
0.00
-0.01
0
10
20
30
40
50

Figure 5

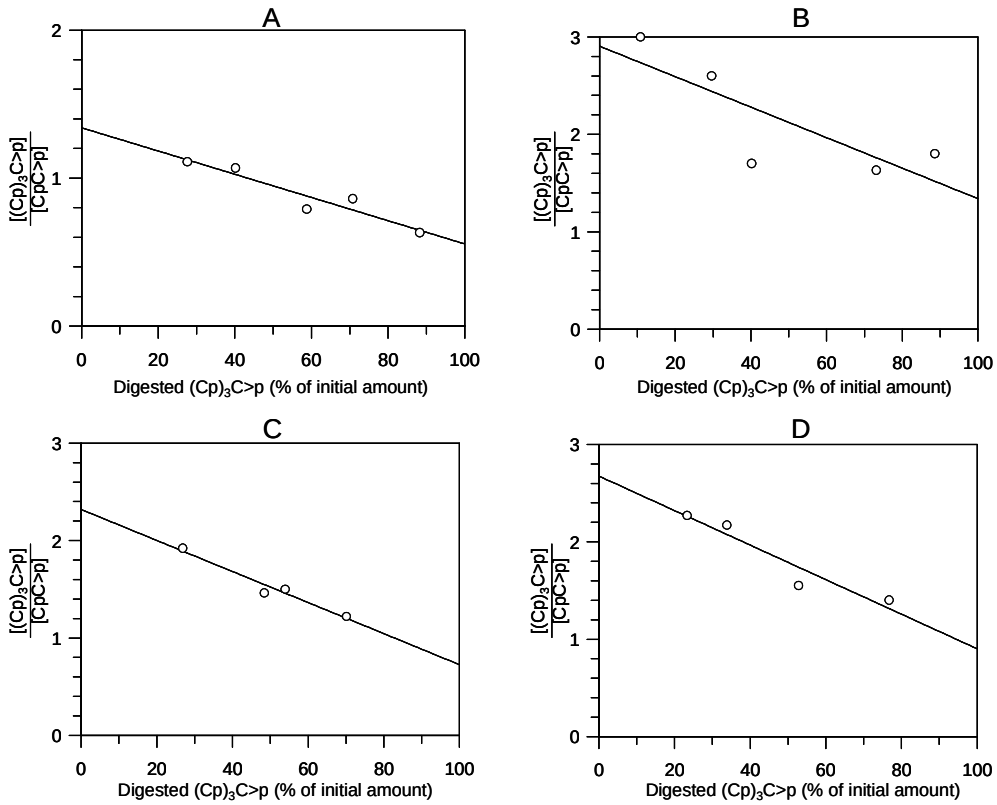
A
B
C
D
[(Cp)3C>p]/[CpC>p]
Digested (Cp)3C>p (% of initial amount)
0
20
40
60
80
100
1
2
3

Figure 6

A

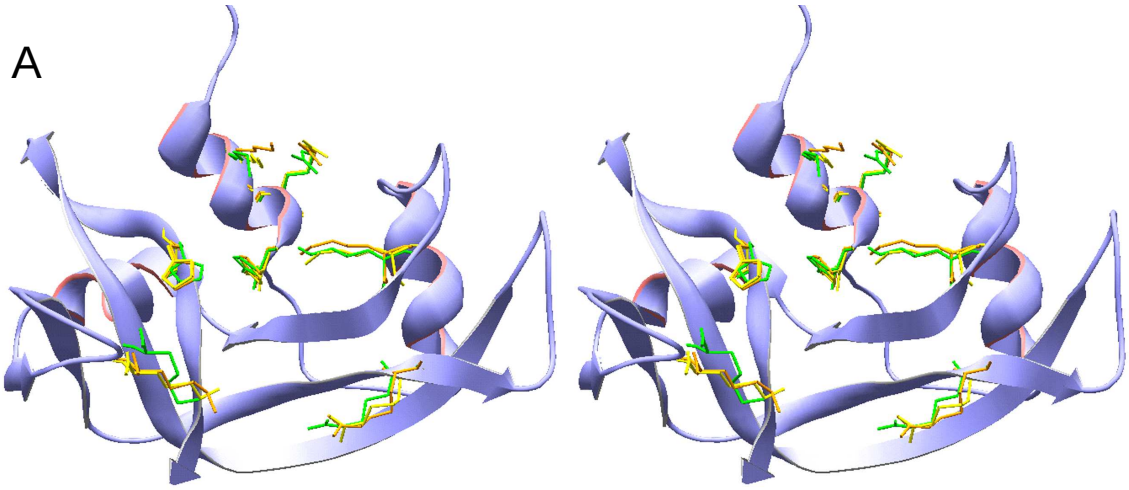

B

```
Hum. 1-    KESRAKKFQR QHMDSDSSPS SSSTYCNQMM RRRNMTQGRC KPVNTFVHEP LVDVQNVCFQ
Bov. 1-    KETAAAKFER QHMDSSTSAA SSSNYCNQMM KSRNLTKDRC KPVNTFVHES LADVQAVCSQ

Hum. 61-   EKVTCKNGQG NCYKSNSSMH ITDCRLTNGS RYPNCAYRTS QKERHIIVAC EGSPYVPVHF
Bov. 61-   KNVACKNGQT NCYQSYSTMS ITDCRETGSS KYPNCAYKTT QANKHIIVAC EGNPYVPVHF

Hum. 121-  DASVEDST
Bov. 121-  DASV
```

Figure 7

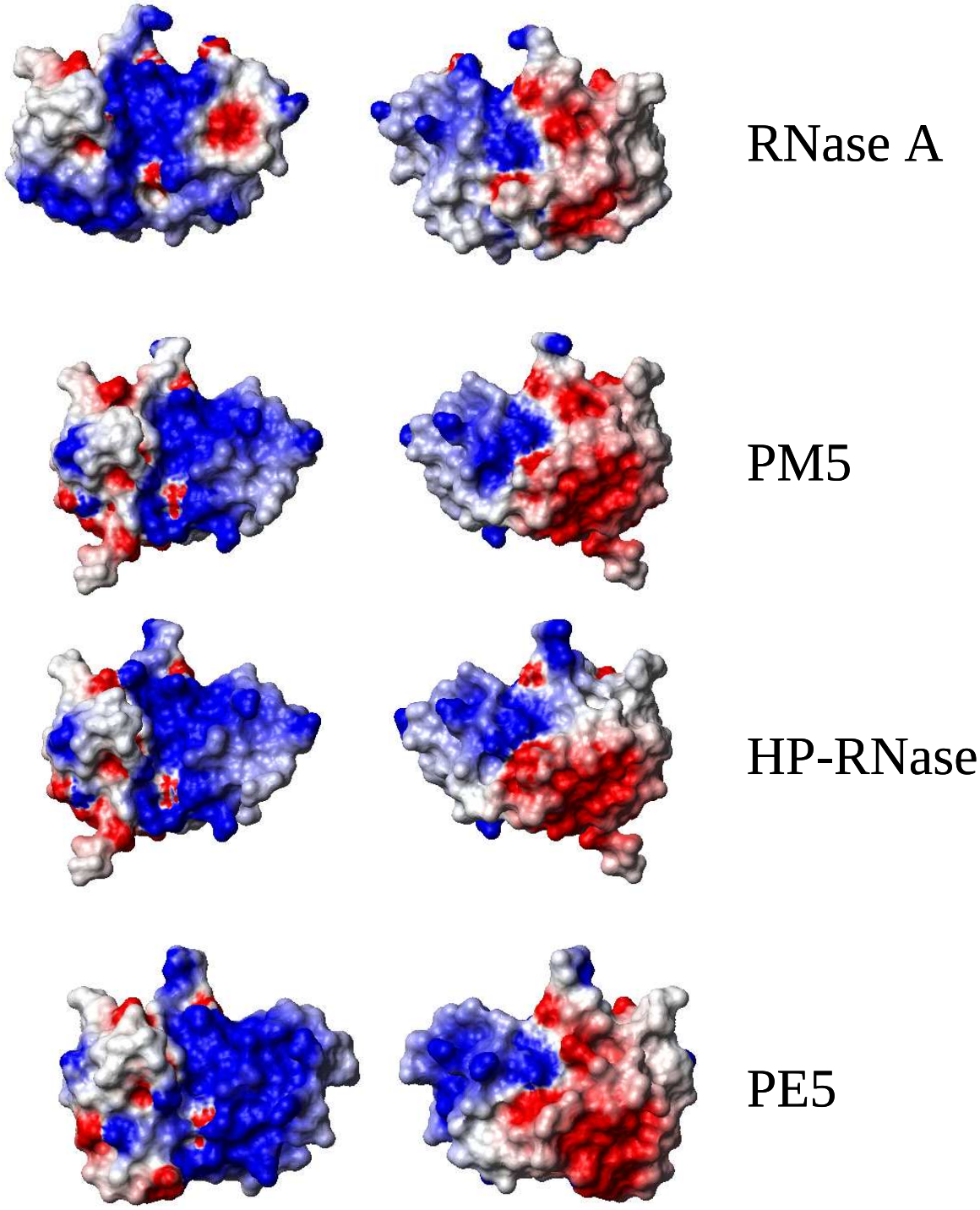

Figure 8

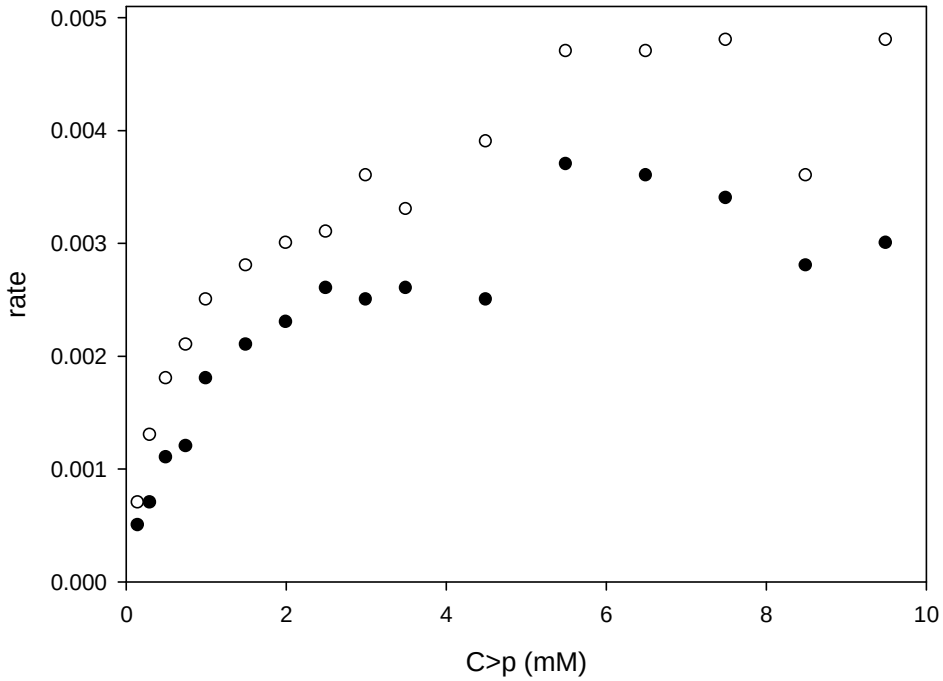

Discussió General

Un dels interessos del grup de recerca en el qual s'ha realitzat aquest treball consisteix en aprofundir en les bases moleculars que determinen la citotoxicitat de certes ribonucleases, a fi d'obtenir variants citotòxiques de l'HP-RNasa. A més llarg termini, aquestes variants podrien ser emprades com a agents quimioterapèutics ja que, degut el seu origen humà, aquestes proteïnes serien probablement menys immunogèniques que altres ribonucleases citotòxiques com l'onconasa, d'origen amfibi, o la BS-RNasa, d'origen boví.

Tal i com s'ha explicat a la introducció (veure apartat 3.1.) el mecanisme de citotoxicitat inclou un seguit de diferents etapes. En una primera etapa s'ha de produir una interacció de la RNasa amb la membrana plasmàtica de les cèl·lules tumorals, que determini la seva internalització fins a un orgànul concret. Seguidament s'ha de produir la translocació de l'enzim al citoplasma des d'aquest orgànul. Finalment, la RNasa citotòxica ha de degradar el RNA de la cèl·lula, cosa que implica que ha de conservar les seves característiques estructurals i catalítiques, així com evitar l'acció de l'inhibidor citoplasmàtic de RNases. Els esforços per obtenir variants citotòxiques de RNases s'han centrat en afavorir la seva internalització, ja sigui mitjançant la seva cationització (Futami et al., 2001, Futami *et al.*, 2002) o conjugant-les a lligands de receptors membranals (Rybak i Newton, 1999), o en impedir la formació del complex RNasa-RI a través de la generació d'impediments estèrics (Di donato *et al.*, 1994; Di Gaetano *et al.*, 2001; Piccoli *et al.*, 1999).

Un dels objectius d'aquesta tesi ha estat estudiar la internalització d'aquestes proteïnes fins a l'orgànul on són translocades al citoplasma ja que és un dels aspectes menys coneguts del mecanisme de citotoxicitat. Com a RNasa citotòxica model hem estudiat la onconasa. Vàrem escollir aquesta proteïna ja que presenta una velocitat d'endocitosis molt superior a la HP-RNasa (Bosch *et al.*, 2004). A més, l'onconasa es troba en fase III d'assajos clínics per al tractament de determinats tipus de neoplàsies (Costanzi *et al.*, 2005) cosa que fa que es pugui considerar l'exemple més paradigmàtic d'aquest grup de RNases citotòxiques.

Utilitzant variants dominant-negatives de diferents proteïnes implicades en la ruta d'endocitosi depenent de clatrina i AP-2 (Eps15, dinamina, intersectina, rab5) s'ha pogut determinar que el camí d'entrada a la cèl·lula es realitza a través del complex AP-2 i de vesícules dependents de clatrina. S'ha investigat quin camí segueix l'onconasa a través dels diferents tipus de compartiments endocítics, en cèl·lules HeLa. S'ha observat que aquesta s'acumula en les vesícules de reciclatge i que aquesta acumulació és necessària per a la seva citotoxicitat. Donat que el destí final d'aquests compartiments és fusionar-se amb la membrana cel·lular els resultats obtinguts indiquen que el pas per aquest compartiment és indispensable per

a la translocació al citoplasma de l'onconasa. A la vegada, aquest resultats, juntament amb el fet que l'onconasa s'internalitza molt ràpidament (Bosch *et al.*, 2004) indiquen que aquesta RNasa s'internalitza després de la unió a algun tipus de receptor cel·lular. Aquesta propietat no és compartida per altres RNases no citotòxiques com la HP-RNasa que s'internalitza molt més lentament, probablement per un mecanisme d'endocitosi en fase fluida, i que a més es concentra en els endosomes tardans/lisosomes (Bosch *et al.*, 2004). Hi ha la possibilitat que la direccionalització al compartiment de reciclatge sigui una manera d'augmentar la citotoxicitat d'altres RNases. Així, per exemple, la conjugació de la RNasa A a una molècula de transferrina (que en la cèl·lula és dirigida als endosomes de reciclatge) augmenta la citotoxicitat de la nova variant 10.000 vegades (Rybak i Newton, 1999).

També s'ha intentat caracteritzar la translocació de la variant citotòxica PE5 portant a terme el mateix tipus d'experiments d'expressió transitòria de moduladors de l'endocitosi. Degut a què aquesta proteïna presenta una velocitat d'internalització molt menor no va ésser possible obtenir resultats d'aquests experiments. El principal problema radicava en què per assegurar una mínima internalització de RNasa calien temps d'incubació amb les cèl·lules molts superiors als màxims que mantenien una expressió significativa dels moduladors de les vies endocítiques. Cal destacar aquí que treballs previs del grup han mostrat que PE5 segueix la via de degradació que la condueix cap als lisosomes i que no es va trobar cap evidència de què una fracció de les molècules PE5 seguís la via de trànsit retrògrada envers l'aparell de Golgi o el reticle endoplasmàtic ni tampoc que es localitzés en els endosomes de reciclatge. Finalment, l'estudi de la citotoxicitat en presència de drogues disruptores del trànsit intracel·lular indica que la seva toxicitat es veu afavorida amb l'increment del pH (Bosch *et al.*, 2004) igual com s'ha observat per a l'onconasa indicant que el pH afecta de la mateixa manera la translocació de les diferents RNases assajades.

Tot i que no s'ha pogut caracteritzar la via d'entrada de PE5, resultats previs al grup indicaven que aquesta variant arriba al nucli cosa que indicaria que està dotada d'una senyal de localització nuclear. L'enzim, que arribaria al citoplasma a partir d'algun punt del sistema endosomal, seria conduït ràpidament al nucli de la cèl·lula per mitjà d'un mecanisme de transport actiu i es concentraria al nucleol, on probablement catalitzaria la degradació del rRNA provocant la mort de la cèl·lula (Bosch *et al.*, 2004). A partir de l'anàlisi de la seqüència de PE5 no va ser possible localitzar a les bases de dades quin era el motiu que era reconegut per la maquinària d'import nuclear. Tal i com es descriu en el capítol II de resultats, a partir de la comparació d'un model de l'estructura de PE5 amb el d'altres proteïnes importades al nucli es va proposar que certs residus bàsics de la RNasa podien formar part d'aquest NLS. La substitució d'aquests residus i l'anàlisi del transport nuclear de les variants resultants van

mostrar que aquest NLS està format, almenys en part, per tres regions de la proteïna disposades al llarg de 90 residus. Malgrat estar molt separades en la seqüència, aquestes regions es troben molt properes en l'estructura i en una disposició que recorda molt a la que presenten els residus bàsics en un NLS bipartit. En aquesta estructura, els residus Arg89 i Arg90 i el residu Lys1 es troben respectivament disposat de manera anàloga als llocs d'unió a importines principal i secundari en un NLS bipartit. Els NLS han estat clàssicament considerats com seqüències lineals de proteïnes. El NLS de PE5 constituiria des d'aquest punt de vista una nova classe de NLSs en la què residus allunyats en la seqüència mimetitzarien en l'estructura la disposició de residus d'un NLS bipartit. Aquests resultats tenen implicacions de cara a les estratègies d'identificació de NLSs en bases de dades i són un nou exemple de la gran versatilitat de la importina α per a reconèixer un ampli espectre de senyals.

Un aspecte que ha quedat per dilucidar és la relació existent entre la presència d'un NLS i la citotoxicitat. Tot i que no s'ha trobat cap altra explicació de la citotoxicitat de PE5 queda pendent de caracteritzar la citotoxicitat de diferents variants en les quals s'elimini aquest NLS. De totes maneres, treballs realitzats pel grup de recerca han mostrat que quan a una RNasa no citotòxica que se li incorpora la seqüència d'un NLS (en concret el NLS bipartit de l'antigen Tlarge del virus SV_{40}) en el llaç exposat $\beta_4\beta_5$, aquesta nova variant presenta una activitat citotòxica que no presenta en canvi una altra variant a la que s'insereix allà mateix una seqüència de la mateixa composició però que no és un NLS (scrambled NLS). Aquest resultat suggereix que la direccionalització de RNases a nucli és una nova estratègia vàlida per a dotar aquests enzims d'activitat citotòxica (Tubert, 2005).

Tal com s'ha comentat anteriorment a la introducció, una altra estratègia per dotar una proteïna d'activitat citotòxica és que presenti una estructura quaternària. Aquest és el cas per exemple de la BS-RNasa (D'Alessio *et al.*, 1997) o d'alguns dímers artificials de la HP-RNasa o la RNasa A (Catanzano *et al.*, 1997; Piccoli et al., 1999). En el grup de recerca s'havia construït anteriorment una variant de la HP-RNasa, denominada PM8 (Canals *et al.*, 1999), la qual tot i que en solució es trobava majoritàriament en forma monomèrica, la seva estructura cristal·logràfica era un dímer (Canals *et al.*, 2001). En aquest dímer s'observa un intercanvi de dominis N-terminals tal com succeeix en el cas de la BS-RNasa (Mazzarella *et al.*, 1993) i el dímer minoritari de la RNasa A (Liu *et al.*, 1998). Les dues subunitats de l'estructura dimèrica es mantenen unides en la interfície primària per interaccions hidrofòbiques entre els residus Phe8 i Met13 del domini intercanviat i la resta de l'altra subunitat. La interfície secundària de PM8 es troba estabilitzada per ponts d'hidrogen entre els residus Gln101 i Ser20 i interaccions iòniques entre els residus Glu103 i Arg104 de cada subunitat. Aquestes interaccions no són suficientment fortes per mantenir estable la forma dimèrica de PM8 en solució (veure capítol III

de resultats). Donada la facilitat de dissociació del dímer de PM8 i que únicament són citotòxics aquells dímers de RNasa units covalentment, es va procedir a la construcció d'una nova variant dimèrica, estabilitzada per un enllaç disulfur entre les dos subunitats, denominada PM8E103C. Aquesta variant no és capaç d'evadir l'RI, degut probablement a que l'enllaç disulfur es pot reduir fàcilment, i conseqüentment PM8E103C no presenta citotoxicitat (veure apèndix).

De l'estudi de la formació i estabilitat dels dímers covalent i no covalent s'ha arribat a proposar un model per al mecanisme de dimerització d'aquesta variant de la HP-RNasa. Aquest model de dimerització podria ser anàleg al proposat per la BS-RNasa on es postula que primer es forma un dímer que no presenta intercanvi de dominis i posteriorment, s'intercanvia el domini N-terminal. Aquesta segona etapa es produiria com a conseqüència de l'estabilització de cada pèptid xarnera per part de residus de l'altra subunitat en una conformació que facilitaria l'intercanvi. Per altra banda, resulta interessant destacar que mentre que un 70% de les molècules del dímer de la BS-RNasa presenten el domini N-terminal intercanviat, pràcticament totes les molècules del dímer PM8E103C l'intercanvien. Aquesta diferència probablement està relacionada amb el grau d'estabilització del pèptid xarnera, que és molt superior en el dímer de PM8 que en la BS-RNasa.

L'anàlisi del patró de trencament de substrats polimèrics per l'HP-RNasa mostra que aquest enzim presenta un comportament molt més endonucleolític que el descrit per a la RNasa A (Cuchillo *et al.*, 2002). A diferència de la RNasa A, a la qual se li suposa una funció de digestió de RNA exogen, no es coneix la funció de la HP-RNasa però aquest enzim podria estar implicat en la degradació de RNA tant de cadena simple com doble (Sorrentino and Libonati, 1997; Sorrentino 1998; Libonati and Sorrentino, 2001, Sorrentino et al., 2003). Aquesta divergència en les seves funcions podria explicar el canvi de comportament en quan al patró de digestió. La RNasa A hauria patit una pressió selectiva per a ser un enzim més exonucleolític que permetés la generació de nucleòtids que puguessin ser assimilats més fàcilment en la digestió. En canvi la funció de l'HP-RNasa podria estar implicada en la inactivació de certs RNAs que induïssin canvis en l'expressió gènica on una activitat més endonucleasa seria més adequada. El comportament endonucleolític de la HP-RNasa és en part degut a la presència de dos residus bàsics (R4 i K6) en l'extrem N-terminal de l'enzim. Aquests dos residus podrien generar un nou centre de fixació de fosfat (p_3) o alternativament reforçar el subseti p_2. Amb les dades de què es disposa en aquest moment no és possible discernir entre les dues opcions. La resolució de l'estructura de l'enzim amb un deoxinucleòtid de mida definida permetria assignar clarament quin paper juguen aquests dos residus bàsics. La caracterització cinètica del dímer PM8E103C suggereix que només un dels dos centres catalítics és funcional. Quan s'ha caracteritzat cinèticament el dímer de PM8, emprant C>p com a substrat, s'ha trobat un comportament

similar al monòmer ja que en l'estructura de PM8 els residus dels dos centres actius es troben disposats d'una manera equivalent als de la RNasa A. És de suposar que la inactivació d'un dels dos centres es produeix com a conseqüència de la unió del substrat a l'altre centre actiu. Per contra no hem observat un comportament alostèric de la variant dimèrica a elevades concnetracions de C>p a diferència del descrit per la BS-RNasa (Piccoli and D'Alessio, 1984).

D'una manera general, aquesta tesi contribueix al coneixement de diferents aspectes de les funcions biològiques de lesRNases, tant pel que fa a la citotoxicitat com a d'altres aspectes ja sigui el mecanisme de formació d'oligòmers o la caracterització de l'activitat enzimàtica.

Conclusions

1. The endocytosis of onconase in Jurkat cells is affected by the expression of the dominant-negative version of Eps15, dynamin and intersectin in a dose-response manner. Onconase labeled with gold is concentrated within coated pits at the plasma membrane when it is incubated with Jurkat cells at 37 ºC. All together these results show that in Jurkat cells, onconase is endocyted via an AP-2/ clathrin-dependent pathway.

2. Dominant negative versions of dynamin, Eps15 and intersectin effectors are able to protect Jurkat transfected cells from the pro-apoptotic effect of onconase showing that onconase toxicity is dependent of its endocytosis through the AP-2/clathrin-dependent pathway.

3. In HeLa cells, onconase does not significantly colocalize with established late endosome/lysosome markers such as the lysosomal membrane proteins (Lamp-1, Lamp-2, Lamp-3), internalized dextran, LBPA or the mannose 6-phosphate receptor. Onconase-containing structures are also negative for calnexin or TGN46, indicating that this protein is neither transported to the endoplasmic reticulum nor to the trans-Golgi network. Onconase is concentrated within the receptor recycling compartment at the center of the cell together with fluorescent transferrin.

4. When onconase is internalized in HeLa cells it colocalizes very efficiently with Rab11 and transferrin in the pericentriolar recycling compartment at the center of the cell but not with Rab4 and Rab5. These data show that onconase follows transferrin internalization pathway i.e. from coated pits to the recycling compartment.

5. Onconase and tranferrin uptake is inhibited by the dominant negative version of Rab5 (Rab5S34N) but are not affected by the dominant negative version of Rab7 (Rab7N125I) that impairs transport to late endosomes. Hence, onconase internalization is regulated by Rab5 and onconase intracellular routing is restricted to early endosomes.

6. Cells overexpressing dominant negatives Rab5 are less sensitive to onconase than control cells whereas dominant negative or activated version of Rab7 does not affect onconase toxicity. These results indicate that onconase toxicity is regulated by Rab5 but not by Rab7.

7. Tetanus toxin expression enhances onconase toxicity by 32% whereas the proteolytically inactive E234Q mutant has no significant effect. This result indicates that the recycling compartment enables onconase translocation to the cytosol and that a higher onconase concentration in this compartment favors its toxicity.

8. Neutralization of endosomal pH with NH_4Cl, monensin or bafilomicyn on HeLa and A431 cells lines increases onconase toxicity. This effect is more apparent when the pH is more drastically affected, i.e. using bafilomicyn. Bafilomicyn does not modify the efficiency of onconase colocalisation with established markers of the endocytic pathway, indicating that endosome neutralisation did not affect onconase intracellular routing. All these results show that onconase translocation to the cytosol from recycling endosomes is facilitated by the endosomal pH neutralization.

9. PE5 is able to specifically interact with Xenopus laevis importin α.

10. The substitution of residues Lys1, Arg31, Arg32 or Arg33 of PE5 by Ala or Glu impairs the nuclear import of the resulting variants in an in vitro assay. This effect is not due to a general desestabilization of the recombinant protein.

11. The superposition of a model of PE5 with the structure of a bipartite NLS shows that residues Lys1 as well as Arg89 and 90 of PE5 are located in a disposition that closely resembles that of the most critical basic residues of the major and minor binding sites of a bipartite NLS. The position of residues Arg31 and 32 closely matches with those residues of the linker of bipartite NLS, that in some cases make interactions with importin α. Thus NLS of PE5 is constituted by residues that are located for apart in the sequence but that are brought together in the three-dimensional structure of the protein in a disposition that resembles a classical bipartite NLS.

12. Size-exclusion chromatography allows clear discrimination between the different forms of PM8 and their quantification. At 29 ºC in a 20% (v/v) ethanol buffer, a significant fraction of the protein is found in dimeric form without the appearance of higher oligomers.

13. The dissociation constant of the dimeric form of PM8 is 5 mM at 29ºC.

14. The thermal unfolding process of monomeric PM8 has been monitored by UV-absorbance spectroscopy and by differential scanning calorimetry. The process is reversible and only one transition is observed which begin at 39ºC. These experiments show that a previous dissociation of the exchangeable domain from the main protein body does not take place before the dimerization process.

15. The construction of a new variant of PM8 stabilized by a disulfide bond between the two subunits, namely PM8E103C; does not endow the enzyme with citotòxica properties against HeLa cell probably because it is not able to evade the RI.

16. The study of the degree of swapping between the protomers in the purified dimer of PM8E103C analysed by cross-linking of His-12 and His-119 of both active sites shows that nearly 100% of the dimer is interchanging their N-terminal moieties. The absence of nonswapped dimers indicates that, when PM8E103C is in the dimeric conformation, the N-terminal domain of one subunit is settled much more stably over the other subunit.

17. The results presented here suggest a model for the dimerization of PM8 that is different to that postulated for the dimerization of the homologous bovine pancreatic ribonucleases. In this model, an open interface is formed first and then intersubunit interactions stabilize the hinge loop in a conformation that completely displaces the equilibrium between nonswapped and swapped dimers to the latter ones.

18. The analysis of the pattern of oligonucleotide formation by HP-RNase shows that the enzyme does not act randomly and follows a more endonucleolytic pattern when compared with RNase A. The enzyme prefers the binding and cleavage of longer substrate molecules specially when the phosphodiester bond broken is 9-11 nucleotides apart from at least one of the ends of the substrate molecule.

19. Deletion of two positives charges on the N-terminus of HP-RNase (Arg4 and Lys6) modifies the pattern of external/internal phosphodiester bond cleavage preference leading to a more exonucleolytic enzyme.

20. Analysis of the catalytic constants and the cleavage pattern of polymeric substrate by a dimeric variant of HP-RNase (PM8E103C) suggest that the interaction of one active site with the substrate likely induces a conformational change on the enzyme that precludes the cleavage of the substrat by the other active site.

Bibliografia

Avitabile, F. Alfano, C., Spadaccini, R., Crescenzi, O., D'Ursi, A.M., D'Alessio, G., Tancredi, T. and Picone, D. (2003) The swapping of terminal arms in ribonucleases: comparison of the solution structure of monomeric bovine seminal and pancreatic ribonucleases2003

Ardelt, B., Ardelt, W. And Darzynkiewicz, Z. (2003) Cytotoxic ribonucleases and RNA interference (RNAi). *Cell Cycle*, **2**, 22-24.

Argent, R. H. Roberts, L.M., Wales, R., Robertus, J.D. and Lord, J. M. (1994) Introduction of a disulfide bond into ricin A chain decreases the cytotoxicity of the ricin holotoxin. *J. Biol. Chem.*, **269**, 26705-26710.

Barnard, E. A. (1969) Biological function of pancreatic ribonuclease. *Nature*, **221**, 340-344.

Bartholeyns, J. and Baudhuin, P. (1976) Inhibition of tumor cell proliferation by dimerized ribonuclease. *Proc Natl Acad Sci USA*, **73**, 573-576.

Bartholeyns, J., Peeters-Joris, C., Reychler, H. And Baudhuin, P. (1975) Hepatic nucleases. 1. Methods fort he specific determination and characterization in rat liver. *Eur. J. Biochem.*, **57**, 205-211.

Beintema, J. J. (1998) Introduction: the ribonuclease A superfamily. *Cell Mol Life Sci*, **54**, 763-765.

Beintema, J. J., Schuller, C., Irie, M. and Carsana, A. (1988) Molecular evolution of the ribonuclease superfamily. *Prog Biophus Mol Biol*, **51**, 165-192.

Bennet, M.J., Schlunegger, M. P. and Eisenberg, D. S. (1995) 3D Domain swapping: A mechanism for oligomer assembly. *Protein Sci*, 4, 2455-2468.

Boix, E., Wu, Y., Vasandani, V. M., Saxena, S. K., Ardelt, W., Ladner, J. and Youle, R., J. (1996) Role of the N terminus n RNase A homologues: differences in catalytic activity, ribonuclease inhibitor interaction and cytotoxicity. *J Mol Biol*, **257**, 992-1007.

Borkakoti, N. (1983) Enzyme specificity: base recognition and hydrolysis of RNA by ribonuclease A. *FEBBS Lett*, **162**, 367-373.

Bosch, M., Benito, A., Ribó, M., Puig, T., Beaumelle, B. and Vilanova, M. (2004) A nuclear localization sequence endows human pancreatic ribonuclease with cytotoxic activity. *Biochemistry*, **43**, 2167-2177.

Bracale, A., Spalletti-Cernia, D., Mastronicola, M., Castaldi, F., Mannucci, R., Nitsch, L. and D'Alessio, G. (2002) Essential stations in the intracellular pathway of cytotoxic bovine seminal ribonuclease. *Biochem J*, **362**, 553-560.

Bracale, A., Castaldi, F., Nitsch, L. and D'Alessio, G (2003) A role for the intersubunit disulfides of seminal RNase in the mechanism of its antitumor action. *Eur J Biochem*, 270, 1980-1987.

Canals, A., Ribó, M., Benito, A., Bosch, M., Mombelli, E. and Vilanova, M. (1999) Production of engineered human pancreatic ribonucelases, solving expression and purification problems, and enhancing thermostability. *Protein Expr Purif*, **17**, 169-181.

Canals, A., Pous, J., Guasch, A., Benito., A., Ribó, M., Vilanova, M. and Coll, M. (2001) The structure of an engineered domain-swapped ribonuclease dimmer and its implications for the evolution of proteins toward oligomerization.*Structure*, **9**, 967-976.

Catanzano F, Graziano G, Cafaro V, D'Alessio G, Di Donato A, Barone G. (1997) From ribonuclease A toward bovine seminal ribonuclease: a step by step thermodynamic analysis. *Biochemistry* **36**, 14403-14408.

Costanzi J, Sidransky D, Navon A, Goldsweig H. (2005) Ribonucleases as a novel pro-apoptotic anticancer strategy: review of the preclinical and clinical data for ranpirnase. *Cancer Invest* **23**, 643-650

Crestfield, A. M., Stein, W. H. and Moore, S. (1962) On the aggregation of bovine pancreatic ribonuclease. *Arch Biochem Biophys Suppl*, 1,217-222.

Cuchillo, C. M., Parés, X., Guasch, A., Barman, T., Travers, F. and Nogués, M. V. (1993) The role of 2',3'-cyclic phosphodiesters in the bovine pancreatic ribonuclease A catalysed cleavage of RNA: intermediates or products? *FEBS Lett*, **333**, 207-210.

Cuchillo, C., Vilanova, M. and Nogués, M.V. (1997) *A "Ribonucleases: Structures and Functions"*Academic Press, New York.

Cuchillo CM, Moussaoui M, Barman T, Travers F, Nogues MV. (2002) The exo- or endonucleolytic preference of bovine pancreatic ribonuclease A depends on its subsites structure and on the substrate size.*Protein Sci.*, **11**, 117-128.

D'Alessio, G., Di Donato, A., Mazzarella, L. and Piccoli, R. (1997) A "Ribonucleases: Structures and Functions" (D'Alessio, G. and Riordan , J.F., Ed.), pp.383-423, Academic Press, Nova York.

Darzynkiewicz, Z., Carter, S.P., Mikulski, S. M., Ardelt, W. J. and Shogen, K. (1988) Cytostatic and cytotoxic effects of Pannon (P-30 Protein), a novel anticancer agent. *Cell Tissue Kinet*, **21**¸169-182.

delCardayré, S. B., and Raines, R. T. (1994) Structural determinants of enzymatic processivity. *Biochemistry*, **33**, 6031-6037.

Deutscher, M. P. (1988) The metabolic role of RNases. *Trends Biochem Sci*, **13**, 136-139.

Deutscher, M. P. (1993) Ribonuclease multiplicity, diversity, and complexity. *J Biol Chem*, **268**, 13011-13014.

Deutscher, M. P. and Li, Z. (2001) Exoribonucleases and their multiple roles in RNA metabolism. *Prog Nucleic Acid Res Mol Biol*, **66**, 67-105.

Diederichs, K., Jacques, S., Boone, T. and Karplus, P.A. (1991) Low-resolution structure of recombinant human granulocyte-macrophage colony stimulating factor. *J Mol Biol*, **221**, 55-60.

Di Donato, A. Canfaro, V. and D'Alessio, G. (1994) Ribonuclease A can be transformed into a dimeric ribonuclease with antitumor activity. *J Biol Chem*, **269**, 17394-17396.

Di Gaetano, S., D'Alessio, G. and Piccoli, R. (2001) Second generation antitumour human RNase: significance of its structural and functional features for the mechanism of antitumour action. *Biochem J*, **358**, 241-247.

Donadio, S., Tamburrini, M., Di Donato, A., Piccoli, R. and D'Alessio, G. (1986) Site-directed alkylation and site-site interactions in bovine seminal ribonuclease. *Eur J Biochem*, **157**, 475-480.

Ercole, C., Avitabile, F., Del Vecchio, P., Crescenzi, O., Tancredi, T. and Picone, D. (2003) Role of the hinge peptide and the intersubunit interface in the swapping of N-termini in dimeric bovine seminal RNase. *Eur J Biochem*, **270**,4729-4735.

Findlay, D., Herries, D. G., Mathias, A. P., Rabin, B. R. and Ross, C. A. (1961) The active site and mechanism of action of bovine pancreatic ribonuclease. *Nature*, **190**, 781-784.

Follmann, H., Wieker, H. J. and Witzel, H. (1967) On the mechanism of ribonuclease reactio. 2. The pre-ordering in the substrate as the accelerating factor in dinucleside phosphates and analogous compunds. *Eur J Biochem*, **1**, 234-250.

Futami J, Maeda T, Kitazoe M, Nukui E, Tada H, Seno M, Kosaka M, Yamada H. (2001) Preparation of potent cytotoxic ribonucleases by cationization: enhanced cellular uptake and decreased interaction with ribonuclease inhibitor by chemical modification of carboxyl groups. *Biochemistry*, **40**, 7518-7524.

Futami J, Nukui E, Maeda T, Kosaka M, Tada H, Seno M, Yamada H. (2002) Optimum modification for the highest cytotoxicity of cationized ribonuclease. *J Biochem* (Tokyo). **132**, 223-228.

Gilliland, G. L. (1997) *A "Ribonucleases: Structures and Functions"*Academic Press, New York.

Gotte, G., Laurents, D.V. and Libonati, M. (2005) Three-dimensional domain-swapped oligomers of ribonuclease A: identification of a fifth tetramer, pentamers and hexamers, and detection of trace heptameric, octameric and nonameric species. *Biochim Biophys Acta*, **1764**, 44-54.

Gotte, G. and Libonati, M. (2004) Oligomerization of ribonuclease A: two novel three-dimensional domain-swapped tetramers. *J Biol Chem*, **279**, 36670-36679.

Gotte, G., Bertoldi, M. and Libonati, M. (1999) Structural versatility of bovine ribonuclease A. Distinct conformers of trimeric and tetrameric aggregates of the enzyme. *Eur J Biochem*, **265**, 680-687.

Gotte, G., Testolin, L., Costanzo, C., Sorrentino, S., Armado, U. and Libonati, M. (1997) Cross-linked trimers of bovine ribonuclease A: activity on double-stranded RNA and antitumor action. *FEBS Lett*, **415**, 308-312.

Gotte, G., Vottariello, F. and Libonati, M. (2003) Thermal aggregation of ribonuclease A. A contribution to the understanding of the role of 3D domain swapping in protein aggregation. *J Biol Chem*, **278**, 10763-10769.

Green, S.M., Gittis, A.G. Meeker, A.K. and Lattman, E.E. (1995) One-step evolution of a dimer from a monomeric protein. *Nat Struct Biol*, **2**, 746-751.

Haigis, M. C., Kurten, E. L., Abel, R. L. and Raines, R. T. (2002) KFERQ sequence in ribonuclease A-mediated cytotoxicity. *J Biol Chem*, **277**, 11576-11581.

Haigis, M. C., and Raines, R. T. (2003) Secretori ribonucleases are internalized by a dynamin-independent endocytic pathway. *J. Cell Sci*, **116**, 313-324.

Harder, J. and Schroder, J. M. (2002) RNase 7, a novel innate immune defense antimicrobial protein of healthy human skin. *J Biol Chem*, **277**, 46779-46784.

Heringa, J., and Taylor, W.R. (1997) Three-dimensional domain duplication, swapping and stealing. *Curr Opin Struct Biol*, ***7***, 416-21.

Hlinak, Z., Matousek, J. and Madlafousek, J. (1981) The effect of bull seminal ribonuclease on reproductive organs and sexual behaviour in male rats. *Physiol Bohemoslov*, **30**, 539-542.

Iordanov, M. S., Ryabinina, O.P. Wong, J., Dinh, T. H., Newton, D. L., Rybak, S. M. and Magun, B.E. (2000) Molecular determinants of paoptosis induced by the cytotoxic ribonuclease onconase: evidence for cytotoxic mechanisms different from inhibition of protein synthesis. *Cancer Res*, **60**, 1983-1994.

Irie, M., Mikami, F., Monma, K., Ohgi, K., Watanabe, H., Yamagychi, R. and Nagase, H. (1984a) Kinetic studies on the cleavage of oligouridylic acids and poly U by bovine pancreatic ribonuclease A. *J Biochem (Tokio)*, **96**, 89-96.

Irie, M., Watanabe, F., Ohgi, K., Tobe, M., Matsumura, G., Arata, Y., Hirose, T. and Inamaya S. (1984b) Some evidence suggesting the existence of P2 and B3 sites in the active site of bovine pancreatic ribonuclease A. *J Biochem (Tokio)*, **95**, 751-759.

Irie, M. (1997) Structures and functions of ribonucleases. *Yakugaku Zasshi*. **117**, 561-582.

Iwama, M., Ogawa, U., Sasaki, N., Nitta, K., Takayanagi, YY., Ohgi, K., Tsuji, T. and Irie, M. (2001) Effect of modification of the carboxyl groups of the sialic acid binding lectin from bullfrog (*Rana catesbeiana*) oocyte on anti-tumor activity. *Biol Pharm Bull*, **24**, 978-981.

Janowski R., Kozak M., Jankowska E., Grzonka Z., Grubb A., Abrahamson M. and Jaskolski M. (2001) Human cystatin C, an amyloidogenic protein, dimerizes through three-dimensional domain swapping. *Nat Struct Biol*, **8**, 316-320.

Kim, J.S. and Raines, R.T. (1993) Bovine seminal ribonuclease produced form a synthetic gene. *J Biol Cem*, **268**, 17392-17396.

Kim, J.S., Soucek, J., Matousek, J. and Raines, R.T. (1995) Mechanism of ribonuclease cytotoxicity. *J Biol Chem*, **270**¸31097-31102.

Kim, J.S., Soucek, J., Matousek, J. and Raines, R.T. (1995) Structural basis for the biological activities of bovine seminal ribonuclease. *J Biol Chem*, **270**¸ 10525-10530.

Klink, T.A. and Raines, R.T. (2000) Conformational stability is a determinant of ribonuclease A cytotoxicity. *J Biol Chem*, **275**, 17463-17467.

Knaus K.J., Morillas M., Swietnicki W., Malone M., Surewicz W.K., Yee V.C. (2001) Crystal structure of the human prion protein reveals a mechanism for oligomerization. *Nat Struct Biol*, **8**, 770-774.

Kobe, B. and Deisenhofer, J. (1993) Crystal structure of porcine ribonuclease inhibitor, a protein with leucine-rich repeats. *Nature*, **366**,751-756.

Kobe, B. and Deisenhofer, J. (1996) Mechanism of ribonuclease inhibitor by ribonuclease inhibitor protein based on the crystal structure of its complex with ribonuclease A. *J Mol Biol*, **264**, 1028-1043.

Kojima, K. (1993) Molecular aspects of the plasma membrane in tumor cells. *Nagoya J Med Sci*, **56**, 1-18.

Lee, J.E. and Raines, R.T. (2005) Cytotoxicity of bovine seminal ribonuclease: monomer versus dimer. *Biochemistry*, **44** 15760-15767.

Lee, F.S., Shapiro, R. and Vallee, B.L. (1989) Tight-binding inhibition of angiogenin and ribonuclease A by placental ribonuclease inhibitor. *Biochemistry*, **28**¸ 225-230.

Lee, F.S. and Vallee, B.L. (1993) Structure and action of mammalian ribonuclease (angiogenin) inhibitor. *Prog Nucleic Acid Res Mol Biol*, **44**, 1-30.

Leland, P.A., Schultz, L.W., Kim, B.M. and Raines R.T. (1998) Ribonuclease A variants with potent cytotoxic activity. *Proc Natl Acad Sci USA*, **95**,10407-10412.

Leland, P.A., Staniszewski, K.E., Kim, B.M. and Raines, R.T. (2001) Endowing human pancreatic ribonuclease with toxicity for cancer cells. *J. Biol. Chem.*, **276**,43095-43102.

Ledoux, L. (1955) Action of ribonuclease on certain ascites tumours. *Nature (London)*, **175**, 258-259.

Ledoux, L. (1955) Action of ribonuclease on two solid tumours *in vivo*. *Nature (London)*, **176**, 36-37.

Liao, Y.D., Huang, H.C., Chan, H.J. and Kuo, S.J. (1996) Large-scale preparation of a ribonuclease from *Rana catesbeiana* (bullfrog)oocytes and characterization of its specific cytotoxic activity against tumor cells. *Protein Expr Purif*, **7**, 194-202.

Libonati, M., Bertoldi, M. and Sorrentino, S. (1996) The activity on double-stranded RNA of aggregates of ribonuclease A higher than dimmers increases as function of the size of the aggregates. *Biochem J*, **318**,287-290.

Libonati, M. (1969) Molecular aggregates of ribonucleases. Some enzymatic properties. *Ital J Biochem*, **18**, 407-417.

Libonati, M., Malorni, M.C., Parente, A. and D'Alessio, G. (1975) Degradation of double-stranded RNA by a monomeric derivative of ribonuclease BS-1. *Biochim Biophys Acta*, **402**, 83-87.

Libonati, M. and Sorrentino, S. (2001) Degradation of double-stranded RNA by mammalian pancreatic-type ribonucleases. *Methods Enzymol*, **341**, 234-248.

Libonati, M. and Floridi, A. (1969) Breakdown of double-stranded RNA by bull semen ribonuclease. *Eur J Biochem*, **8**, 81-87.

Lin, J.J., Newton, D.L., Mikulski, S.M., Kung, H.F., Youle, R.J. and Rybak, S.M. (1994) Characterization of the mechanism of cellular and cell free protein synthesis inhibition by an anti-tumor ribonuclease. *Biochem Biophys Res Commun*, **2204**, 156-162.

Liu, Y., Hart, P.J. schlunegger, M.P. and Eisenberg, D. (1998) The crystal structure of a ·D domain-swapped dimmer of RNase A at 2.1-Å resolution. *Proc Natl Acad Sci USA*, ***95****, 3437-3442.*

Liu, Y., Gotte, G., Libonati, M. and Eisenberg, D. (2001) A domain-swapped RNase A dimer with implications for amyloid formation. *Nat Struct Biol*, **3**, 211-214.

Liu, Y., Gotte, G., Libonati, M. and Eisenberg, D. (2002) Structures of the two 3D domain-swapped RNase A trimers. *Prot Sci*, **11**, 371-380.

Mastronicola, M.R., Piccoli, R. and D'Alessio, G (1995) Key extracellular and intracellular steps in the antitumor action of seminal ribonuclease. *Eur J Biochem*, **230**, 242-249.

Mancheño, J.M., Gasset, M., Onaderra, M., Gavilanes, J.G and D'Alessil, G. (1994) Bovine seminal ribonuclease destabilizes negatively charged membranes. *Biochem Biophys Res Commun*, **199**, 119-124.

Matousek, J., Pouckova, P., Soucek, J. and Skvor, J. (2002) PEG chains increase aspermatogenic and antitumor activity of RNase A and BS-RNase enzymes. *J. Controlled Release*, **82**, 29-37.

Matousek, J. and Grozdanovic, J. (1973) The effect of bovine seminal ribonuclease (AS RNase on cells of Crocker tumor in mice. *Experientia*, **29**, 858-859.

Matousek, J., Gotte, G., Pouckova, P., Soucek, J., Slavik, T., Vottariello, F. and Libonati, M. (2003) Antitumor and other biological actions of oligoers of ribonuclease A. *J Biol Chem*, **278**, 23817-23822.

Moussaoui, M., Guash, A., Boix, E., Cuchillo, C.M and Nogués, M.V. (1996) The role of non-catalytic binding subsites in the endonuclease activity of bovine pancreatic ribonuclease A. *J Biol Chem*, **271**, 4687-4692.

Mazzarella, L., Capasso, S., Demasi, D., Di Lorenzo, G., Mattia, C.A. and Zagari, A. (1993) Bovine seminal ribonuclease: structure at 1.9 Å resolution. *Acta Crystallogr*, **D 49**, 389-402.

Milburn, M.V., Hassell, A.M., Kambert, M.H., Jordan, S.R., Proudfoot, A.E., Graber, P. and Wells, T.N. (1993) A novel dimmer configuration revealed by the crystal structure at 2.4A resolution of human interleukin-5. *Nature*, **363**, 172-176.

Mishra, N.C. "Molecular Biology of Nucleases" CRC Press, Boca Raton, FL, 1995.

Monti, D.M. and D'Alessio G. (2004) Cytosolic RNase inhibitor only affects RNases with intrinsic cytotoxicity.. *J Biol Chem*, **279**, 39195-39198.

Murthy, B.S., De Lorenzo, C., Piccoli, R., D'Alessio, G. and Sirdehmunk, R. (1996) Effects of protein RNase inhibitor and substrate on the quaternary structures of bovine seminal RNase. *Biochemistry*, **35**, 3880-3885.

Murthy, B.S., and Sirdeshmukh, R. (1992) Sensitivity of monomeric and dimeric forms of bovine seminal ribonuclease to human placental ribonuclease inhibitor. *Biochem J*, **281**, 343-348.

Newton, D.L., Boqué, L., Wlodawer, A., Huang, C.Y. and Rybak, S.M. (1998) Single amino acid substitutions at the N-terminus of a recombinant cytotoxic ribonuclease markedly influence biochemical and biological properties. *Biochemistry*, **37**, 5173-5183.

Nitta, K., Ozaki, K., Ishikawa, M., Furusawa, S., Hosono, M., Kawauchi, H., Sasaki, K., Takayanagi, Y., Tsuiki, S. and Hakomori, S. (1994) Inhibition of cell proliferation by *Rana catesbeiana* and *Rana japonica* lectins belonging to the ribonucleasesuperfamily. *Cancer Res*, **54**¸920-927.

Nitta, K., Takayanagi, G., Kawauchi, H. and Halomori, S. (1987) Isolation and characterization of *Rana catesbeiana* lectin and demonstration of the lectin-binding glycoprotein of rodent and human tumor cell membranes. *Cancer Res*, **47**, 4877-4883.

Nogués, M.V., vilanova, M. and Cuchillo, C.M. (1995) Bovine pancreatic ribonuclease A as a modelo f an enzyme with mutiple substrate binding sites. *Biochem Biophys Acta*, **1253**, 16-24.

Nogués, M.V., Moussaoui, M., Boix, E., Vilanova, M., Ribó, M. and Cuchillo, C.M. (1998) The contribution of noncatalytic phosphate-binding subsites to the mechanism of bovine pancreatic ribonuclease A. *Cell Mol Life Sci*, **54**, 766-774.

Ogawa, Y., Iwama, M., Ohgi, K., Tsuji, T., Irie, M., Itagaki, T., Kobayashi, H. and Inokuchi, N. (2002) Effect of replacing the aspartic acid/glutamic residues of bullfrog sialic acid binding lectin with asparagines/glutamine and arginine on the inhibition of cell proliferation in murine leukaemia P388 cells. *Biol Pharm Bull*, **25**, 722-727.

Parés, X., Nogués, M.V., de Llorens, R and cuchillo, C.M. (1991) Structure and function of ribonuclease A binding subsites. *Essays Biochem*, **26**, 89-103.

Parge, H.E., Arvai, A.S., Murtari, D.J., Reed, S.I. and Tainer, J.A. (1993) Human CksHs2 atomic atructure: A role for its hexameric assembli in cell cycle control. *Science*, **262**, 387-395.

Piccoli, R., Di Gaetano, S., De Lorenzo, C., Grauso, M., Monaco, C., Spalletti-Cernia, D., Laccetti, P., Cinatl, J., Matousek, J. and D'Alessio, G. (1999) A dimeric mutant of human pancreatic ribonuclease with selective cytotosicity toward malignant cells. *Proc Natl Acad Sci USA*, **96**, 7768-7773.

Piccoli, R. and D'Alessio, G. (1984) relationship between nonhyperbolic kinetics and dimeric structure in ribonucleases. *J Biol Chem*, **259**, 693-695.

Piccoli, R., Tamburrini, M., Piccialli, G., Di Donato, A., Parente, A. and D'Alessio, G. (1992) The dual-mode quaternary structure of seminal RNase. *Biochemistry*, **89**, 1870-1874.

Piccoli, R., Di Donato, A. and D'Alessio., G. (1988) Co-operativity in seminal ribonuclease function. Kinetic studies. *Biochem J*, **253**, 329-336.

Piccoli, R., Di Donato, A., Dudkin, S. and D'Alessio, G. (1982) Bovine seminal ribonuclease: non-hyperbolic kinetics in the second reaction step. *FEBS Lett*, **140**, 307-310.

Picone, D., Di Fiore, A., Ercole, C., Franzese, M., Sica, F., Tomaselli, S. and Mazzarella, L. (2005) The role of the hinge loop in domain swapping. *J Biol Chem*, **280**, 13771-13778

Reddi, K.K. (1975) Nature and possible origin of human serum ribonuclease. *Biochem Biophys Res Commun*, **67**, 110-118.

Richards, F.M. and Wyckoff, H.W. (1971) "The enzymes" (Ed. Boyer, P.D.), **4**, 647-806.

Roth, J.S. and Juster, H. (1972) On the absence of ribonuclease inhibitor in rat liver nuclei. *Biochim Biophys Acta*, **287**, 474-476.

Rushizky,. G. W., Knight, C.A. and Sober, H.A. (1961) Studies on the preferential specificity of pancreatic ribonuclease as deduced from partial digests. *J Biol Chem*, **236**, 2732-2737.

Rybak, S.M., Saxena, S.K., Ackerman, E.J. and Youle, R. J. (1991) Cytotoxic potential of ribonuclease and ribonuclease hybrid proteins. *J Biol Chem*, **266**, 21202-21207.

Rybak, S.M. and Newton, D.L. (1999) Natural and engineered cytotoxic ribonucleases: the therapeutic potential. *Exp Cell Res*, **253**¸ 325-335.

Sakakibara, F., Kawauchi, H., Takayanagi, G. and Ise, H. (1979) Egg lectin of *Rana japonica* and its receptor glycoprotein of Ehrlich tumor cells. *Cancer Res*, **39**, 1347-1352.

Saxena, S.K., Gravell, M., Wu, Y.N., Mikulski, S.M., Shogen, K., Ardelt, W. and Youle, R.J. (1996) Inhibition of HIV-1 production and selective degradation of viral RNA by an amphibian ribonuclease. *J Biol Chem*, **271**, 20783-20788.

Saxena, S.K., Rybak, S.M., Winkler, G., Meade, H.M., McGray, P., Youle, R.J. and Ackerman, E.J. (1991) Comparision of RNases and toxins upon injection into Xenopus oocytes. *J Biol Chem*, **266**, 21208-21214.

Saxena, S.K., Sirdeshmukh, R., Ardelt, W., Mikulski, S.M., Shogen, K. and Youle, R.J. (2002) Entry into cells and selective degradation of tRNAs by a cytotoxic member of the RNase A family. *J Biol Chem*, **277**, 15142-15146.

Schein, C.H. (1997) From housekeeper to microsurgeon: the diagnostic and therapeutic potential of ribonucleases. *Nat Biotechnol*, **15**, 529-536.

Schmitz, A., Herrgen,H., Winkeler, A. and Herzog, V. (2000) Cholera toxin is exported from microsomes by the Sec61p complex. *J Cell Biol*, **148**, 1203-1212.

Sica, F., Di Fiore, A., Merlino, A. and Mazzarella, L. (2004) Structure and stability of the non-covalent swapped dimmer of bovine seminal ribonuclease. *J Biol Chem*, **279**, 36753-36760.

Sierakowska, H and Shugar, D. (1977) Mammalian nucleolytic enzymes. *Proc Nucleic Acid Res Mol Biol*, **20**, 59-130.

Sorentino, S. (1998) Human extracellular ribonucleases: multiplicity, molecular diversity and catalytic properties of the major RNase types. *Cell Mol Lifie Sci*, **54**, 785-794.

Sorrentino, S., Naddeo, M., Russo, A. and D'Alessio, G. (2003) Degradation of double-stranded RNA by human pancreatic ribonuclease: crucial role of noncatalytic basic amino acid residues. *Biochemistry*, **42**, 10182-10190.

Sorrentino, S. and Libonati, M. (1994) Human pancreatic-type and nonpancreatic-type ribonucleases: a direct side-by-side comparison of their catalytic properties. *Arch Biochem Biophys*, **312**, 340-348.

Sorrentino, S. and Libonati, M. (1997) Structure-function relationships in human ribonucleases: main distinctive features of the major RNase types. *FEBS Lett*, **404**, 1-5.

Soucek, J., Pouckova, P., Matousek, J., Stockbauer, P., Dostal, J. and Zadinova, M. (1996) Antitumor action of bovine seminal ribonuclease. *Neoplasma*, **43**, 335-340.

Suzuki, M., Saxena, S.K., Boix, E., Prill, R.J., Vasandani, V.M., Ladner, J.E., Sung, C. and Youle, R.J. (1999) Engineering receptor-mediated cytotoxicity into human ribonucleases by steric blockade of inhibitor interaction. *Nat Biotechnol*, **17**, 265-270.

Tamburrini, M., Scala, G., Verde, C., Ruoco, M.R., Parente, A., Venuta, S. and D'Alessio, G. (1990) Immunosupressive activity of bovine seminal RNase on T-cell poliferation. *Eur J Biochem*, **190**, 145-148.

Taniguchi, T. and Libonati, M. (1974) Action of ribonuclease BS-1 on a DNA-RNA hybrid. *Biochem Biophys Res Commun*, **58**, 280-286.

Tarnowski, G.S., Kassel, R.L., Mountain, I.M., Blackburn, P., Wilson, G. and Wang, D. (1976) Comparison fo antitumor activities of pancreatic ribonucleases and its cross-linked dimmer. *Cancer Res*, **36**, 4074-4078.

Thompson, J.E., Venegas, F.D. and Raines, R.T. (1994) Energetics of catalysis by ribonucleases: fate of the 2',3'-cyclic phophodiester intermediate. *Biochemistry*, **33**, 7408-7414.

Tubert, Pere (2005) Treball de Recerca. Incorporació de seqüències NLS (d'import nuclear) amb la finalitat de dotar de citotoxicitat a la ribonucleasa pancreàtica humana (HP-RNasa).

Usher, D.A., Richardson, D.I., Jr. and Eckstein, F. (1970a) Absolute stereochemistry of the second step of ribonuclease action. *Nature*, **228**, 663-665.

Usher, D.A., Richardson, D.I., Jr. and Oakenfull, D.G. (1970b) Models of ribonuclease action. II. Specific acid, specific base, and neutral pathways for hydrolysis of a nucleotide diester analog. *J Am Chem Soc*, **92**, 4699-4712.

Vasandani, V.M., Wu, Y.N., Mikulski, S.M., Youle, R.J. and Sung, C. (1996;)Molecular determinants in the plasma clearance and tissue distribution of ribonucleases of the ribonuclease A superfamily. *Cancer Res*, **56**, 4180-4186.

Vasandani, V.M.,Burris, J.A. and Sung, C. (1999) Reversible nephrotoxicity of onconase and effect of lysine pH on renal onconase uptake. *Cancer Chemother Pharmacol*, **44**, 164-169.

Vescia, S., Tramontano, D., Augusti-Tocco, G. and D'Alessio, G. (1980) In vitro studies on selective inhibition of tumor cell growth by seminal ribonuclease. *Cancer Res*, **40**, 3740-3744.

Vicentini, A.M., Kieffer, B., Mathies, R., Meyhack, B., Hemmings, B.A., Stone, S.R. and Hofsteenge, J. (1990) Protein chemical and kinetic characterization of recombinant porcine ribonuclease inhibitor expressed in *Saccharomyces cerevisiae*. *Biochemistry*, **29**, 8827-8834.

Witzel, H. and Barnard, E.A (1962a) Mechanism and binding sites in the ribonuclease reaction I. Kinetic studies on the second step of the reaction. *Biochem Biphys Res Commun*, **7**, 289-294.

Witzel, H. and Barnard, E.A (1962b) Mechanism and binding sites in the ribonuclease reaction II. Kinetic studies on the first step of the reaction. *Biochem Biphys Res Commun*, **7**, 295-299.

Wlodawer, A. and Sjolin,L. (1983) Structure of ribonuclease A: results of joint neutron and X-ray refinement at 2.0-A resolution. *Biochemistry*, **22**, 2720-2728.

Wu, Y., Mikulski, S.M., Ardelt, W., Rybak, S.M. and Youle, R.J. (1993) A cytotoxic ribonuclease. Study of the mechanism of onconase cytotoxicity. *J Biol Chem*, **270**, 17476-17481.

Wu, Y., Saxena, S.K., Ardelt, W., Gadina, M., Mikulski, S.M., De Lorenzo, C., D'Alessio, G. and Youle, R.J. (1995) A study of the intracellular routing of cytotoxic ribonucleases. *J Biol Chem*, **270**, 17476-17481.

Yan, Y., Winograd, E., Viel, A., Cronin, T., Harrison, S.C. and Branton, D. (1993) Crystal structure of the repetitive segments of spectrin. *Science*, **262**, 2027-2030.

Youle, R.J., Wu, Y.N., Mikulski, S.M., Shogen, K., Hamilton, R.S. Newton, D., D'Alessio, G. and Gravel, M. (1994) RNase inhibition of human immunodeficiency virus infection of H9 cells. *Proc Natl Acad Sci USA*, **91**, 6012-6016.

Youle, R.J. and D'Alessio, G. (1997) *Antitumor RNases in "Ribonucleases: Structures and Functions"*. Academic Press, Nova York.

Zhang, J., dyer, K.D. and Rosenberg, H.F. (2002) RNase 8, a novel RNase A superfamily ribonuclease expressed uniquely in placenta. *Nucleic Acids Res*, **30**, 1169-1175.

Zhou, H.M. and Strydom, D.J. (1993) The amino acid sequence of human ribonuclease 4, a highly conserved ribonuclease that cleaves specifically on the 3' side of uridine. *Eur J Biochem*, **217**, 401-410.

Apèndix

Anàlisis de la capacitat citotòxica de PM8E103C

1. Anàlisis de la interacció amb l'inhibidor proteic de ribonucleases.

Tal com s'ha esmentat a la introducció d'aquesta tesi, un dels factors que contribueixen a la capacitat citotòxica de certes RNases citotòxiques, com la onconasa i la BS-RNasa és l'habilitat per escapar l'RI (Leland *et al.*, 1998; Haigis *et al.*, 2002; Haigis *et al.*, 2003; Matousek et al., 2003; Lee and Raines, 2005). En el cas de la BS-RNasa, aquesta només presenta activitat citotòxica quan es troba en forma dimèrica per intercanvi de dominis i es creu que aquesta estructura quaternària produeix un impediment estèric per la unió del RI. Era doncs, molt interessant assajar la interacció del dímer de PM8E103C amb l'RI per tal d'avaluar les seves possibilitats com a agent citotòxic. Es va descartar assajar la citotoxicitat del dímer de PM8 ja que la forma dimèrica presentava una estabilitat molt inferior (veure capítol 3). Prèviament, en el grup s'havia realitzat un modelat molecular de la interacció del dímer de PM8 amb l'RI (Canals *et al.*, 2001). Aquest model indicava que un cop una molècula d'RI interaccionava amb una de les dues subunitats del dímer, no era possible la interacció d'una segona molècula amb l'altra subunitat per impediment estèric, deixant accessible al substrat un dels centres catalítics. Per tal de valorar la capacitat d'escapament a l'RI de la forma dimèrica de PM8E103C es va procedir a la realització d'un assaig d'escapament al inhibidor en gel d'agarosa. En aquest assaig qualitatiu de la formació del complex RNasa-RI s'analitza electroforèticament la degradació dels rRNA 16S i 23S d'*E. Coli* per part de cadascuna de les proteïnes recombinants incubades amb diferents concentracions d'inhibidor. Com a control negatiu s'utilitzà la HP-RNasa que no escapa al inhibidor, mentre que com a control positiu es va utilitzar l'onconasa.

Els resultats obtinguts de l'anàlisi d'escapament a l'RI es presenten a la Figura 5.1.A on s'observa que l'onconasa és capaç de degradar el rRNA tant en presència com en absència de RI i, per altra banda, que la HP-RNasa només degrada rRNA en absència de RI. Tal com s'esperava, la forma monomèrica de PM8E103C tampoc escapa a l'RI. Per altra banda, aquest assaig sembla indicar que el dímer de PM8E103C tampoc és capaç d'evadir l'acció del RI. Aquest fet, es podria explicar perquè la concentració de DTT inclosa a l'assaig (10 mM), necessària per a poder mantenir l'estructura del inhibidor activa, fos suficient per reduir el pont disulfur que estabilitza l'estructura dimèrica de PM8E103C. Per això, es va repetir l'assaig sense afegir DTT en el tampó de reacció, tot i que com que la solució estoc de RI conté 8 mM de DTT, la reacció es realitzà a una concentració de 0.4 mM de DTT. Tal i com es pot observar a la Figura 5.1.B, no hi havia diferències en el comportament de cap enzim a aquesta nova concentració de DTT.

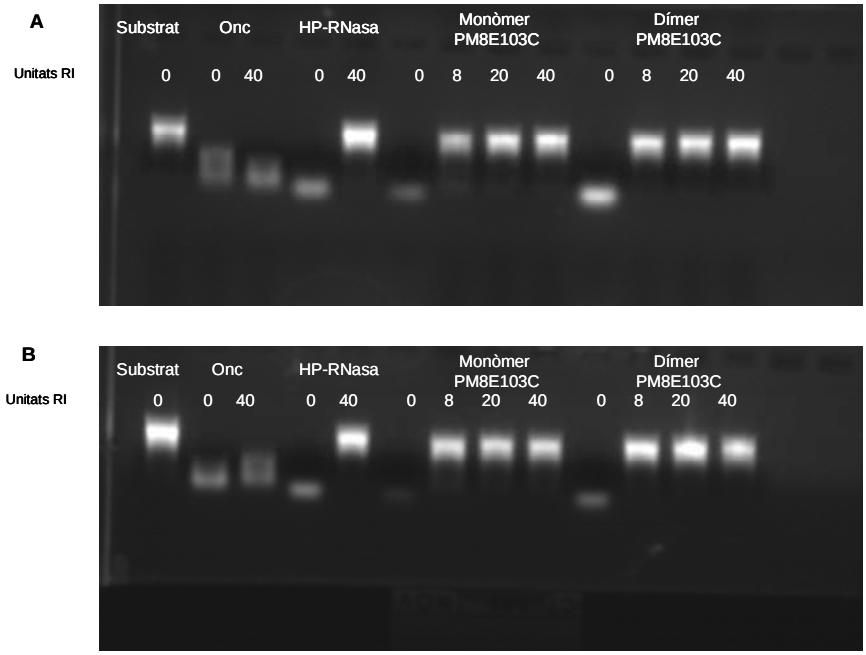

Figura 5.1.: Assaig d'escapament a l'RI de diferents RNases en presència de 10 mM (A) i 0,4 mM (B) de DTT. La inhibició per part del RI es va determinar qualitativament seguint unl protocol descrit prèviament (Bosch et al., 2004). S'incubaren 15 ng de RNasa en tampó Hepes 20 mM amb les concentracions de RI indicades a la figura (una unitat es defineix com la quantitat de RI necessària per inhibir al 50% 5ng de RNasa A), en un volum total de 20 µl. Després d'incubar 10 min a 25 ºC, es va afegir el substrat de l'enzim a cada tub, i es va incubar 10 min més a 25 ºC. Finalment, la reacció es va aturar afegint tampó sacarosa 40% (p/v), 0.2% dietilpolicarbonat, 0.25% (p/v) blau de bromofenol. La degradació del substrat es va visualitzar en un gel d'agarosa a 1,5% en el que s'incloïa una mostra de substrat no degradat. El substrat degradat presenta una mobilitat electroforètica superior.

S'ha descrit que la introducció de dues Cys a la posició 89 de la HP-RNasa, permeti la formació d'una estructura dimèrica però que la presència de 5 mM de DTT per a la realització de l'assaig d'escapament al RI trenca aquesta estructura (Suzuki *et al.*, 1999). Per tal de comprovar aquesta hipòtesis, es va determinar per cromatografia de gel-filtració la presència de la forma monomèrica quan s'incubava DPM8E103C durant 10 minuts en tampó Hepes 20 mM en presència i absència de DTT 0,4 mM. Tal i com es pot observar a la Figura 5.2, aquesta concentració de DTT era suficient com per produir la dissociació completa de la forma dimèrica de PM8E103C.

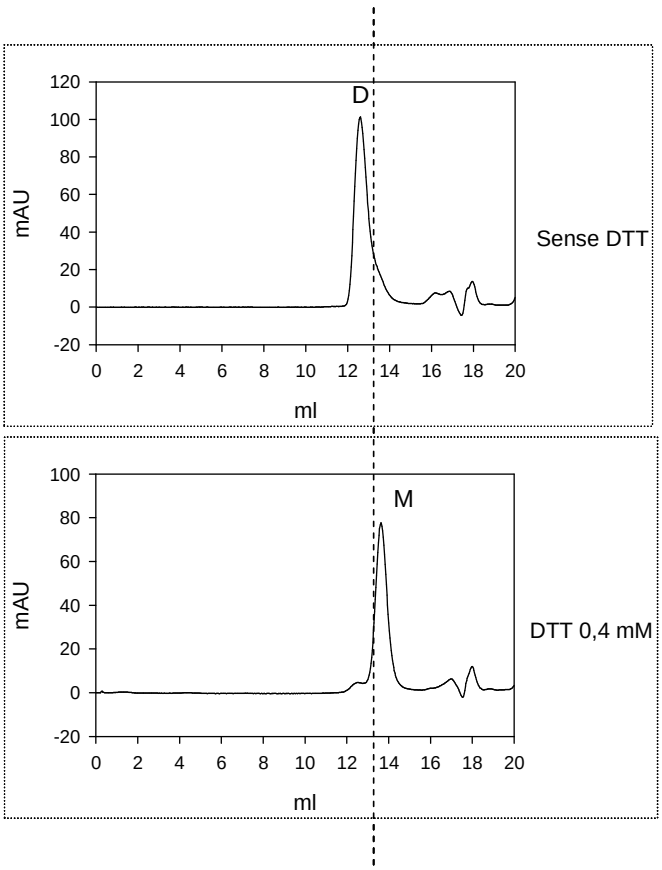

Figura 5.2: Caracterització cromatogràfica del dímer de PM8E103C en absència (A) i presència (B) de DTT. Es mostren els perfils cromatogràfics de la variant dimèrica de ribonucleasa pancreàtica humana PM8E103C en la columna gel filtració G75 HR10/30. Els pics corresponents a la forma dimèrica i monomèrica s'assenyalen amb D i M respectivament.

2. Propietats citotòxiques en cultius cel·lulars.

Malgrat de no ser capaç d'escapar *in vitro* a l'acció de l'inhibidor a aquestes concentracions de DTT, es va voler comprovar si aquesta RNasa dimèrica presentava activitat citotòxica. Per això, es van realitzar assajos de citotoxicitat sobre la línia cel·lular HeLa (carcinoma cèrvix). Aquesta capacitat es va mesurar aplicant concentracions creixents de cada una de les proteïnes sobre la línia cel·lular i mesurant la síntesis proteica amb la incorporació de ^{35}S-metionina.

A la Figura **5.3** es representen les corbes dosi-resposta de l'acció del dímer de PM8E103C. Com a control positiu es va utilitzar l'onconasa per a la qual es va obtenir un valor de IC_{50} (definit com la concentració de RNasa que provoca una reducció del 50% del valor de la síntesis proteica) de 0,3 µM. Aquest valor és del mateix ordre de magnitud que els descrits prèviament (Bosch *et al.*, 2004). Tal i com es pot observar, la variant dimèrica no va presentar una activitat citotòxica significativa (veure Figura **5.3**). Aquests resultats poden ser deguts a què l'entorn citosòlic on les RNases exerceixen la seva acció citotòxica, presenta un caràcter reductor que podria induir la dissociació del dímer i per tant el monòmer generat podria ser capturat per l'RI.

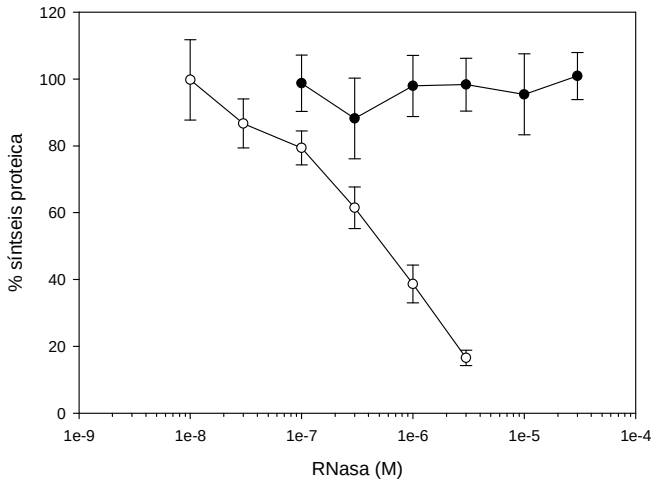

Figura 5.3.: Citotoxicitat de la variant dimèrica de PM8E103C i de l'onconasa. Representació del percentatge de síntesi proteica en cèl·lules HeLa. Es van fer créixer les cèl·lules en medi DMEM suplementades amb 10% de FCS, 50 U/ml de penicil·lina i 50 U/ml d'estreptomicina. Per a l'assaig de citotoxicitat, s'utilitzaren 2500 cèl·lules en plaques de 96 pous i després de 96 hores d'incubació amb la RNasa (• DPM8E103C, o Onc) s'adicionà ^{35}S-metionina (500.000 c.p.m./pou) durant 24 hores més. Es lisaren les cèl·lules en amb NaOH i es precipitaren les proteïnes amb TCA al 15%. Les proteïnes foren recollides en filtres de fibra de vidre, rentades amb TCA al 5% i resuspeses en líquid d'escintil·lació per tal de ser contades al contador corresponent. Com a control negatiu, s'utilitzaren les mateixes cèl·lules tractades amb cicloheximidia 1mM (Bosch *et al*.,2004). Els resultats per a cada experiment individual són la mitjana de quatre determinacions.